Chapter 5

Coherent Control of Momentum

The linear momentum transfer of photon via absorption and stimulated emission provides a way of imparting momentum to a particle. Combinations of laser pumping techniques, with suitable timing, frequency detuning, polarization, intensity and direction can be used to control the translational momentum and kinetic energy of the molecules. By coherently controlling the momentum and kinetic energy of molecules, the c.m. entropy can also be changed at the expense of changing the internal entropy.

We derive the general expression for the rate of a mean system variable which linearly depends on the dissipation. This gives expressions for the rate of mean kinetic energy, the rate of mean internal energy, and the mean force. The rates of mean center of mass kinetic energy and the mean force are also related to the momentum probability density and its rate. We show that the momentum probability density and the external entropy can change even if there is no dissipation.

The Doppler shift and recoil shift frequencies provide a way for selectively transferring the population with a narrow momentum class of using lasers in the so-called Raman velocity selection scheme [313]. A gas of molecules can also be coherently accelerated or decelerated during coherent population transfer. This can be achieved using the STIRAP scheme [285] with the inclusion of the momentum state. We use the density matrix equations including the center of mass momentum states and spontaneous emissions from the excited state of a three-level Λ system to study the mechanical effects of velocity selection and STIRAP processes. The expression for predicting the selected momentum width as a function of Rabi frequencies, detunings and pulse length is derived. We describe a deceleration method using repeated STIRAP processes. The rate of momentum transfer, which is the light force are shown to be very large by using short pulses. In the final Section, we use the Wigner function to study the quasi phase space evolution of a spatially narrow pulse of molecules in a harmonic potential trap. The momentum squeezing is obtained after a quarter trap period. This is extended for repeated squeezing.

5.1 Equation of Motion (Rate of Mean Operator)

The expectation value of an operator is defined as $\langle\hat{O}\rangle \doteq Tr\{\hat{\rho}(t)\hat{O}\} = \sum_n \langle n|\hat{\rho}(t)\hat{O}|n\rangle$ where $|n\rangle$ are the time independent basis. By using $\frac{\partial\hat{\rho}}{\partial t} = \frac{1}{i\hbar}[\hat{H},\hat{\rho}(t)]$, we obtain

$$\frac{d}{dt}\langle\hat{O}\rangle = \langle\frac{\partial}{\partial t}\hat{O}\rangle + \frac{1}{i\hbar}\langle[\hat{O},\hat{H}]\rangle \tag{5.1}$$

where the trace is over the system and reservoir time independent basis which as $\langle\hat{O}\rangle \doteq Tr_{SR}\{\hat{\rho}(t)\hat{O}\}$.

If $\hat{O}_S$ is the system operator and the state of the system is governed by the master equation $\frac{\partial\hat{\rho}_S}{\partial t} = \frac{1}{i\hbar}[\hat{H}_o + \hat{V}_{SL},\hat{\rho}_S(t)] + \mathcal{L}\hat{\rho}_S(t)$, with $\mathcal{L}\hat{\rho}_S(t)$ as the dissipative Liouvillean, we have

$$\frac{d}{dt}\langle\hat{O}_S\rangle_S = \langle\frac{\partial}{\partial t}\hat{O}_S\rangle_S + \frac{1}{i\hbar}\langle[\hat{O}_S,\hat{V}_{SL}]\rangle_S + Tr_S\{\hat{O}_S\mathcal{L}\hat{\rho}_S(t)\} \tag{5.2}$$

where the trace is over the system $\langle\hat{O}_S\rangle_S \doteq Tr_S\{\hat{\rho}_S(t)\hat{O}_S\}$.

Alternatively, if the trace in Eq. 5.1 is over the reservoir as well $\langle\hat{O}_S\rangle \doteq Tr_{SR}\{\hat{\rho}_S(t)\hat{O}_S\}$, we replace $\hat{H} = \hat{H}_o + \hat{V}_{SL} + \hat{V}_{SR}$ and Eq. 5.1 becomes

$$\frac{d}{dt}\langle\hat{O}_S\rangle = \langle\frac{\partial}{\partial t}\hat{O}_S\rangle + \frac{1}{i\hbar}\langle[\hat{O}_S,\hat{H}_o]\rangle + \frac{1}{i\hbar}\langle[\hat{O}_S,\hat{V}_{SL}]\rangle + \frac{1}{i\hbar}Tr_{SR}\{\hat{\rho}[\hat{O}_S,\hat{V}_{SR}]\} \tag{5.3}$$

By comparing Eqs. 5.1 and 5.3, with $\langle\hat{O}_S\rangle = \langle\hat{O}_S\rangle_S$ and $[\hat{O}_S,\hat{H}_o] = 0$, we find that $\hat{O}_S\mathcal{L}\hat{\rho}_S(t) = \frac{1}{i\hbar}Tr_R\{\hat{\rho}[\hat{O}_S,\hat{V}_{SR}]\}$. If we replace $\hat{\rho}(t) \stackrel{?}{=} \hat{\rho}_S(t)\otimes\hat{\rho}_R$, the last term in Eq. 5.3 is zero in the case of thermal reservoir since $Tr_R\{\hat{\rho}_R\hat{V}_{SR}\} = 0$, which implies that $Tr_S\{\hat{O}_S\mathcal{L}\hat{\rho}_S(t)\}$ is zero too and the evolution of the mean operator is independent of the dissipative effect. However, this is not true because $\hat{\rho}(t) \neq \hat{\rho}_S(t)\otimes\hat{\rho}_R$ the dissipative term $Tr_S\{\hat{O}_S\mathcal{L}\hat{\rho}_S(t)\}$ gives a finite contribution.

5.1.1 Rate of Internal Energy

The rate of the mean internal energy operator is

$$\frac{d}{dt}\langle\hat{H}_I\rangle = \frac{1}{i\hbar}Tr_S\{\hat{\rho}^i_S(t)[\hat{H}_I,\hat{V}^i_{SL}]\} + Tr_S\{\hat{H}_I\mathcal{L}\hat{\rho}^i_S(t)\} \tag{5.4a}$$

$$= i\int d^3P\sum_{L,a,b}\hbar\Omega_{Lab}\omega_{ab}(\pi_{ba}-\pi_{ab}) + \sum_a\int\hbar\omega_a\langle a\mathbf{P}|\mathcal{L}\hat{\rho}_S(t)|a\mathbf{P}\rangle d^3P \tag{5.4b}$$

where $\hat{H}_I = \hbar\sum_a\omega_a|a\rangle\langle a|$, $\pi_{ba}(\mathbf{P},t) \doteq \langle b,\mathbf{P}|\hat{\rho}^i_S(t)|a,\mathbf{P}+\hbar\mathbf{k}_L\rangle e^{-i(\omega_L-\omega_{ab})t}$ and $\omega_{ab} \doteq \omega_a - \omega_b$. We have used the facts that the internal operator is diagonal in both the momentum basis and internal state basis $\langle a\mathbf{P}|\hat{H}_I|b\mathbf{P}'\rangle = \hbar\omega_a\delta_{ab}\delta(\mathbf{P}-\mathbf{P}')$.

As an example, we consider a two level system with the internal energy operator $\hat{H}_I = \hbar\omega_e S^+S^- + \hbar\omega_g S^-S^+$, the rate of internal energy can be evaluated as

$$\frac{d\langle\hat{H}_I\rangle}{dt} = \hbar\omega_o \int d^3P\{i\Omega(\pi_{ge}(\mathbf{P},t) - \pi_{eg}(\mathbf{P},t)) - \Gamma\left(\overline{n}+1\right)\rho_{ee}(\mathbf{P},t) + \Gamma\overline{n}\rho_{gg}(\mathbf{P}-\hbar\mathbf{k}_L,t)\} \tag{5.5a}$$

At steady state, we can show that $\frac{d}{dt}\langle\hat{H}_I\rangle = 0$ (as expected) by inserting the standard results [151], generalized to include the center of mass momentum dependence and the mean thermal photon number at resonant $\overline{n} \doteq (e^{\beta\hbar\omega_o} - 1)^{-1}$ as

$$i\{\pi_{ge}(\mathbf{P},t) - \pi_{eg}(\mathbf{P},t)\}_{st} = \frac{\Omega\Gamma f(\mathbf{P},t)}{(\gamma^2 + \bar{\Delta}^2 + 2\Omega^2)} \tag{5.6}$$

$$\rho_{ee}(\mathbf{P},t)_{st} = \frac{f(\mathbf{P},t)}{2}\{1 - \frac{(\gamma^2+\bar{\Delta}^2)}{(2\overline{n}+1)(\gamma^2+\bar{\Delta}^2+2\Omega^2)}\} \tag{5.7}$$

$$\rho_{gg}(\mathbf{P}-\hbar\mathbf{k}_L,t)_{st} = \frac{f(\mathbf{P}-\hbar\mathbf{k}_L,t)}{2}\{1 + \frac{(\gamma^2+\bar{\Delta}^2)}{(2\overline{n}+1)(\gamma^2+\bar{\Delta}^2+2\Omega^2)}\} \tag{5.8}$$

where $\int f(\mathbf{P},t)d^3P = 1$ and $\gamma \doteq \Gamma(\overline{n}+\frac{1}{2})$.

5.1.2 Rate of Kinetic Energy

The time derivative of the kinetic energy operator is related to the force operator $\hat{\mathbf{F}} \doteq \frac{d}{dt}\hat{\mathbf{P}} = -\nabla\hat{V} = -\nabla\hat{V}_{SL} - \nabla\hat{V}_{SR}$ as

$$\frac{d}{dt}\hat{H}_{cm} = \frac{d}{dt}(\frac{\hat{P}^2}{2M}) = \frac{1}{2M}\{\hat{\mathbf{P}}\cdot\hat{\mathbf{F}} + \hat{\mathbf{F}}\cdot\hat{\mathbf{P}}\} = \frac{i\hbar}{2M}\{\nabla\cdot(\nabla\hat{V}) + (\nabla\hat{V})\cdot\nabla\} \tag{5.9}$$

The time derivative of the mean kinetic energy is

$$\frac{d}{dt}\langle\hat{H}_{cm}\rangle = \frac{1}{i\hbar}\frac{1}{2M}Tr_S\{\hat{\rho}_S(t)(\hat{P}^2\hat{V}_{SL} - \hat{V}_{SL}\hat{P}^2)\} + Tr_S\{\frac{\hat{P}^2}{2M}\mathcal{L}\hat{\rho}_S(t)\} \tag{5.10}$$

In the case of unitary evolution, only the first term on the right hand side of Eq. 5.10 contributes. For two level system, we replace the Eq. 8.94 of Appendix IV, and obtain

$$\begin{aligned}\frac{d}{dt}\langle\hat{H}_{cm}\rangle &= -i\int d^3P\sum_L \frac{\hbar\Omega_L}{2}(\frac{\hat{\mathbf{P}}\cdot\mathbf{k}_L}{M} - \frac{\hbar\mathbf{k}_L^2}{2M}) \times \\ &\{\chi_L(\mathbf{P})(\pi_{ge}(\mathbf{P},t) + \pi_{eg}^{arw}(\mathbf{P},t)) - \chi_L^*(\mathbf{P})(\pi_{ge}^{arw}(\mathbf{P},t) + \pi_{eg}(\mathbf{P},t))\}\end{aligned} \tag{5.11}$$

where the Röntgen correction term is $\chi_L(\mathbf{P}) \doteq \sum_{q=+,-,\mathbf{0}} C_q\{\epsilon_{Lq}^*\frac{\omega_{\parallel,L}(\mathbf{P})}{\omega_L} + \kappa_{Lq}^*\frac{\omega_{\perp,L}(\mathbf{P})}{\omega_L}\}$ and the rotating wave parameters and the anti-rotating parameters are defined respectively as

$$\pi_{eg}(\mathbf{P},t) \doteq \hat{\rho}_{eg}(\mathbf{P},\mathbf{P}-\hbar\mathbf{k})e^{i\bar{\Delta}_{L\mathbf{P}}t} \quad , \quad \pi_{eg}^{arw}(\mathbf{P},t) \doteq \hat{\rho}_{eg}(\mathbf{P}-\hbar\mathbf{k},\mathbf{P})e^{-i\bar{\sigma}_{L\mathbf{P}}t} \tag{5.12}$$

$$\bar{\Delta}_L \doteq \Delta_L - \frac{\hat{\mathbf{P}}\cdot\mathbf{k}_L}{M} + \frac{\hbar\mathbf{k}_L^2}{2M} \quad , \quad \bar{\sigma}_L \doteq \sigma_L - \frac{\hat{\mathbf{P}}\cdot\mathbf{k}_L}{M} + \frac{\hbar\mathbf{k}_L^2}{2M} \tag{5.13}$$

From Eq. 8.37 of Appendix II, ϵ^*_{Lq} and κ^*_{Lq} have the same exponential phase factors. Thus, in rotating wave approximation (RWA), we can rewrite Eq. 5.11 as

$$\frac{d}{dt}\langle \hat{H}_{cm}\rangle = -i\int d^3P \sum_L \frac{\hbar\Omega_L}{2}\left(\frac{\hat{\mathbf{P}}\cdot\mathbf{k}_L}{M} - \frac{\hbar\mathbf{k}_L^2}{2M}\right)\chi_L(\mathbf{P})(\pi_{ge}(\mathbf{P},t) - \pi_{eg}(\mathbf{P},t)) \tag{5.14}$$

Thus, the mean kinetic energy can change, depending on the real parameter, the 'absorption' $v(\mathbf{P},t) \doteq i(\pi_{ge}(\mathbf{P},t) - \pi_{eg}(\mathbf{P},t))$. For continuous laser pumping in the absence of dissipation, we use Eq. 8.105 to obtain the solutions for π_{ge} and $\frac{d}{dt}\langle \hat{H}_{cm}\rangle = \rho_{gg}(\mathbf{P},0)\frac{1}{2}\Omega_L \sin\Omega_L t \int d^3P(\frac{\hbar\mathbf{P}\cdot\mathbf{k}_L}{M} + \frac{\hbar^2\mathbf{k}_L^2}{2M})$. Here, v oscillates around zero value, so on average there is no change in the kinetic energy. The oscillation rate and amplitude can be very large if high intensity laser is used. The Doppler shift is dependent on the direction of the wavevector $\mathbf{k}_L$, so it is possible to rectify the kinetic rate so that $\frac{d}{dt}\langle \hat{H}_{cm}\rangle \neq 0$ by reversing the direction of $\mathbf{k}_L$ during every period of π/Ω_L so that $\mathbf{P}\cdot\mathbf{k}_L \sin\Omega_L t$ is always positive. This shows that *coherent control without dissipation* can change the kinetic energy of a system.

5.1.3 Mean Momentum and Mean Force

From Eq. 5.2 and 5.18, the rate of mean momentum or mean force can also be expressed as

$$\mathbf{F} = \frac{d}{dt}\langle\hat{\mathbf{P}}\rangle = -\langle\nabla\hat{V}_{SL}\rangle + Tr_S\{\hat{\mathbf{P}}\mathcal{L}\hat{\rho}_S(t)\} \tag{5.15}$$

where we have used $[\hat{\mathbf{P}},\hat{V}_{SL}] = [-i\hbar\nabla,\hat{V}_{SL}] = -i\hbar\nabla\hat{V}_{SL}$. It should be noted that the second term has often been neglected in the analysis of light force in the existing laser cooling theories [168], [166], [169].The first and second terms on right-hand-side of Eq. 5.15 can be expanded as

$$\langle\nabla\hat{V}_{SL}\rangle = Tr_S(\hat{\rho}_S\nabla\hat{V}_{SL}) = \int\sum_\alpha\langle\alpha,\mathbf{P}|\hat{\rho}_S\nabla\hat{V}_{SL}|\alpha,\mathbf{P}\rangle d^3P \tag{5.16}$$

$$Tr_S\{\hat{\mathbf{P}}\mathcal{L}\hat{\rho}_S(t)\} = \int\mathbf{P}\sum_\alpha\langle\alpha,\mathbf{P}|\mathcal{L}\hat{\rho}_S|\alpha,\mathbf{P}\rangle d^3P \tag{5.17}$$

5.1.4 Relationships with $f(\mathbf{P},t)$

The mean momentum and the rate of mean momentum (or mean forced) can be written as

$$\langle\hat{\mathbf{P}}\rangle = Tr_S(\hat{\mathbf{P}}\hat{\rho}_S(t)) = \int d^3P\sum_\alpha\langle\mathbf{P},\alpha|\hat{\mathbf{P}}\hat{\rho}_s(t)|\mathbf{P},\alpha\rangle = \int f(\mathbf{P},t)\mathbf{P}d^3P \tag{5.18}$$

$$\mathbf{F} = \frac{d}{dt}\langle\hat{\mathbf{P}}\rangle = \int\frac{df(\mathbf{P},t)}{dt}\mathbf{P}d^3P \tag{5.19}$$

where $f(\mathbf{P},t) \doteq \sum_\alpha \langle \mathbf{P},\alpha|\hat{\rho}(t)|\mathbf{P},\alpha\rangle$ is the momentum probability distribution, with $\langle \mathbf{P}',\alpha|\hat{\rho}(t)|\mathbf{P},\alpha\rangle = \pi_{\alpha\alpha}(t)\delta(\mathbf{P}-\mathbf{P}')$.

Similarly, the mean kinetic energy and its rate are related to the probability density and first derivative as

$$\langle \hat{H}_{cm}\rangle = \frac{\langle P^2\rangle}{2M} = \frac{1}{2M}\int f(\mathbf{P},t)\mathbf{P}^2 d^3P \tag{5.20}$$

$$\frac{d}{dt}\langle \hat{H}_{cm}\rangle = \frac{1}{2M}\int \frac{df(\mathbf{P},t)}{dt}\mathbf{P}^2 d^3P \tag{5.21}$$

We can combine Eqs. 5.15, 5.16 and 5.17 to obtain

$$\frac{df(\mathbf{P},t)}{dt} = -\frac{\mathbf{P}}{P^2}\cdot\sum_\alpha \langle \alpha,\mathbf{P}|\hat{\rho}_S\nabla\hat{V}_{SL}|\alpha,\mathbf{P}\rangle + \sum_\alpha \langle \alpha,\mathbf{P}|\mathcal{L}\hat{\rho}_S|\alpha,\mathbf{P}\rangle \tag{5.22}$$

Equation 5.22 shows that $\frac{df(\mathbf{P},t)}{dt}$ is finite and that the momentum distribution can change even if there is no dissipation. From Eqs. 4.32,4.33 it is clear that the *external c.m. entropy can change in a non-dissipative process.*

5.1.5 Rate of Phase Operator

The phase space operator is defined as $\hat{\mathbf{R}}\cdot\hat{\mathbf{P}} = \hbar^2(\frac{\partial^2}{\partial X\partial P_x} + \frac{\partial^2}{\partial Y\partial P_y} + \frac{\partial^2}{\partial Z\partial P_z}) = \sum_i \hat{R}_i\hat{P}_i$ and the time derivative is

$$\frac{d}{dt}(\hat{\mathbf{R}}\cdot\hat{\mathbf{P}}) = \hat{\mathbf{R}}\cdot\hat{\mathbf{F}} + \hat{\mathbf{v}}\cdot\hat{\mathbf{P}} \tag{5.23}$$

where $\hat{\mathbf{F}} \doteq \frac{d}{dt}\hat{\mathbf{P}}$ and $\hat{\mathbf{v}} \doteq \frac{d}{dt}\hat{\mathbf{R}}$.

When the Hamiltonian is of the form $\hat{H} = \frac{\hat{\mathbf{P}}^2}{2M} + V(\hat{\mathbf{R}})$ as in the dipole approximation Hamiltonian, it is clear that $\hat{\mathbf{F}} = -\nabla\hat{V}(\hat{\mathbf{R}})$ and $\hat{\mathbf{v}} = \frac{\hat{\mathbf{P}}}{M}$ so

$$\frac{d}{dt}(\hat{\mathbf{R}}\cdot\hat{\mathbf{P}}) = -\hat{\mathbf{R}}\cdot\nabla\hat{V} + 2\hat{H}_{cm} \tag{5.24}$$

However, in the minimal coupling Hamiltonian, $\hat{H} = \frac{\hat{\mathbf{P}}^2}{2M} + V(\hat{\mathbf{R}},\hat{\mathbf{P}})$ and the equations are more complicated $\hat{\mathbf{F}} = -\nabla\hat{V}(\hat{\mathbf{R}},\hat{\mathbf{P}})$ and $\hat{\mathbf{v}} = \frac{\hat{\mathbf{P}}}{M} + \nabla_P\hat{V}(\hat{\mathbf{R}},\hat{\mathbf{P}})$ so $\frac{d}{dt}(\hat{\mathbf{R}}\cdot\hat{\mathbf{P}}) = -\hat{\mathbf{R}}\cdot\nabla\hat{V} + 2\hat{K} + \nabla_P\hat{V}\cdot\hat{\mathbf{P}}$. This shows another reason in favor of using the dipole Hamiltonian. For a bounded potential, the mean $\langle\hat{\mathbf{R}}\cdot\hat{\mathbf{P}}\rangle$ must be time independent [224]. This gives the *quantum virial theorem,*

$$\langle\hat{\mathbf{R}}\cdot\nabla\hat{V}\rangle_{st} = 2\langle\hat{H}_{cm}\rangle_{st} \tag{5.25}$$

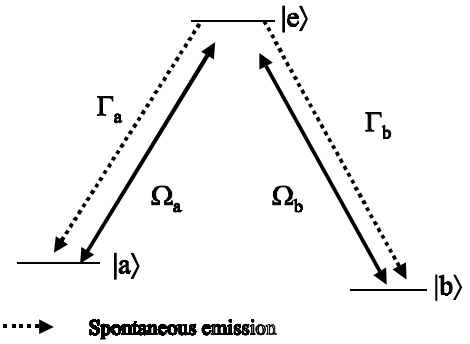

Figure 5.1: Schematic of a three-level Λ scheme with two-sided laser couplings and spontaneous emissions, used for Raman velocity selection and STIRAP deceleration.

5.2 Bloch Equations for Three-Level Λ System

In Ref. [1], we have proposed a laser cooling scheme for molecules which use the lasers for coherent population and momentum transfers in a three-level Λ (Raman) scheme, namely to achieve velocity selection and deceleration. This requires efficient and complete population transfer from one state to another without populating the excited state, in order to avoid spontaneous decay to unwanted levels that will reduce the transfer efficiency.

The Schrödinger equation is preferable for simplicity in the analysis when the laser pulse duration is much shorter than the decay rate of the excited state and in the large detuning regime. For small detuning and long pulses, the spontaneous decay must be considered using a full master equation. It also enables the light forces to be evaluated though the coherences of the density matrix elements.

In the following, we present the density matrix theory which leads to the theory of Raman velocity selection and deceleration with repeated STIRAP technique. The generalized Bloch equations for 3-level Λ system (see Fig. 5.1) including the c.m. momentum and spontaneous emissions is derived from the master equation in Chapter III, Eq. 3.37 in the weak field limit of Eq. 3.85. We consider the case where the two decaying channels do not interfere (no spontaneously generated coherences). Thus, we obtain the dissipative parts for the Bloch equations from Eqs. 3.154 by setting the terms with $\Gamma_{1,o2}$ and $\Gamma_{2,o1}$ to zero. The same results are obtained within the timescale $t >> 1/(\omega_{o1} - \omega_{o2})$ such that the terms with $e^{\pm i\omega_{o12}t}$ average to zero. Thus, we obtain the full Bloch equations are:

$$
\begin{aligned}
\frac{d}{dt}\pi_{ee}(\mathbf{P},t) &= i\Omega_a(t)\{\pi_{ae}(\mathbf{P},t)-\pi_{ea}(\mathbf{P},t)\}+i\Omega_b(t)\{\pi_{be}(\mathbf{P},t)-\pi_{eb}(\mathbf{P},t)\} \qquad (5.26)\\
&\quad -\Gamma_{tot}\pi_{ee}(\mathbf{P},t)+\Gamma_a\overline{n}_a\pi_{aa}(\mathbf{P}+\hbar\mathbf{k}_a,t)+\Gamma_b\overline{n}_b\pi_{bb}(\mathbf{P}+\hbar\mathbf{k}_b,t)\\
\frac{d}{dt}\pi_{aa}(\mathbf{P},t) &= -i\Omega_a(t)\{\pi_{ae}(\mathbf{P},t)-\pi_{ea}(\mathbf{P},t)\}+\Gamma_a(\overline{n}_a+1)\pi_{ee}(\mathbf{P}-\hbar\mathbf{k}_a,t)-\Gamma_a\overline{n}_a\pi_{aa}(\mathbf{P},t)\\
\frac{d}{dt}\pi_{bb}(\mathbf{P},t) &= -i\Omega_b(t)\{\pi_{be}(\mathbf{P},t)-\pi_{eb}(\mathbf{P},t)\}+\Gamma_b(\overline{n}_b+1)\pi_{ee}(\mathbf{P}-\hbar\mathbf{k}_b,t)-\Gamma_b\overline{n}_b\pi_{bb}(\mathbf{P},t)\\
\frac{d}{dt}\pi_{ea}(\mathbf{P},t) &= (i\bar{\Delta}_{\mathbf{P}a}-\frac{\Gamma_{\perp a}}{2})\pi_{ea}(\mathbf{P},t)+i\Omega_a(t)(\pi_{aa}(\mathbf{P},t)-\pi_{ee}(\mathbf{P},t))+i\Omega_b(t)\pi_{ba}(\mathbf{P},t)\\
\frac{d}{dt}\pi_{ae}(\mathbf{P},t) &= (-i\bar{\Delta}_{\mathbf{P}a}-\frac{\Gamma_{\perp a}}{2})\pi_{ae}(\mathbf{P},t)-i\Omega_a(\pi_{aa}(\mathbf{P},t)-\pi_{ee}(\mathbf{P},t))-i\Omega_b\pi_{ab}(\mathbf{P},t)\\
\frac{d}{dt}\pi_{eb}(\mathbf{P},t) &= (i\bar{\Delta}_{\mathbf{P}b}-\frac{\Gamma_{\perp b}}{2})\pi_{eb}(\mathbf{P},t)+i\Omega_b(t)(\pi_{bb}(\mathbf{P},t)-\pi_{ee}(\mathbf{P},t))+i\Omega_a(t)\pi_{ab}(\mathbf{P},t)\\
\frac{d}{dt}\pi_{be}(\mathbf{P},t) &= (-i\bar{\Delta}_{\mathbf{P}b}-\frac{\Gamma_{\perp b}}{2})\pi_{be}(\mathbf{P},t)-i\Omega_b(\pi_{bb}(\mathbf{P},t)-\pi_{ee}(\mathbf{P},t))-i\Omega_a\pi_{ba}(\mathbf{P},t)\\
\frac{d}{dt}\pi_{ab}(\mathbf{P},t) &= -\{i(\bar{\Delta}_{\mathbf{P}a}-\bar{\Delta}_{\mathbf{P}b})+\frac{1}{2}(\Gamma_a\overline{n}_a+\Gamma_b\overline{n}_b)\}\pi_{ab}(\mathbf{P},t)-i\Omega_b\pi_{ae}(\mathbf{P},t)+i\Omega_a\pi_{eb}(\mathbf{P},t)\\
\frac{d}{dt}\pi_{ba}(\mathbf{P},t) &= \{i(\bar{\Delta}_{\mathbf{P}a}-\bar{\Delta}_{\mathbf{P}b})-\frac{1}{2}(\Gamma_a\overline{n}_a+\Gamma_b\overline{n}_b)\}\pi_{ba}(\mathbf{P},t)+i\Omega_b\pi_{ea}(\mathbf{P},t)-i\Omega_a\pi_{be}(\mathbf{P},t)
\end{aligned}
$$

where the following density matrix elements are defined by averaging over the other two momentum dimensions:

$$
\begin{aligned}
\pi_{ee}(\mathbf{P},t) &\doteq \langle\mathbf{P},e|\hat{\rho}(t)|\mathbf{P},e\rangle=\rho_{ee}(\mathbf{P},t) \qquad (5.27)\\
\pi_{qq}(\mathbf{P},t) &\doteq \langle\mathbf{P}-\hbar\mathbf{k}_q,g_q|\hat{\rho}(t)|\mathbf{P}-\hbar\mathbf{k}_q,g_q\rangle=\rho_{qq}(\mathbf{P}-\hbar\mathbf{k}_q,t) \qquad (5.28)\\
\pi_{eq}(\mathbf{P},t) &\doteq \langle\mathbf{P},e|\hat{\rho}(t)|\mathbf{P}-\hbar\mathbf{k}_q,g_q\rangle=\rho_{eq}(\mathbf{P},\mathbf{P}-\hbar\mathbf{k}_q,t)e^{-i\bar{\Delta}_{\mathbf{P}q}t} \qquad (5.29)\\
\pi_{q'q}(\mathbf{P},t) &\doteq \langle\mathbf{P}-\hbar\mathbf{k}_{q'},g_{q'}|\hat{\rho}(t)|\mathbf{P}-\hbar\mathbf{k}_q,g_q\rangle e^{i\bar{\Delta}_{\mathbf{P}q't}}e^{-i\bar{\Delta}_{\mathbf{P}q}t} \qquad (5.30)\\
\pi_{ee}(\mathbf{P}-\hbar\mathbf{k}_q,t) &\doteq \int_{-\hbar k_o'}^{\hbar k_o'} d^3p' N_q(\mathbf{p}')\pi_{ee}\langle\mathbf{P}-\hbar\mathbf{k}_q+\mathbf{p}'). \qquad (5.31)\\
\Gamma_{tot} &\doteq \Gamma_a(\overline{n}_a+1)+\Gamma_b(\overline{n}_b+1) \qquad (5.32)\\
\Gamma_{\perp a,b} &\doteq \Gamma_{a,b}(2\overline{n}_{a,b}+1)+\Gamma_{b,a}(\overline{n}_{b,a}+1) \qquad (5.33)
\end{aligned}
$$

where $\rho_{ab}(\mathbf{P},\mathbf{P}',t)\doteq\langle\mathbf{P},a|\hat{\rho}(t)|\mathbf{P}',b\rangle$, with $q,q'\in a,b$ and $\bar{\Delta}_{\mathbf{P}q}=\Delta_q-\omega_{\mathbf{P}q}+\omega_{rq}$ is the effective detuning, $\Delta_q=k_qc-\omega_{eq}$ is the laser detuning, $\omega_{eq}=\frac{1}{\hbar}(E_e-E_q)$ is the internal energy levels spacing, $\omega_{\mathbf{P}q}=\frac{\mathbf{P}\cdot\mathbf{k}_q}{M}$ is the Doppler frequency, $\omega_{rq}=\frac{\hbar k_q^2}{2M}$ is the recoil frequency, $\Gamma_q\doteq C_q^2\Gamma$ with Γ the free-space spontaneous emission rate, and $\Omega_q=C_qdE_q$ the Rabi frequencies.

For the purpose of graphical computation, it is useful to define the density matrix elements $\pi_{ab}(P,t)$ along a particular momentum dimension P by averaging over the other

two (transverse) momentum dimensions $P_\perp$ through the definitions

$$\begin{aligned}
\pi_{ee}(P,t) &\doteq \int\int \langle P_\perp, P, e|\hat{\rho}(t)|P_\perp, P, e\rangle d^2P_\perp = \rho_{ee}(P,t) \\
\pi_{qq}(P,t) &\doteq \int\int \langle P_\perp, P-\hbar k_q, g_q|\hat{\rho}(t)|P_\perp, P-\hbar k_q, g_q\rangle d^2P_\perp = \rho_{qq}(P-\hbar k_q,t) \\
\pi_{eq}(P,t) &\doteq \int\int \langle P_\perp, P, e|\hat{\rho}(t)|P_\perp, P-\hbar k_q, g_q\rangle d^2P_\perp e^{i\omega_q t} = \rho_{eq}(P,P-\hbar k_q,t)e^{i\omega_q t} \\
\pi_{q'q}(P,t) &= \int\int \langle P_\perp, P-\hbar k_{q'}, g_{q'}|\hat{\rho}(t)|P_\perp, P-\hbar k_q, g_q\rangle d^2P_\perp e^{i(\omega_q-\omega_{q'})t} \\
&= \rho_{q'q}(P-\hbar k_{q'}, P-\hbar k_q, t)e^{i(\omega_q-\omega_{q'})t}
\end{aligned} \tag{5.34}$$

5.2.1 Analytical Solutions

Using the $P(t) = P(t_o)e^{L(t-t_o)} + \int_0^t A(t-\tau)e^{L\tau}d\tau$ as the formal solution of $\frac{d}{dt}P = LP + A$, we integrate Eqs. 5.26 for $\bar{n} = 0$. We use the identity $\int_0^\infty a(t-x)e^{\Delta x}dx = -\frac{1}{\Delta}[a(t) + \frac{da(t)}{dt}\frac{1}{\Delta} + \frac{d^2a(t)}{dt^2}\frac{1}{\Delta^2} + \frac{d^3a(t)}{dt^3}\frac{1}{\Delta^3}...]$ and keep the terms up to $\frac{1}{\Delta^2}$ and after lengthy calculations we have the excited-ground coherences

$$\begin{aligned}
\beta_a\pi_{ea} &= \pi_{ea}(P,0)e^{\mathcal{D}_a t} - \frac{1}{\mathcal{D}_a}\{i\Omega_a(t)f_a^a(t)(\pi_{aa}-\pi_{ee}) + i\Omega_b(t)f_a^b(t)\pi_{ba}\} \\
&\quad -\frac{1}{\mathcal{D}_a^2}\{2\Omega_a^2\pi_{ae} + i\Omega_a(2\Gamma_a+\Gamma_b)\pi_{ee} + \Omega_a\Omega_b(2\pi_{be}-\pi_{eb}) - \Omega_b(\bar{\Delta}_a-\bar{\Delta}_b)\pi_{ba}\}
\end{aligned} \tag{5.35}$$

$$\begin{aligned}
\beta_a^*\pi_{ae} &= \pi_{ae}(P,0)e^{\mathcal{D}_a^* t} - \frac{1}{\mathcal{D}_a^*}\{-i\Omega_a(t)f_a^{a*}(t)(\pi_{aa}-\pi_{ee}) - i\Omega_b(t)f_a^{b*}(t)\pi_{ab}\} \\
&\quad -\frac{1}{\mathcal{D}_a^{*2}}\{2\Omega_a^2\pi_{ea} - i\Omega_a(2\Gamma_a+\Gamma_b)\pi_{ee} + \Omega_a\Omega_b(2\pi_{eb}-\pi_{be}) - \Omega_b(\bar{\Delta}_a-\bar{\Delta}_b)\pi_{ab}\}
\end{aligned} \tag{5.36}$$

$$\begin{aligned}
\beta_b\pi_{eb} &= \pi_{eb}(P,0)e^{\mathcal{D}_b t} - \frac{1}{\mathcal{D}_b}\{i\Omega_b(t)f_b^b(t)(\pi_{bb}-\pi_{ee}) + i\Omega_a(t)f_b^a(t)\pi_{ab}\} \\
&\quad -\frac{1}{\mathcal{D}_b^2}\{2\Omega_b^2\pi_{be} + i\Omega_b(2\Gamma_b+\Gamma_a)\pi_{ee} + \Omega_b\Omega_a(2\pi_{ae}-\pi_{ea}) - \Omega_a(\bar{\Delta}_b-\bar{\Delta}_a)\pi_{ab}\}
\end{aligned} \tag{5.37}$$

$$\begin{aligned}
\beta_b^*\pi_{be} &= \pi_{be}(P,0)e^{\mathcal{D}_b^* t} - \frac{1}{\mathcal{D}_b^*}\{-i\Omega_b(t)f_b^{b*}(t)(\pi_{bb}-\pi_{ee}) - i\Omega_a(t)f_b^{a*}(t)\pi_{ba}\} \\
&\quad -\frac{1}{\mathcal{D}_b^{*2}}\{2\Omega_b^2\pi_{eb} - i\Omega_b(2\Gamma_b+\Gamma_a)\pi_{ee} + \Omega_b\Omega_a(2\pi_{ea}-\pi_{ae}) - \Omega_a(\bar{\Delta}_b-\bar{\Delta}_a)\pi_{ba}\}
\end{aligned} \tag{5.38}$$

and the ground-ground coherence

$$\pi_{ab} \simeq \frac{K^2\pi_{ab}(P,0)e^{-iKt}}{K^2+(\Omega_a^2+\Omega_b^2)} + \frac{(\Omega_a\pi_{eb}-\Omega_b\pi_{ae})(\bar{\Delta}_a-\bar{\Delta}_b)}{K^2+(\Omega_a^2+\Omega_b^2)} + \frac{\Omega_b\Omega_a(2\pi_{ee}-\pi_{aa}-\pi_{bb})}{K^2+(\Omega_a^2+\Omega_b^2)} + \frac{-i\Omega_b\pi_{ae}(\partial_b+\mathcal{D}_a^*)+i\Omega_a\pi_{eb}(\partial_a+\mathcal{D}_b)}{K^2+(\Omega_a^2+\Omega_b^2)} \quad (5.39)$$

with the definitions $f_{a,b}^{a,b}(t) \doteq (1+\frac{\partial_{a,b}}{\mathcal{D}_{a,b}}), \partial_{a,b}(t) \doteq \frac{1}{\Omega_{a,b}(t)}\frac{d\Omega_{a,b}(t)}{dt}, \beta_{a,b} \doteq (1-\frac{(2\Omega_{a,b}^2+\Omega_{b,a}^2)}{\mathcal{D}_{a,b}{}^2})$, $\mathcal{D}_{a,b} \doteq (i\bar{\Delta}_{a,b}-\frac{\Gamma_{\perp a,b}}{2})$ and $K \doteq (\bar{\Delta}_{\mathbf{P}a}-\bar{\Delta}_{\mathbf{P}b})-i\frac{1}{2}(\Gamma_a\overline{n}_a+\Gamma_b\overline{n}_b)$.

Large Detuning Condition

The above results are valid only when the detuning is sufficiently large to allow for the expansions in orders of $\frac{1}{\mathcal{D}}$ and the neglect of terms higher than $\frac{1}{\mathcal{D}^3}$. If the detuning is sufficiently large,

$$\frac{\Omega_{a,b}}{|\mathcal{D}_{a,b}|} < 1 \text{ or } \Omega_{a,b}^2 << \bar{\Delta}_{a,b}^2 + (\frac{\Gamma_{\perp a,b}}{2})^2 \quad (5.40)$$

we can even neglect all terms with $\frac{1}{\mathcal{D}^2}$ in the ground-excited coherences. The conditions also give $\beta_{a,b} \to 1$ and Eqs. 5.35-5.38 become

$$\begin{aligned}
\pi_{ea}(P,t) &= \pi_{ea}(P,0)e^{\mathcal{D}_a t} - \frac{1}{\mathcal{D}_a}\{i\Omega_a(t)f_a^a(t)(\pi_{aa}-\pi_{ee})+i\Omega_b(t)f_a^b(t)\pi_{ba}\} \\
\pi_{ae}(P,t) &= \pi_{ae}(P,0)e^{\mathcal{D}_a^* t} - \frac{1}{\mathcal{D}_a^*}\{-i\Omega_a(t)f_a^{a*}(t)(\pi_{aa}-\pi_{ee})-i\Omega_b(t)f_a^{b*}(t)\pi_{ab}\} \\
\pi_{eb}(P,t) &= \pi_{eb}(P,0)e^{\mathcal{D}_b t} - \frac{1}{\mathcal{D}_b}\{i\Omega_b(t)f_b^b(t)(\pi_{bb}-\pi_{ee})+i\Omega_a(t)f_b^a(t)\pi_{ab}\} \\
\pi_{be}(P,t) &= \pi_{be}(P,0)e^{\mathcal{D}_b^* t} - \frac{1}{\mathcal{D}_b^*}\{-i\Omega_b(t)f_b^{b*}(t)(\pi_{bb}-\pi_{ee})-i\Omega_a(t)f_b^{a*}(t)\pi_{ba}\} \quad (5.41)
\end{aligned}$$

Slow Pulse Evolution

For pulses, the time evolution of the Rabi frequencies can be represented by the Gaussian pulse-shape, $\Omega_{a,b} = \Omega_{a,b0}e^{-(t-t_{a,b0})^2/\sigma_{a,b}^2}$ which give the well-defined widths $\sigma_{a,b}$ and have $\partial_{a,b}(t) = -\frac{2(t-t_{a,b0})}{\sigma_{a,b}^2} \simeq \frac{4}{\sigma_{a,b}}$. If the pulse evolves sufficiently slow such that the pulse duration is much larger than the inverse of frequency detuning,

$$\frac{\partial_{a,b}}{|\mathcal{D}|} \sim \frac{4}{\bar{\Delta}\sigma_{a,b}} << 1 \quad (5.42)$$

we can set $f_{a,b}^{a,b}(t) \simeq 1$ in Eqs. 5.41. Assuming that there are no coherences initially, we obtain

$$\begin{aligned}
\pi_{ea}(P,t) &= -\frac{1}{\mathcal{D}_a}\{i\Omega_a(t)(\pi_{aa}-\pi_{ee})+i\Omega_b(t)\pi_{ba}\} \\
\pi_{ae}(P,t) &= -\frac{1}{\mathcal{D}_a^*}\{-i\Omega_a(t)(\pi_{aa}-\pi_{ee})-i\Omega_b(t)\pi_{ab}\} \\
\pi_{eb}(P,t) &= -\frac{1}{\mathcal{D}_b}\{i\Omega_b(t)(\pi_{bb}-\pi_{ee})+i\Omega_a(t)\pi_{ab}\} \\
\pi_{be}(P,t) &= -\frac{1}{\mathcal{D}_b^*}\{-i\Omega_b(t)(\pi_{bb}-\pi_{ee})-i\Omega_a(t)\pi_{ba}\} \qquad (5.43)
\end{aligned}$$

Now, we can eliminate the excited coherences $\pi_{ea}(P,t), \pi_{eb}(P,t)$ and their conjugates in Eqs. 5.26 using Eqs. 5.43. This gives the effective two-level equations

$$\begin{aligned}
\frac{d}{dt}\pi_{aa}(P,t) &= -i\Omega_a\{\frac{1}{\mathcal{D}_a^*}\{i\Omega_a(\pi_{aa}-\pi_{ee})+i\Omega_b\pi_{ab}\}+\frac{1}{\mathcal{D}_a}\{i\Omega_a(\pi_{aa}-\pi_{ee})+i\Omega_b\pi_{ba}\}\} \qquad (5.44)\\
\frac{d}{dt}\pi_{bb}(P,t) &= -i\Omega_b\{\frac{1}{\mathcal{D}_b^*}\{i\Omega_b(\pi_{bb}-\pi_{ee})+i\Omega_a\pi_{ba}\}+\frac{1}{\mathcal{D}_b}\{i\Omega_b(\pi_{bb}-\pi_{ee})+i\Omega_a\pi_{ab}\}\} \\
\frac{d}{dt}\pi_{ab}(P,t) &= -i(\bar{\Delta}_a-\bar{\Delta}_b)\pi_{ab}+\frac{1}{\mathcal{D}_a^*}\{\Omega_b\Omega_a(\pi_{aa}-\pi_{ee})+\Omega_b^2\pi_{ab}\}+\frac{1}{\mathcal{D}_b}\{\Omega_a\Omega_b(\pi_{bb}-\pi_{ee})+\Omega_a^2\pi_{ab}\} \\
\frac{d}{dt}\pi_{ba}(P,t) &= i(\bar{\Delta}_a-\bar{\Delta}_b)\pi_{ba}+\frac{1}{\mathcal{D}_a}\{\Omega_b\Omega_a(\pi_{aa}-\pi_{ee})+\Omega_b^2\pi_{ba}\}+\frac{1}{\mathcal{D}_b^*}\{\Omega_a\Omega_b(\pi_{bb}-\pi_{ee})+\Omega_a^2\pi_{ba}\}
\end{aligned}$$

Detuned out of Linewidth

For the detuning greater than the transverse linewidth

$$\bar{\Delta}_{a,b} > \frac{\Gamma_{\perp a,b}}{2} \qquad (5.45)$$

we can replace $\frac{1}{\mathcal{D}_{a,b}} \sim \frac{1}{i\bar{\Delta}_{a,b}}(1+\frac{\Gamma_{\perp a,b}}{2i\bar{\Delta}_{a,b}})$ in Eqs. 5.44. By defining the real parameters: $u=\pi_{ab}+\pi_{ba}$ $(dispersion)$, $v=-i(\pi_{ab}-\pi_{ba})$ $(absorption)$ and $w=\pi_{aa}-\pi_{bb}(inversion)$, first introduced by Feynman, Vernon and Hellwarth [223] for a two level system, Eqs. 5.44 can be rewritten as

$$\begin{aligned}
\frac{d}{dt}u &= \bar{\Delta}_{eff}v-(\frac{\Gamma_{\perp a}\Omega_b^2}{2\bar{\Delta}_a^2}+\frac{\Gamma_{\perp b}\Omega_a^2}{2\bar{\Delta}_b^2})u-\Omega_b\Omega_a\{\frac{\Gamma_{\perp a}}{\bar{\Delta}_a^2}(\pi_{aa}-\pi_{ee})+\frac{\Gamma_{\perp b}}{\bar{\Delta}_b^2}(\pi_{bb}-\pi_{ee})\} \qquad (5.46)\\
\frac{d}{dt}v &= -(\frac{\Gamma_{\perp a}\Omega_b^2}{2\bar{\Delta}_a^2}+\frac{\Gamma_{\perp b}\Omega_a^2}{2\bar{\Delta}_b^2})v-\bar{\Delta}_{eff}u+\Omega_b\Omega_a\{\frac{2}{\bar{\Delta}_a}(\pi_{aa}-\pi_{ee})-\frac{2}{\bar{\Delta}_b}(\pi_{bb}-\pi_{ee})\} \qquad (5.47)\\
\frac{d}{dt}w &= -(\frac{\Gamma_{\perp a}}{2\bar{\Delta}_a^2}-\frac{\Gamma_{\perp b}}{2\bar{\Delta}_b^2})\Omega_a\Omega_b u-\Omega_{eff}v-\frac{\Gamma_{\perp a}\Omega_a^2}{\bar{\Delta}_a^2}(\pi_{aa}-\pi_{ee})+\frac{\Gamma_{\perp b}\Omega_b^2}{\bar{\Delta}_b^2}(\pi_{bb}-\pi_{ee}) \qquad (5.48)\\
\frac{d}{dt}f &= -(\frac{\Gamma_{\perp a}}{2\bar{\Delta}_a^2}+\frac{\Gamma_{\perp b}}{2\bar{\Delta}_b^2})\Omega_a\Omega_b u-Rv-\frac{\Gamma_{\perp a}\Omega_a^2}{\bar{\Delta}_a^2}(\pi_{aa}-\pi_{ee})-\frac{\Gamma_{\perp b}\Omega_b^2}{\bar{\Delta}_b^2}(\pi_{bb}-\pi_{ee}) \qquad (5.49)
\end{aligned}$$

where

$$\bar{\Delta}_{eff} \doteq \bar{\Delta}_a - \bar{\Delta}_b + \frac{\Omega_a^2}{\bar{\Delta}_b} - \frac{\Omega_b^2}{\bar{\Delta}_a} \text{ the Stark-shifted two-photon detuning} \quad (5.50)$$

$$\Omega_{eff} \doteq \Omega_b\Omega_a\{\frac{1}{\bar{\Delta}_a} + \frac{1}{\bar{\Delta}_b}\} \text{ the effective Rabi frequency} \quad (5.51)$$

$$R \doteq \Omega_b\Omega_a\{\frac{1}{\bar{\Delta}_a} - \frac{1}{\bar{\Delta}_b}\} \quad (5.52)$$

Elimination of Excited State

The excited state population can be expressed up to second order in $\frac{1}{\Gamma_{tot}^2}$ using the first of Eqs. 5.26

$$\begin{aligned}\pi_{ee}(P,t) &= \pi_{ee}(P,0)e^{-\Gamma_{tot}t} + \frac{1}{\Gamma_{tot}}\{i\Omega_a\{\pi_{ae} - \pi_{ea}\} + i\Omega_b\{\pi_{be} - \pi_{eb}\}\} \\ &-\frac{1}{\Gamma_{tot}^2}\{i\Omega_a(\partial_a - i\bar{\Delta}_a - \frac{\Gamma_{\perp a}}{2})\pi_{ae} - i\Omega_a(\partial_a + i\bar{\Delta}_a - \frac{\Gamma_{\perp a}}{2})\pi_{ea}\} \\ &-\frac{1}{\Gamma_{tot}^2}\{i\Omega_b(\partial_b - i\bar{\Delta}_b - \frac{\Gamma_{\perp b}}{2})\pi_{be} - i\Omega_b(\partial_b + i\bar{\Delta}_a - \frac{\Gamma_{\perp b}}{2})\pi_{eb}\} \\ &-\frac{1}{\Gamma_{tot}^2}\{2\Omega_a^2\pi_{aa} + 2\Omega_b^2\pi_{bb} - 2(\Omega_a^2 + \Omega_b^2)\pi_{ee} - 2i\Omega_a i\Omega_b(\pi_{ba} + \pi_{ab})\} \quad (5.53)\end{aligned}$$

By using the following relations,

$$\pi_{ea} + \pi_{ae} = (\frac{1}{\mathcal{D}_a^*} - \frac{1}{\mathcal{D}_a})i\Omega_a(t)(\pi_{aa} - \pi_{ee}) + i\Omega_b(t)(\frac{1}{\mathcal{D}_a^*}\pi_{ab} - \frac{1}{\mathcal{D}_a}\pi_{ba}) \quad (5.54)$$

$$i(\pi_{ae} - \pi_{ea}) = -(\frac{1}{\mathcal{D}_a^*} + \frac{1}{\mathcal{D}_a})\Omega_a(t)(\pi_{aa} - \pi_{ee}) - \Omega_b(t)(\frac{1}{\mathcal{D}_a^*}\pi_{ab} + \frac{1}{\mathcal{D}_a}\pi_{ba}) \quad (5.55)$$

$$\frac{1}{\mathcal{D}_a^*} \pm \frac{1}{\mathcal{D}_b} \sim i(\frac{1}{\bar{\Delta}_a} \mp \frac{1}{\bar{\Delta}_b}) - (\frac{\Gamma_{\perp a}}{2\bar{\Delta}_a^2} \pm \frac{\Gamma_{\perp b}}{2\bar{\Delta}_b^2}) \quad (5.56)$$

we find that the terms with $\frac{1}{\Gamma_{tot}^2}$ in π_{ee} (Eq. 5.53) are at most in the order of $\frac{\Omega^2}{\Gamma^2}$. Thus, we can neglect the terms with $\frac{1}{\Gamma_{tot}^2}$ in Eq. 5.53 if the Rabi frequency is lower than the linewidth,

$$\Omega_{a,b} < \Gamma \quad (5.57)$$

By using Eqs. 5.54 and 5.55, Eq. 5.53 reduces to

$$\pi_{ee}(1 + (\tau_a - \tau_b)) \sim \pi_{ee}(P,0)e^{-\Gamma_{tot}t} + \tau_a\pi_{aa} - \tau_b\pi_{bb} - \frac{\Omega_a\Omega_b}{\Gamma_{tot}}\{\pi_{ab}(\frac{1}{\mathcal{D}_a^*} + \frac{1}{\mathcal{D}_b}) + \pi_{ba}(\frac{1}{\mathcal{D}_a} + \frac{1}{\mathcal{D}_b^*})\} \quad (5.58)$$

where $\tau_{a,b} \doteq \frac{\Gamma_{\perp a,b}}{\Gamma_{tot}} \frac{\Omega_{a,b}^2}{\bar{\Delta}_{a,b}^2}$. The low intensity or large detuning condition of Eq. 5.40 also allows us to neglect $\tau_{a,b}$. Finally, we use Eq. 5.56 to rewrite Eq. 5.58 as

$$\pi_{ee} \sim \pi_{ee}(P,0)e^{-\Gamma_{tot}t} - \frac{\Omega_a\Omega_b}{\Gamma_{tot}}\{(\frac{1}{\bar{\Delta}_b} - \frac{1}{\bar{\Delta}_a})v - (\frac{\Gamma_{\perp a}}{2\bar{\Delta}_a^2} + \frac{\Gamma_{\perp b}}{2\bar{\Delta}_b^2})u\} \tag{5.59}$$

If the one-photon detuning $\bar{\Delta}_{a,b}$ is much greater than the two-photon detuning $\bar{\Delta}_b - \bar{\Delta}_a$, we can set $\frac{1}{\bar{\Delta}_b} - \frac{1}{\bar{\Delta}_a} \sim 0$. The coefficient for u in Eq. 5.59 is in the order $\sim \frac{\Omega_a\Omega_b}{\bar{\Delta}_{a,b}^2}$. Thus, the condition of Eq. 5.40 gives $\pi_{ee}(P,0) \sim \pi_{ee}(P,0)e^{-\Gamma_{tot}t}$. If the excited state is initially unpopulated, it will be essentially unpopulated at later times when the conditions $\Omega_{a,b} < \bar{\Delta}_{a,b}, \Omega_{a,b} < \Gamma < \bar{\Delta}_{a,b}$ are met. Thus, we can write $\pi_{aa} + \pi_{bb} \approx f$,and Eqs. 5.46-5.49 become

$$\begin{aligned}
\frac{d}{dt}u &= -(\frac{\Gamma_{\perp a}\Omega_b^2}{2\bar{\Delta}_a^2} + \frac{\Gamma_{\perp b}\Omega_a^2}{2\bar{\Delta}_b^2})u + \bar{\Delta}_{eff}v - \frac{\Omega_b\Omega_a}{2}(\frac{\Gamma_{\perp a}}{\bar{\Delta}_a^2} + \frac{\Gamma_{\perp b}}{\bar{\Delta}_b^2})f - \frac{\Omega_b\Omega_a}{2}(\frac{\Gamma_{\perp a}}{\bar{\Delta}_a^2} - \frac{\Gamma_{\perp b}}{\bar{\Delta}_b^2})w \\
\frac{d}{dt}v &= -\bar{\Delta}_{eff}u - (\frac{\Gamma_{\perp a}\Omega_b^2}{2\bar{\Delta}_a^2} + \frac{\Gamma_{\perp b}\Omega_a^2}{2\bar{\Delta}_b^2})v + Rf + \Omega_{eff}w \\
\frac{d}{dt}w &= (\frac{\Gamma_{\perp b}}{2\bar{\Delta}_b^2} - \frac{\Gamma_{\perp a}}{2\bar{\Delta}_a^2})\Omega_a\Omega_b u - \Omega_{eff}v - (\frac{\Gamma_{\perp a}\Omega_a^2}{2\bar{\Delta}_a^2} - \frac{\Gamma_{\perp b}\Omega_b^2}{2\bar{\Delta}_b^2})f - (\frac{\Gamma_{\perp a}\Omega_a^2}{2\bar{\Delta}_a^2} + \frac{\Gamma_{\perp b}\Omega_b^2}{2\bar{\Delta}_b^2})w \\
\frac{d}{dt}f &= -(\frac{\Gamma_{\perp a}}{2\bar{\Delta}_a^2} + \frac{\Gamma_{\perp b}}{2\bar{\Delta}_b^2})\Omega_a\Omega_b u - Rv - (\frac{\Gamma_{\perp a}\Omega_a^2}{2\bar{\Delta}_a^2} + \frac{\Gamma_{\perp b}\Omega_b^2}{2\bar{\Delta}_b^2})f - (\frac{\Gamma_{\perp a}\Omega_a^2}{2\bar{\Delta}_a^2} - \frac{\Gamma_{\perp b}\Omega_b^2}{2\bar{\Delta}_b^2})w
\end{aligned} \tag{5.60}$$

For symmetric system where $\Gamma_{\perp b} = \Gamma_{\perp a}$, Eqs. 5.60 reduce to

$$\begin{aligned}
\frac{d}{dt}u &= -\frac{\Gamma_\perp}{2}\chi_+ u + \bar{\Delta}_{eff}v - \frac{\Gamma_\perp}{2}d_+\Omega_b\Omega_a f - \frac{\Gamma_\perp}{2}d_-\Omega_b\Omega_a w \\
\frac{d}{dt}v &= -\bar{\Delta}_{eff}u - \frac{\Gamma_\perp}{2}\chi_+ v + Rf + \Omega_{eff}w \\
\frac{d}{dt}w &= -\frac{\Gamma_\perp}{2}d_-\Omega_a\Omega_b u - \Omega_{eff}v - \frac{\Gamma_\perp}{2}\pi_- f - \frac{\Gamma_\perp}{2}\pi_+ w \\
\frac{d}{dt}f &= -\frac{\Gamma_\perp}{2}d_+\Omega_a\Omega_b u - Rv - \frac{\Gamma_\perp}{2}\pi_+ f - \frac{\Gamma_\perp}{2}\pi_- w
\end{aligned} \tag{5.61}$$

where we define $\chi_\pm = \frac{\Omega_b^2}{\bar{\Delta}_a^2} \pm \frac{\Omega_a^2}{\bar{\Delta}_b^2}, \pi_\pm = \frac{\Omega_a^2}{\bar{\Delta}_a^2} \pm \frac{\Omega_b^2}{\bar{\Delta}_b^2}, d_\pm = \frac{1}{\bar{\Delta}_a^2} \pm \frac{1}{\bar{\Delta}_b^2}$. Equations 5.61 are grossly dependent on the decay rate $\Gamma_\perp$.

Near two-photon detuning

For close to two-photon detuning $\bar{\Delta}_a \sim \bar{\Delta}_b$ we have $\chi_\pm \sim \pi_\pm \sim \frac{\Omega_b^2}{\bar{\Delta}^2} \pm \frac{\Omega_a^2}{\bar{\Delta}^2}, R \to 0, \bar{\Delta}_{eff} \to \frac{\Omega_a^2 - \Omega_b^2}{\bar{\Delta}}, \Omega_{eff} \to \Omega_b\Omega_a\frac{2}{\bar{\Delta}}$. The required condition to neglect the terms which

contain $\Gamma_\perp$ in Eqs. 5.61 is $\Gamma_\perp << \bar{\Delta}\frac{\Omega_a\Omega_b}{\Omega^2_{a,b}}$ which is the previously imposed condition Eq. 5.45. So, Eqs. 5.61 reduce to

$$\begin{aligned}
\frac{d}{dt}u &= \bar{\Delta}_{eff}v \\
\frac{d}{dt}v &= -\bar{\Delta}_{eff}u + Rf + \Omega_{eff}w \\
\frac{d}{dt}w &= -\Omega_{eff}v \\
\frac{d}{dt}f &= -Rv
\end{aligned} \tag{5.62}$$

Bloch vector equation

In general, $\Omega_{a,b}(t)$ are time dependent while $\bar{\Delta}(P)$ is momentum dependent, so Ω_{eff} and $\bar{\Delta}_{eff}$ depend on both P and t; and the Bloch vector equations cannot be solved analytically by Laplace transform. For close to two-photon detuning $R \doteq \Omega_b\Omega_a\{\frac{1}{\bar{\Delta}_a} - \frac{1}{\bar{\Delta}_b}\} \rightarrow 0$ and Eqs. 5.62 can be written in the well-known Bloch vector equation

$$\frac{d}{dt}\mathbf{S} = \mathbf{T} \times \mathbf{S} \tag{5.63}$$

where $\mathbf{S} \doteq (u, v, w)$ is the Bloch vector, and $\mathbf{T} \doteq (-\Omega_{eff}, 0, -\bar{\Delta}_{eff})$ is the 'angular momentum' associated to the precession of the Bloch vector. Equation 5.63 gives simple geometrical picture in analogy to the two-level system. Complete inversion can occur under either one of the two circumstances:

a)First, $\tan\Theta = (\Omega_{eff}/\bar{\Delta}_{eff}) = \frac{2\Omega_b\Omega_a}{\Omega_a^2 - \Omega_b^2}$ changes adiabatically from $\bar{\Delta}_{eff}/\Omega_{eff} \rightarrow +\infty$ at $t = 0$ to $\bar{\Delta}_{eff}/\Omega_{eff} \rightarrow -\infty$ at $t \rightarrow \infty$. Here, adiabaticity means that $\frac{d}{dt}\Theta << |\mathbf{T}|$ which gives

$$\bar{\Delta}_{eff}\frac{d\bar{\Delta}_{eff}}{dt} - \Omega_{eff}\frac{d\Omega_{eff}}{dt} << \frac{(\Omega^2_{eff} + \bar{\Delta}^2_{eff})^{3/2}}{\Omega_{eff}\bar{\Delta}_{eff}} \tag{5.64}$$

This principle was first noted by Oreg, Hioe and Eberly [263] and later coined the name *STIRAP (Stimulated Raman Adiabatic Passage)* [285] where it was found that complete inversion can also occur when the detuning is small (close to one-photon resonance).

b)Second, is the π-pulse condition. When $\bar{\Delta}_a = \bar{\Delta}_b$ and $\Omega_a = \Omega_b$, we have zero effective detuning, $\bar{\Delta}_{eff} = 0$ with $R = 0$ and $\Omega_{eff} = 2\Omega^2(t)/\bar{\Delta}$. The $\mathbf{T}$ vector remains orthogonal to w-axis and does not change direction. For complete inversion, the Bloch vector $\mathbf{S}$ would need to rotate by π around $\mathbf{T}$. From Eq. 5.62 the inversion satisfies the differential equation

$$\frac{d^2w}{dt^2} = \frac{ds}{dt}\frac{dw}{dt} - \Omega^2_{eff}w \tag{5.65}$$

where $s \doteq \ln \Omega_{eff}$, $\frac{ds}{dt} = \frac{1}{\Omega_{eff}} \frac{d\Omega_{eff}}{dt}$ which has the general solution

$$w(t) = w(0) \cos(\int_0^t \frac{2\Omega^2(t')}{\bar{\Delta}} dt') \tag{5.66}$$

It is clear that complete inversion occurs when $\int_0^\tau \frac{2\Omega^2(t')}{\bar{\Delta}} dt' = \pi$, in agreement with the geometrical picture of Eq. 5.63. These conditions are the basis for *Raman velocity selection.*

5.2.2 Exact Solutions for Continuous Wave Lasers

For continuous wave laser we can assume a time independent Rabi frequencies $\Omega_{a,b}$, and Eq. 5.62 can be solved exactly by Laplace transform

$$\begin{pmatrix} u \\ v \\ w \\ f \end{pmatrix} = \begin{pmatrix} 1 - \frac{\bar{\Delta}_{eff}^2(1-\cos At)}{A^2} & \frac{\bar{\Delta}_{eff}}{A} \sin At & \frac{\bar{\Delta}_{eff}\Omega_{eff}(1-\cos At)}{A^2} & \frac{\bar{\Delta}_{eff}R(1-\cos At)}{A^2} \\ -\frac{\bar{\Delta}_{eff}}{A} \sin At & \cos At & \frac{\Omega_{eff}}{A} \sin At & \frac{R}{A} \sin At \\ \frac{\bar{\Delta}_{eff}\Omega_{eff}(1-\cos At)}{A^2} & -\frac{\Omega_{eff}}{A} \sin At & 1 - \frac{\Omega_{eff}^2(1-\cos At)}{A^2} & -\frac{\Omega_{eff}R(1-\cos At)}{A^2} \\ \frac{\bar{\Delta}_{eff}R(1-\cos At)}{A^2} & -\frac{R}{A} \sin At & -\frac{\Omega_{eff}R(1-\cos At)}{A^2} & 1 - \frac{R^2(1-\cos At)}{A^2} \end{pmatrix} \begin{pmatrix} u_o \\ v_o \\ w_o \\ f_o \end{pmatrix} \tag{5.67}$$

where $\bar{\Delta}_{eff}, \Omega_{eff}$ and R are defined by Eqs. 5.50-5.52 and

$$A^2 \doteq \bar{\Delta}_{eff}^2 + R^2 + \Omega_{eff}^2 \tag{5.68}$$

If we use the initial conditions $u_o(P) = v_o(P) = 0, w_o(P) = f_o(P) = \pi_{aa}(P,0)$ we find

$$u(P,t) = w_o \frac{(\bar{\Delta}_a - \bar{\Delta}_b + \frac{\Omega_a^2}{\bar{\Delta}_b} - \frac{\Omega_b^2}{\bar{\Delta}_a})}{A^2} \frac{2\Omega_b\Omega_a}{\bar{\Delta}_a} (1 - \cos At) \tag{5.69}$$

$$v(P,t) = w_o \frac{2\Omega_b\Omega_a}{\bar{\Delta}_a A} \sin At \tag{5.70}$$

$$w(P,t) = w_o \left(1 - \frac{1}{A^2} \frac{2\Omega_b^2\Omega_a^2}{\bar{\Delta}_a} (\frac{1}{\bar{\Delta}_a} + \frac{1}{\bar{\Delta}_b}) (1 - \cos At)\right) \tag{5.71}$$

$$f(P,t) = w_o \left(1 - \frac{1}{A^2} \frac{2\Omega_b^2\Omega_a^2}{\bar{\Delta}_a} (\frac{1}{\bar{\Delta}_a} - \frac{1}{\bar{\Delta}_b}) (1 - \cos At)\right) \tag{5.72}$$

Equations 5.71 and 5.72 give the results of Ref. [314] (Eq. 21) at two-photon resonance:

$$\pi_{aa}(P,t) = \pi_{aa}(P,0) \left(1 - \frac{1}{A^2} \frac{2\Omega_b^2\Omega_a^2}{\bar{\Delta}_a^2} (1 - \cos At)\right) \tag{5.73}$$

$$\pi_{bb}(P,t) = \pi_{aa}(P,0) \frac{4\Omega_b^2\Omega_a^2}{\bar{\Delta}_a\bar{\Delta}_b A^2} \sin^2 \frac{1}{2} At \tag{5.74}$$

These equations will be used for deriving the relationship between pulse duration, Rabi frequency and selected momentum width.

5.3 Analytical Light Force for Λ System

The evaluation of the light force acting on the particles is useful as it shows how the kinetic effect of light can be used to reduce the kinetic energy of the particles and also gives the order of magnitude for deceleration.

By taking the spatial gradient the interaction potential, Eq. 5.108 gives

$$\nabla \hat{V}^i_{SL}(\hat{\mathbf{R}},t) = -\hbar \sum_{q=a,b} \{\nabla\Omega_q(\mathbf{R},t) + i\mathbf{k}_q\Omega_q(\mathbf{R},t)\}\{|e\rangle\langle q|\hat{\pi}_q e^{-i\Delta_q t} + |q\rangle\langle e|\hat{\pi}^\dagger_q e^{i\Delta_q t}\} \quad (5.75)$$

and tracing over the internal and radiation states with projection onto $|\mathbf{P}\rangle\langle\mathbf{P}|$, we have the *light force density* $\mathbf{F}(\mathbf{P},t) \doteq -\langle|\mathbf{P}\rangle\langle\mathbf{P}|\nabla\hat{V}^i_{SL}\rangle$ on a particle with momentum $\mathbf{P}$ at time t which can be decomposed into the *gradient force* $\mathbf{F}(\mathbf{P},t)_{grad}$ and the *reactive force* $\mathbf{F}(\mathbf{P},t)_{reac}$

$$\mathbf{F}(\mathbf{P},t) = \hbar \sum_{q=a,b} (\nabla\Omega_q(\mathbf{R},t) + i\mathbf{k}_q\Omega_q(\mathbf{R},t))\rho_{qe}(\mathbf{P},t)e^{-i\bar{\Delta}_{q\mathbf{P}}t} + c.c. \quad (5.76)$$

$$\mathbf{F}(\mathbf{P},t)_{grad} = \hbar \sum_{q=a,b} \nabla\Omega_q\{\pi_{qe}(\mathbf{P},t) + \pi_{eq}(\mathbf{P},t)\} \quad (5.77)$$

$$\mathbf{F}(\mathbf{P},t)_{reac} = \hbar \sum_{q=a,b} \mathbf{k}_q\Omega_q i\{\pi_{qe}(\mathbf{P},t) - \pi_{eq}(\mathbf{P},t)\} \quad (5.78)$$

where $\pi_{qe}(\mathbf{P},t) \doteq \rho_{qe}(\mathbf{P}-\hbar\mathbf{k}_q,\mathbf{P},t)e^{-i\bar{\Delta}_{q\mathbf{P}}t}$ and $\rho_{qe}(\mathbf{P}-\hbar\mathbf{k}_q,\mathbf{P},t) \doteq \langle\mathbf{P}-\hbar\mathbf{k}_q,g_q|\hat{\rho}(t)|\mathbf{P},e\rangle$. The variable $\mathbf{R}$ in Ω_q has been assumed as a c-number instead of an operator. If it is quantized, it gives additional kinetic effect to the particle interaction. Equation 5.76 follows from Eq. 5.2 with the dissipative part being neglected for velocity selection and STIRAP processes.

The gradient force $\mathbf{F}(\mathbf{P},t)_{grad}$ is proportional to the spatial gradient of the Rabi frequencies and the dispersion u parameter. The Rabi frequency Ω_q contains the position dependence through two parameters; the electric field and the polarization (in the case of more than one laser) as shown in Appendix I (Eq. 8.13). This is also shown in Ref. [58]. The spatial gradient in the polarization gives the *polarization gradient force* behind the polarization gradient cooling. The electric field gradient gives the so-called *dipole force* used for trapping of atoms in the large detuning regime [93]. Although it has a shallow trap depth (around mK), the dipole trap can provide a large trapping force and has been used to increase the density of the trapped atoms [102]. The dipole potential can be varied for evaporative cooling and has been used to obtain the all-optical BEC [13]. Laser deflections of atomic beam [84], channeling [82] and dispersion [79] of atoms through a standing wave and the optical Stern-Gerlach effect [81] are also due to the dipole force. The superpositions of laser fields create the optical lattice which has periodic variations of light intensity, has been used for coherent acceleration of BEC [214] and for cooling towards BEC[213].

The reactive force $\mathbf{F}(\mathbf{P},t)_{reac}$ is proportional to the absorption parameter v. For discrete momentum points, the light force on a particle with momentum $\mathbf{P}$ can be computed

as $\mathbf{F}(\mathbf{P},t) = \mathbf{f}(\mathbf{P},t)\Delta^3 P$ where $\Delta^3 P$ is the discretized volume of each momentum point. Thus, the momentum averaged force is obtain by integration $\mathbf{F}(t) = \int \mathbf{f}(\mathbf{P},t)d^3P$.

The time and momentum dependent dipole force, Eq. 5.76 can be computed analytically from Eqs. 5.43 for $|\bar{\Delta}_{a,b}| >> \frac{\Gamma_{\perp a,b}}{2}$ and $\pi_{ee} \simeq 0$

$$\begin{aligned}\mathbf{F}(\mathbf{P},t)_{grad} &= \hbar\nabla\Omega_a\{-\frac{2\Omega_a}{\bar{\Delta}_a}(\pi_{aa}-\pi_{ee}) - \frac{\Omega_b}{\bar{\Delta}_a}u\} + \hbar\nabla\Omega_b\{-\frac{2\Omega_b}{\bar{\Delta}_b}(\pi_{bb}-\pi_{ee}) - \frac{\Omega_a}{\bar{\Delta}_b}u\} \\ &\simeq -\hbar(\frac{\nabla\Omega_a^2}{\bar{\Delta}_a} + \frac{\nabla\Omega_b^2}{\bar{\Delta}_b})f(\mathbf{P},t) - \hbar(\frac{\Omega_b\nabla\Omega_a}{\bar{\Delta}_a} + \frac{\Omega_a\nabla\Omega_b}{\bar{\Delta}_b})u(\mathbf{P},t) \qquad (5.79)\end{aligned}$$

Similarly, the analytical reactive force is

$$\mathbf{F}(\mathbf{P},t)_{reac} = \hbar\Omega_a(t)\Omega_b(t)v(\mathbf{P},t)(\frac{\mathbf{k}_a}{\bar{\Delta}_a} - \frac{\mathbf{k}_b}{\bar{\Delta}_b}) \qquad (5.80)$$

Equation 5.80 shows that there is a finite force from the reactive part even for spatially homogeneous lasers. It provides the deceleration/acceleration force as the result of recoil due to photon absorption/emission. The force is largest when both lasers are counter propagating and smallest when the are co-propagating. For time independent (continuous wave) laser fields, we can replace $v(\mathbf{P},t)$ with the analytical expression of Eq. 5.70 for homogeneous fields, and obtain

$$\mathbf{F}(\mathbf{P},t)_{reac} = \hbar w(\mathbf{P},0)\frac{2\Omega_b^2\Omega_a^2}{\bar{\Delta}_a}\frac{\sin At}{A}(\frac{\mathbf{k}_a}{\bar{\Delta}_a} - \frac{\mathbf{k}_b}{\bar{\Delta}_b}) \qquad (5.81)$$

From Eq. 5.81, the time-averaged force is zero. However, if the direction of $(\frac{\mathbf{k}_a}{\bar{\Delta}_a} - \frac{\mathbf{k}_b}{\bar{\Delta}_b})$ is reversed every period of π/A the force would be rectified. This is the basis for providing continuous deceleration using repeated processes of STIRAP (discussed in Section 5.6.4).

5.4 Pure Internal State for Population Transfer

We show a method to prepare the population in a single internal state. The population in a single state will be used as the initial state for the population transfer techniques in the laser cooling scheme described in Chapter 6. At around $1K$, the level $J = 1$ is highly occupied. It is possible to filtered out the gas in a single rotational level but occupies several magnetic substates. We can use σ^+ and σ^- polarized lasers to pump the populations in states $M = \pm 1$ to $M = 0$ (Fig. 5.2a). If both lasers are switched on simultaneously, the results are shown by the simulated results from four-states Bloch equations (Fig. 5.2b), the creation of partial dark state causes only half instead of all of the total population being transferred to state $M = 0$. The dark state does not absorb the laser photon and cannot be excited but remain in the dark state. It is due to the quantum interference and closely related to the electromagnetic induced transparency (EIT)

[105], [107] and lasing without inversion (LWI) [106]. When σ^+ and σ^- are switched on alternatingly instead of simultaneously, all populations are essentially pumped into $M = 0$ as shown in Fig. 5.2c.

5.5 Raman Velocity Selection

In this section, we use the above results to describe the optimal conditions required to perform a narrow velocity selection from a gas initially in a single quantum state. We designate laser a as the *pump laser* and laser b as the *Stokes laser*, so we wish to transfer the population initially in state $|a\rangle$ to $|b\rangle$.

5.5.1 Two-photon Raman Resonance

For *selected momentum* $P = P_{vs}$ which satisfies the *two-photon Raman resonance* condition

$$\bar{\Delta}_a(P_{vs}) = \bar{\Delta}_b(P_{vs}) = \bar{\Delta}_{vs} \tag{5.82}$$

Eqs. 5.69-5.72 become

$$\begin{aligned} u(P_{vs},t) &= \pi_{aa}(P_{vs},0)\frac{\Omega_a^2-\Omega_b^2}{(\Omega_a^2+\Omega_b^2)^2}2\Omega_b\Omega_a\left(1-\cos A_{vs}t\right) \\ v(P_{vs},t) &= \pi_{aa}(P_{vs},0)\frac{2\Omega_b\Omega_a}{\Omega_a^2+\Omega_b^2}\sin A_{vs}t \\ w(P_{vs},t) &= \pi_{aa}(P_{vs},0)\left(1-(\frac{2\Omega_b\Omega_a}{\Omega_a^2+\Omega_b^2})^2\left(1-\cos A_{vs}t\right)\right) \\ f(P_{vs},t) &= \pi_{aa}(P_{vs},0) \end{aligned} \tag{5.83}$$

where $A_{vs}^2 \doteq \frac{1}{\bar{\Delta}_{vs}^2}(\Omega_a^2+\Omega_b^2)^2$. The two-photon Raman resonance condition gives the general formula

$$(k_a-k_b)c + \tfrac{P_{vs}}{M}(-k_a\cos\theta_a + k_b\cos\theta_b) + \tfrac{\hbar}{2M}(k_a+k_b)(k_a-k_b) = \omega_{ea}-\omega_{eb} \tag{5.84}$$

where P_{vs} is the magnitude of the resonant (or velocity selected) momentum, $\theta_{a,b}$ are the angles between lasers a, b and the momentum direction of the particle momentum and $\omega_{ea,b}$ are the energy separations between states $|a\rangle$ and $|b\rangle$ and the excited state $|e\rangle$.

The two photon detuning for arbitrary momentum $\mathbf{P}$ can be written as

$$\bar{\Delta}_a(\mathbf{P}) - \bar{\Delta}_b(\mathbf{P}) = (\mathbf{P}_{vs}-\mathbf{P})\cdot(\mathbf{k}_a-\mathbf{k}_b)/M \tag{5.85}$$

where we have used $\Delta_a - \omega_{\mathbf{P}_{vs}a} + \omega_{ra} - \Delta_b + \omega_{\mathbf{P}_{vs}b} - \omega_{rb} = 0$, the Raman resonance for $\mathbf{P}_{vs}$.

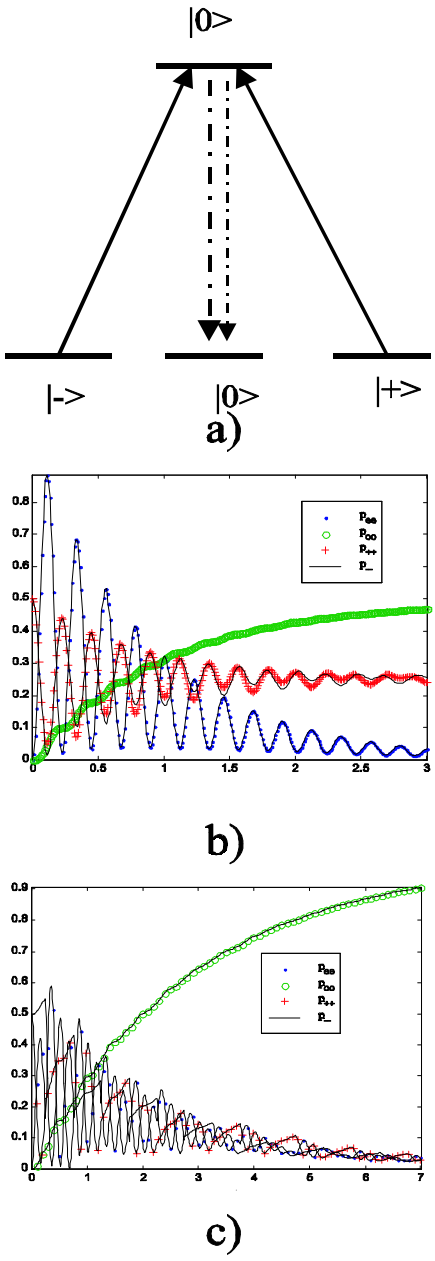

Figure 5.2: Pumping from three degenerate states to a single state in a rotational level. a)Diagram of the four-state pumping scheme. Time evolution of populations for b) simultaneous pumping and c)alternative pumping with σ^+ and σ^- polarized lasers.

For co-propagating lasers($\theta_a = \theta_b$)

$$c - \frac{P_{vs}}{M}\cos\theta + \frac{\hbar}{2M}(k_a + k_b) = \frac{\omega_{ea} - \omega_{eb}}{k_a - k_b} \tag{5.86}$$

We "proof by contradiction" that Raman resonance cannot occur if the Stokes and pump wavevectors are parallel and the two Raman ground levels are degenerate (symmetric Λ scheme), $\omega_{ea} = \omega_{eb}$. In this case, Eq. 5.86 becomes $\cos\theta = \frac{\hbar}{2P_{vs}}(k_a + k_b) + \frac{Mc}{P_{vs}} >> 1$ which contradicts with $-1 \leq \cos\theta \leq 1$ since the momentum is typically nonrelativistic, $P_{vs} << Mc$. If the Raman states are nondegenerate, $\omega_{ea} \neq \omega_{eb}$, the Raman condition may occur if only if $-1 \leq \{\cos\theta = \frac{\hbar}{2P_{vs}}(k_a + k_b) + \frac{M}{P_{vs}}(c - \frac{(\omega_{ea}-\omega_{eb})}{(k_a-k_b)})\} \leq 1$. This is possible if $\omega_{ea,b} = ck_{a,c}$ and $\frac{\hbar}{2P_{vs}}(k_a + k_b) \leq P_{vs}$.

The momentum recoil is along the pump laser direction during absorption but opposite to the Stoke laser direction during stimulated emission. Therefore, co-propagating Raman lasers do not impart appreciable net momentum to a particle.

For counter-propagating lasers($\theta_b = 180^o + \theta_a$)

$$(k_a - k_b)c - \frac{P_{vs}}{M}(k_a + k_b)\cos\theta_a + \frac{\hbar}{2M}(k_a + k_b)(k_a - k_b) = \omega_{ea} - \omega_{eb} \tag{5.87}$$

By fixing the frequency of one of the lasers, say $\omega_a = k_a c$, any velocity class P_{vs} can be selected by tuning $\omega_b = k_b c$ to resonance using (for example) a dye(tunable) laser. Thus, we need to solve for ω_b in the quadratic Eq. 5.87 which is numerically ill-conditioned due to the small recoil term. We can solve for ω_b as following. We fix k_a,and set $\theta_a = 0$, and wish to solve for k_b in $Ak_b^2 + Bk_b + C = 0$ with $A \doteq \frac{\hbar}{2M}, B \doteq (c + \frac{P_{vs}}{M})$ and $C \doteq -\{k_a(c - \frac{P}{M}) - (\omega_{ea} - \omega_{eb}) + \frac{\hbar}{2M}k_a^2\}$. Since ak_b^2 is much smaller than the others, we obtain good approximation with series expansion

$$k_b \approx \frac{k_a(c - \frac{P}{M}) - (\omega_{ea} - \omega_{eb}) + \frac{\hbar}{2M}k_a^2}{(c + \frac{P_{vs}}{M})} - \frac{C^2}{B^3}A - 2\frac{C^3}{B^5}A^2 \tag{5.88}$$

We will use Eq. 5.88 for the simulations of the Raman velocity selection. The first term corresponds to neglecting the quadratic recoil term $\frac{\hbar}{2M}k_b^2$ which leads to a linear equation. Here, the counter-propagating lasers provide $\hbar(k_a + k_b)$ of momentum to the particle. Deceleration (net reduction in momentum) requires that the mean momentum P_o of the narrow distribution is antiparallel to the pump wavevector but parallel to the Stokes wavevector:

$$\mathbf{P}_{vs} \cdot \mathbf{k}_p = P_{vs}k_p\cos\theta_p < 0 \quad \text{and } \mathbf{P}_{vs} \cdot \mathbf{k}_S = P_{vs}k_S\cos\theta_S > 0 \tag{5.89}$$

while the reverse holds for acceleration.

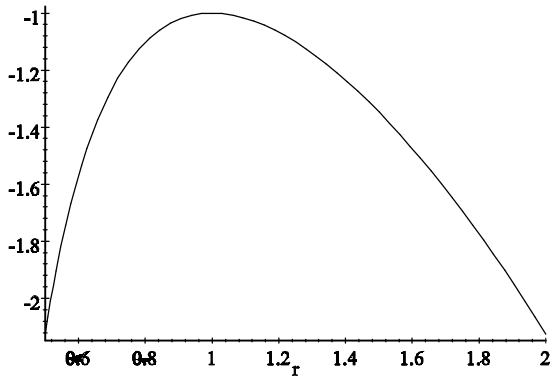

Figure 5.3: Plot of $\cos At$ versus $r \doteq \Omega_b/\Omega_a$ shows that $r = 1$ is the only physical value for complete inversion.

5.5.2 Zero effective detuning $\Omega_a = \Omega_b$

Here, we wish to derive the values of Rabi frequencies which give optimum transfer efficiency. Let $\Omega_b = r\Omega_a$ and we can rewrite Eqs. 5.83 as

$$\begin{aligned} u(P_{vs},t) &= \pi_{aa}(P_{vs},0)\frac{1-r^2}{(1+r^2)^2}2r\,(1-\cos A_{vs}t) \\ v(P_{vs},t) &= \pi_{aa}(P_{vs},0)\frac{2r}{1+r^2}\sin A_{vs}t \\ w(P_{vs},t) &= \pi_{aa}(P_{vs},0)\left(1-(\frac{2r}{1+r^2})^2\,(1-\cos A_{vs}t)\right) \\ f(P_{vs},t) &= \pi_{aa}(P_{vs},0) \end{aligned} \tag{5.90}$$

Complete inversion of the velocity selected population occur when $w(P_{vs},t) = -\pi_{aa}(P_{vs},0)$. From the third of Eq. 5.90, we can plot

$$\cos A_{vs}t = -\frac{1}{2r^2} - \frac{1}{2}r^2 \tag{5.91}$$

The plot of $\cos A_{vs}t$ versus r is shown in Fig. 5.3. Since $-1 \leqslant \cos A_{vs}t \leqslant 1$, it is clear that complete transfer (inversion) efficiency of velocity selected population from state $|a\rangle$ to $|b\rangle$ can only be achieved when $r = 1$ which means when the effective detuning is zero:

$$\Omega_a = \Omega_b \tag{5.92}$$

This condition corresponds to $A_{vs} \doteq \frac{2\Omega^2}{\Delta_{vs}}$, $u(P_{vs},t) = 0, v(P_{vs},t) = \pi_{aa}(P_{vs},0)\sin A_{vs}t$ and $w(P_{vs},t) = -\pi_{aa}(P_{vs},0)\cos A_{vs}t$.

5.5.3 Effective π-pulse (Rabi Frequency-Pulse Duration Relationship)

The required *pulse duration* τ for complete inversion is obtained from Eq. 5.66 when $\cos(\int_0^t \frac{2\Omega^2(t')}{\bar{\Delta}} dt') = -1$ for arbitrary time dependent Rabi frequency. This gives

$$\pi(2n-1) = \int_0^\tau \frac{2\Omega(t)^2}{|\bar{\Delta}_{vs}|} dt \tag{5.93}$$

where $n \geqslant 1$, with $n = 1, n = 2, ...$ correspond to the $\pi, 3\pi, ...$ pulse conditions respectively for complete population transfer. For time independent Rabi frequency, complete inversion occur when $\cos A(P_{vs})\tau = -1$ in the third of Eq. 5.90, $\sin \frac{1}{2}A(P_{vs})\tau = \pm 1$ in Eq. 5.74 or from Eq. 5.93 which give

$$\pi(2n-1) = \tau \frac{2\Omega^2}{|\bar{\Delta}_{vs}|} \tag{5.94}$$

The *Blackman* pulse shape can provide a more efficient velocity selection profile than the square pulse [313]. The corresponding Rabi frequency is

$$\Omega(t) = \Omega_o[a\cos\pi(2t/\tau - 1) + b\cos 2\pi(2t/\tau - 1) + c] \tag{5.95}$$

where τ is the pulse duration with the coefficients $(a, b, c) = (0.5, 0.08, 0.42)$.

From Eq. 5.93, we have the relation of the peak intensity Ω_o^2 with the pulse duration τ and detuning $\bar{\Delta}_{vs}$

$$\Omega_o^2 = (2n-1)|\bar{\Delta}_{vs}|\pi/\{\tau(a^2+b^2+2c^2)\} \approx 5.1569|\bar{\Delta}_{vs}|/\tau \tag{5.96}$$

$$\tau = \frac{|\bar{\Delta}_{vs}|\pi(2n-1)}{(a^2+b^2+2c^2)\Omega_o^2} \tag{5.97}$$

where $(a^2 + b^2 + 2c^2) = 0.6092$.

For Gaussian pulse shape, $\Omega(t) = \Omega_o e^{-(t-t_0)^2/\sigma^2}$, we find the peak intensity is

$$\Omega_o^2 = |\bar{\Delta}_{vs}|\sqrt{\frac{\pi}{2}}/\sigma \approx 6.267|\bar{\Delta}_{vs}|/\tau \tag{5.98}$$

where we have approximated the duration as $\tau = 5\sigma$ following an estimation from Fig. 4.1.

5.5.4 Selected Momentum Width-Square Pulse Duration Relationship

Similarly, we can find the momentum $P_{0.5}$ at the HWHM (half width at half maximum population) around the selected momentum P_{vs} by solving $\pi_{bb}(P_{0.5}, t) = \frac{1}{2}\pi_{bb}(P_{vs}, t)$. From Eq. 5.74, we get

$$\frac{\sin\frac{1}{2}A(P_{0.5})\tau}{A(P_{0.5})\bar{\Delta}(P_{0.5})} = \pm\sqrt{0.5}\frac{\sin\frac{1}{2}A(P_{vs})\tau}{A(P_{vs})\bar{\Delta}(P_{vs})} \tag{5.99}$$

If the detuning Δ_q is much greater than the Doppler width of the velocity selected population $\mathbf{k}\cdot(\mathbf{P}_{0.5}-\mathbf{P}_{vs})/M$, it is a good approximation to set $\bar{\Delta}(P_{0.5}) \approx \bar{\Delta}(P_{vs})$ in the denominator of Eq. 5.99. From Eqs. 5.68-5.51 and Eq. 5.82, we find $D(P_{vs}) = R(P_{vs}) = 0$ and $A(P_{vs}) = B(P_{vs}) = 2\frac{\Omega_a\Omega_b}{\bar{\Delta}_{vs}}$. By using $\sin\frac{1}{2}A(P_{vs})\tau = \pm 1$, $\Omega_a = \Omega_b$ and Eq. 5.94 $\pi = \tau\frac{2\Omega_o^2}{|\bar{\Delta}_{vs}|}$ we have

$$\frac{\sin\frac{1}{2}A(P_{0.5})\tau}{\frac{1}{2}A(P_{0.5})\tau} = \frac{\sqrt{2}}{\pi} \approx 0.45 \tag{5.100}$$

Now, by using $\bar{\Delta}_a(P_{0.5}) - \bar{\Delta}_b(P_{0.5}) = (P_{vs} - P_{0.5})(k_a + k_b)/M$ from Eq. 5.85, we have

$$A(P_{0.5}) \approx \sqrt{(\frac{(P_{vs}-P_{0.5})(k_a+k_b)}{M})^2 + (\frac{2\Omega_o^2}{\bar{\Delta}_{vs}})^2} \tag{5.101}$$

Numerical estimate of Eq. 5.100 gives $A(P_{0.5})\tau \approx 4.02$ and by using Eq. 5.101, we obtain the FWHM (full width at half maximum) momentum width as

$$\Delta P_{vs} = 2|P_{0.5} - P_{vs}| = \frac{2\sqrt{6.3}M}{\tau(k_a+k_a)} \approx \frac{5M}{\tau(k_a+k_a)} \tag{5.102}$$

Replacing τ from Eq. 5.94 into Eq. 5.102 gives

$$\Delta P_{vs} = \frac{10\Omega_o^2 M}{\pi|\bar{\Delta}_{vs}|(k_a+k_a)} \tag{5.103}$$

The correctness of Eqs. 5.102 and 5.94 have been verified through the simulations with density matrix equations (Eq. 5.26) as shown in Fig. 5.5. The existence of side lobes in the selected population π_{vs} shows the inefficiency of using square pulse for velocity selection. Ideally, it is preferable to have the selected population profile to be as close as possible to a rectangular shape.

The relationship between *momentum width and pulse duration* for Blackman pulse is the same as Eq. 5.102 except for the numerical factor, which is found via numerical analysis as

$$\Delta P_{vs} = \frac{7\pi M}{\tau(k_a+k_b)} \tag{5.104}$$

The validity of Eq. 5.104 is seen from Fig. 5.4, where the momentum widths from the velocity selection simulation are numerically measured for different input values of ΔP_{vs} with the corresponding τ_1 calculated from Eq. 5.104.

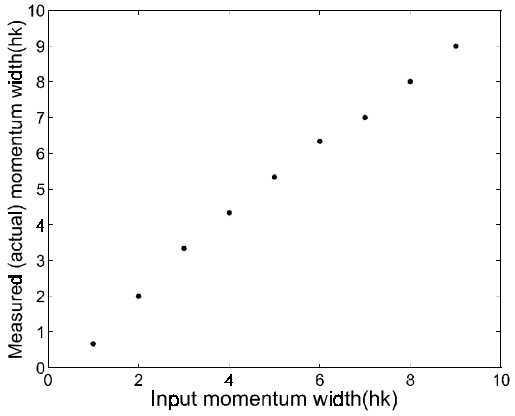

Figure 5.4: Momentum width measured from simulation results versus input momentum width using $\Delta P_{vs} = \frac{7\pi M}{\tau(k_a+k_b)}$.

By replacing Eq. 5.97 into Eq. 5.104, we have

$$\Delta P_{vs} = 4.26\frac{\Omega_o^2 M}{|\Delta_{vs}|(k_a + k_b)} \tag{5.105}$$

By comparing Eq. 5.105 and Eq. 5.103 or Eq. 5.104 with Eq. 5.102, it is clear the Blackman pulse provides a narrower selected momentum width for the same values of Ω_o, $|\Delta_{vs}|$ and τ.

Based on the Raman π-pulse condition (Eq. 5.96), we have simulated the transient and momentum dynamics the velocity selection process using the density matrix equations (Eqs. 5.26) for Blackman pulse, as shown in Fig. 5.6. The profile of the Blackman pulse (Fig. 5.6a) gives a single peak profile(Fig. 5.6b) of the velocity selected population without any side lobes. Thus, the Blackman pulse provides a efficient velocity selection than the square pulse (see Fig. 5.5). An interesting feature is observed from the 3-D graphics of Fig. 5.6c and 5.6d. Initially, the selected population has a wider profile than the width at subsequent time when the pulse goes to zero. There seems to be an 'over-transfer' in the population and the subsequent 'bouncing-back' in the population is manifested in the negative force region in Fig. 5.6. The parameters used for the velocity selection simulations are based on the OH molecular levels (discussed in Chapter 6):

Velocity Selection Parameters with Blackman pulses
$\omega_{ea} = 6.1637 \times 10^{15} s^{-1} (\Gamma_a = 4.2 \times 10^5 s^{-1})$
$\omega_{eb} = 5.4917 \times 10^{15} s^{-1} (\Gamma_b = 3 \times 10^5 s^{-1})$
$\omega_{p1} = 6.1636 \times 10^{15} s^{-1}$ (pump frequency)
$\omega_{S1} = 5.4916 \times 10^{15} s^{-1}$(Stokes frequency)
$\Omega_{op1} = \Omega_{oS1} = 3.4 \times 10^8 s^{-1}$ (pump and Stokes Rabi frequencies
$\tau = 4.45 \mu s$ (pulse duration)

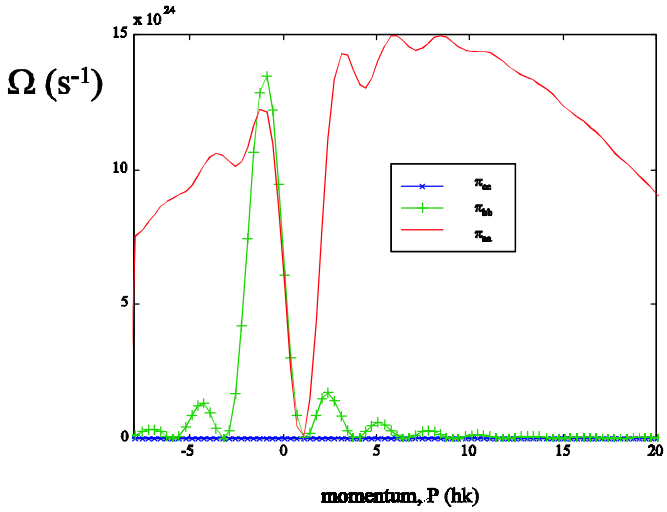

Figure 5.5: Momentum distributions of the velocity selected population and the residual population using square Raman π-pulses.

The transient evolution and the momentum distribution of the reactive force in Fig. 5.6 agrees very well with $\mathbf{F}_{reac}$ from analytical expression Eq. 5.78. The force shows a maximum deceleration of up to $3000ms^{-1}$ during the maximum laser field for peak Rabi frequency.

5.6 Deceleration by Repeated STIRAP

Various techniques of population transfer have been devised. The most famous one is STIRAP [265]. The technological successes in the generation of ultrashort pulses provides advanced frequency chirped lasers for population [266] and optimally controlled pulse-shape have spurred new techniques to control the internal states of molecules [276], [274] via wavepacket engineering with the pulses. The close entanglement between the internal and external degrees provides the momentum transfer during the Raman transitions. The kinetic effect from STIRAP has been used to deflect atomic beam to generate an atom interferometer [283] and to provide an output coupling mechanism for atom laser scheme[262].

It has been shown using the Schrödinger equation that for one-photon resonant with a short lived decaying intermediate state, the diabatic (non-adiabatic) coupling leads to the low transfer efficiency [269]. This may be discouraging for application of STIRAP to molecule where the one-photon detuning should be much smaller than the adjacent levels spacing. However, the rotational levels separation is sufficiently large, typically $10^{10}s^{-1}$.

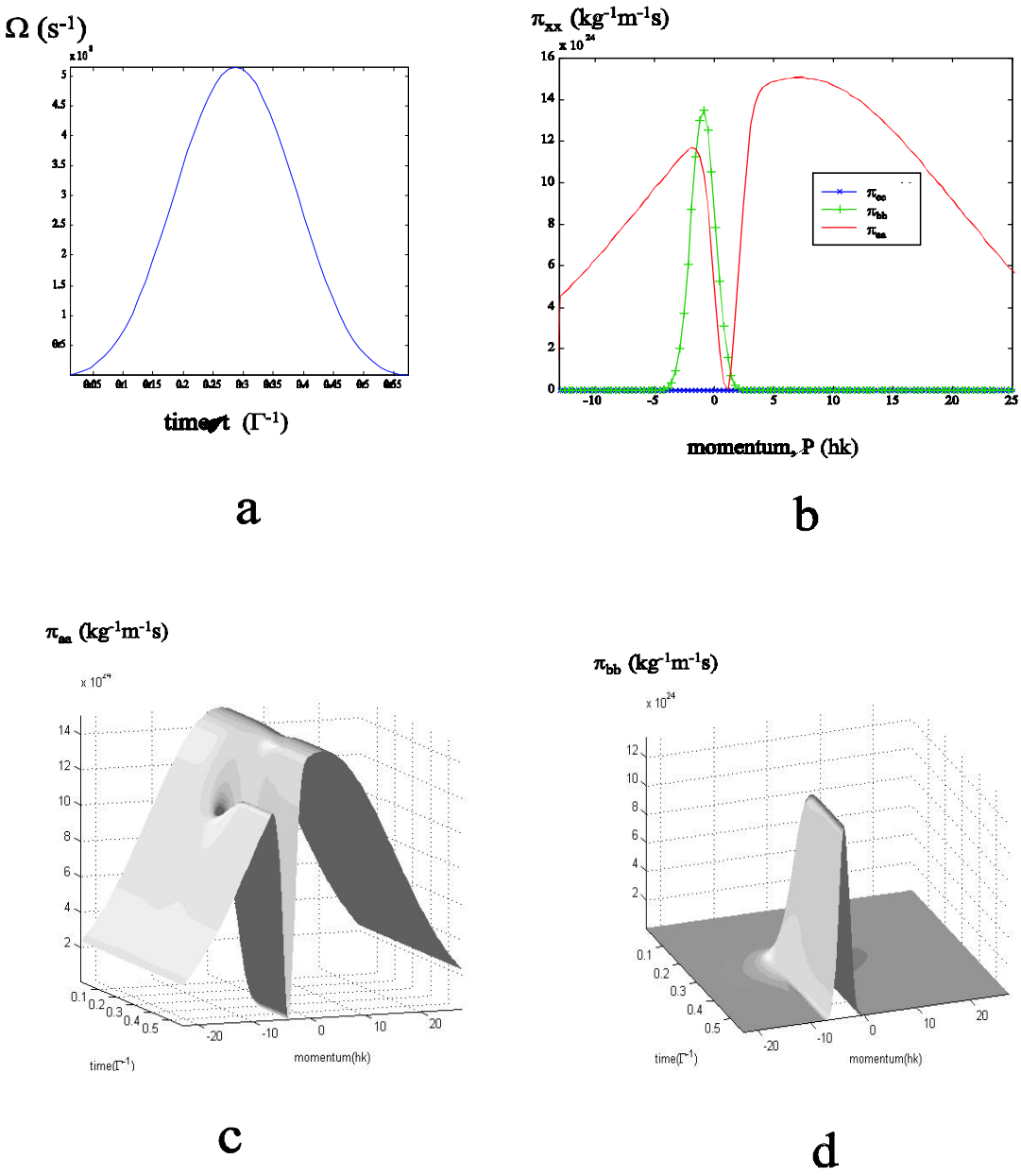

Figure 5.6: Dynamics of Raman velocity selection process: a) time evolution of Blackman pulse, b) momentum distributions of population density in initial $\pi_{aa}(P)$, final (targeted) $\pi_{bb}(P)$ and the excited states $\pi_{ee}(P)$, and momentum-transient distributions of c) initial state $\pi_{aa}(P,t)$, d) final state $\pi_{bb}(P,t)$.

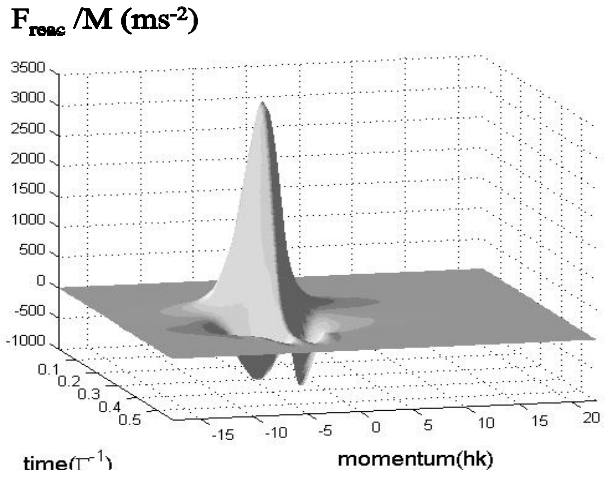

Figure 5.7: Transient and momentum distribution of the reactive force during the process of velocity selection.

This enables the detuning of up to $10^9 s^{-1}$ which is larger than the typical linewidth of the intermediate state.

Population transfer in the case of finite two-photon detuning is more realistic due to Doppler shift when the population has finite momentum width. This has been studied using Schrödinger equation [270]. Population transfer through intermediate continuum in a Λ scheme has also been shown to be inefficient [277]. Studies have also been extended to multilevels system using density matrix approach both algebraically [272] and numerically [271]. There are also works which emphasize on efficiency and non adiabatic mechanism [268].

Despite the many works on STIRAP, the center of mass effect was not considered in most of them except for the application in atom interferometry by Ref. [69]. In the case when repeated cycles of STIRAP are required, the transfer efficiency of each cycle becomes important [284]. There has been much theoretical studies of three-level STIRAP [267] using Schrödinger equation, and simulation with density matrix equations [289] but without considering the center of mass momentum distribution. We wish to use the coherent momentum transfer from the laser photons to decelerate the molecules without affecting the momentum distribution. Thus, we avoid using the optical pumping which involves spontaneous emission process [290]. Periodically switched standing wave lasers at far-off resonance have been used to accelerate ultracold atoms with high efficiency [291]. In the following, we shall develop the theory of STIRAP for Λ scheme including the center of mass momentum as the external quantum states, in addition to the internal states using the Schrödinger equation.

5.6.1 Schrödinger equation

If we neglect the incoherent effect from the radiation-molecule interaction, we have the free Hamiltonian

$$H_o = \sum_P \tfrac{\mathbf{P}^2}{2M}|\mathbf{P}\rangle\langle\mathbf{P}| + \hbar\omega_{oe}|e\rangle\langle e| + \hbar\omega_{oa}|a\rangle\langle a| + \hbar\omega_{ob}|b\rangle\langle b| \tag{5.106}$$

and the coherent laser interaction

$$\begin{aligned} V_{SL}(t) &= -\hbar\Omega_a(|e\rangle\langle a|e^{i(\mathbf{k}_a\cdot\hat{\mathbf{R}}-\omega_a t)} + |a\rangle\langle e|e^{-i(\mathbf{k}_a\cdot\hat{\mathbf{R}}-\omega_a t)}) \\ &\quad -\hbar\Omega_b(|e\rangle\langle b|e^{i(\mathbf{k}_b\cdot\hat{\mathbf{R}}-\omega_b t)} + |b\rangle\langle e|e^{-i(\mathbf{k}_b\cdot\hat{\mathbf{R}}-\omega_b t)}) \end{aligned} \tag{5.107}$$

In interaction picture, we have

$$\begin{aligned} V^i_{SL}(t) &= -\hbar\Omega_a(|e\rangle\langle a|\hat{\pi}_a e^{-i\Delta_a t} + |a\rangle\langle e|\hat{\pi}^\dagger_a e^{i\Delta_a t}) \\ &\quad -\hbar\Omega_b(|e\rangle\langle b|\hat{\pi}_b e^{-i\Delta_b t} + |b\rangle\langle e|\hat{\pi}^\dagger_b e^{i\Delta_b t}) \end{aligned} \tag{5.108}$$

where $\hbar\Omega_q(\mathbf{R},t) \doteq d_{eq}E_q(\mathbf{R},t)$ and $d_{eq} = ||d||C_q$ is the reduced dipole matrix times the transition coefficient and $\Delta_q = \omega_q - \omega_{oq}$ with $q \in a,b$. For state vector $|\Psi^i(\mathbf{P},t)\rangle = \sum_P\{c_a(\mathbf{P}-\hbar\mathbf{k}_a,t)\,|a,\mathbf{P}-\hbar\mathbf{k}_a\rangle + c_b(\mathbf{P}-\hbar\mathbf{k}_b,t)\,|2,\mathbf{P}-\hbar\mathbf{k}_b\rangle + c_e(\mathbf{P},t)\,|e,\mathbf{P}\rangle\}$ we have

$$\tfrac{d}{dt}\begin{pmatrix} c_a(\mathbf{P}-\hbar\mathbf{k_a},t) \\ c_b(\mathbf{P}-\hbar\mathbf{k_b},t) \\ c_e(\mathbf{P},t) \end{pmatrix} = i\begin{pmatrix} 0 & 0 & \Omega_a e^{i\bar{\Delta}_{a\mathbf{P}}t} \\ 0 & 0 & \Omega_b e^{i\bar{\Delta}_{b\mathbf{P}}t} \\ \Omega_a e^{-i\bar{\Delta}_{a\mathbf{P}}t} & \Omega_b e^{-i\bar{\Delta}_{b\mathbf{P}}t} & 0 \end{pmatrix}\begin{pmatrix} c_a(\mathbf{P}-\hbar\mathbf{k_a},t) \\ c_b(\mathbf{P}-\hbar\mathbf{k_b},t) \\ c_e(\mathbf{P},t) \end{pmatrix}$$

where $\bar{\Delta}_{q\mathbf{P}} = \Delta_q - \omega_{q\mathbf{P}} + \omega_{qr}$ with $q \in a,b$, and $\omega_{q\mathbf{P}}$ denotes the Doppler shift and ω_{qr} the recoil shift. By unitary transformation to eliminate $\bar{\Delta}_{q\mathbf{P}}$ and the inclusion of damping from the excited state Γ, we get

$$\frac{d}{dt}\begin{pmatrix} C_a(\mathbf{P}-\hbar\mathbf{k_a},t) \\ C_b(\mathbf{P}-\hbar\mathbf{k_b},t) \\ C_e(\mathbf{P},t) \end{pmatrix} = i\begin{pmatrix} -\bar{\Delta}_{a\mathbf{P}} & 0 & \Omega_a \\ 0 & -\bar{\Delta}_{b\mathbf{P}} & \Omega_b \\ \Omega_a & \Omega_b & i\Gamma \end{pmatrix}\begin{pmatrix} C_a(\mathbf{P}-\hbar\mathbf{k_a},t) \\ C_b(\mathbf{P}-\hbar\mathbf{k_b},t) \\ C_e(\mathbf{P},t) \end{pmatrix} \tag{5.109}$$

where $C_q(\mathbf{P}-\hbar\mathbf{k}_q,t) = c_q(\mathbf{P}-\hbar\mathbf{k}_q,t)e^{-i\bar{\Delta}_{q\mathbf{P}}t}$ and $C_e(\mathbf{P},t) = c_e(\mathbf{P},t)$. For large detuning, Eq. 5.109 has been solved by reducing it to a two-level equation in Ref. [314]. When two-photon resonance $\bar{\Delta}_{a\mathbf{P}_r} = \bar{\Delta}_{b\mathbf{P}_r} = \bar{\Delta}_{\mathbf{P}_r}$ is satisfied for the populations with the momentum $\mathbf{P}_r$, Eq. 5.109 can be transformed into

$$\frac{d}{dt}\begin{pmatrix} a \\ b \\ c \end{pmatrix} = i\begin{pmatrix} 0 & 0 & \Omega_a \\ 0 & 0 & \Omega_b \\ \Omega_a & \Omega_b & \bar{\Delta}_{\mathbf{P}} + i\Gamma \end{pmatrix}\begin{pmatrix} a \\ b \\ c \end{pmatrix} \tag{5.110}$$

where $a \doteq C_a e^{i\bar{\Delta}_{\mathbf{P}}t} = c_a, b \doteq C_b e^{i\bar{\Delta}_{\mathbf{P}}t} = c_b$ and $c \doteq C_e e^{i\bar{\Delta}_{\mathbf{P}}t} = c_e e^{i\bar{\Delta}_{\mathbf{P}}t}$.

Unitary transformation of Eq. 5.110 gives the new basis vectors $|\Psi\rangle$

$$|\Psi_1\rangle = \sin\theta\sin\varphi|a\rangle + \cos\theta\sin\varphi|b\rangle + \cos\varphi|e\rangle \quad (5.111)$$

$$|\Psi_2\rangle = -\sin\theta\cos\varphi|a\rangle - \cos\theta\cos\varphi|b\rangle + \sin\varphi|e\rangle \quad (5.112)$$

$$|\Psi_3\rangle = \cos\theta|a\rangle - \sin\theta|b\rangle \quad (5.113)$$

and the corresponding eigenvalues or light shifts

$$E_1 \doteq \frac{1}{2}D + \frac{1}{2}\sqrt{D^2 + 4\Omega^2} \quad (5.114)$$

$$E_2 \doteq \frac{1}{2}D - \frac{1}{2}\sqrt{D^2 + 4\Omega^2} \quad (5.115)$$

$$E_3 \doteq 0 \quad (5.116)$$

with

$$\tan\theta \doteq \frac{\Omega_a}{\Omega_b} \text{ and } \tan 2\varphi \doteq 2\Omega/D \quad (5.117)$$

where $D \doteq \bar{\Delta} + i\Gamma$ and $\Omega^2 \doteq \Omega_a^2 + \Omega_b^2$. The eigenvalues and eigenvectors have been solved for the case $\Gamma = 0$ in Ref. [267]. For $\bar{\Delta}, \Gamma << \Omega$, the complex eigenvalues Eqs. 5.114-5.116 can be written in real and imaginary parts as $E_1 = \frac{1}{2}\bar{\Delta} + \frac{1}{2}\sqrt{X} + i\Gamma(\frac{1}{2} + \frac{\bar{\Delta}}{\sqrt{X}}), E_2 = \frac{1}{2}\bar{\Delta} - \frac{1}{2}\sqrt{X} + i\Gamma(\frac{1}{2} - \frac{\bar{\Delta}}{\sqrt{X}})$ and $E_3 = 0$ where $X \doteq \left(\bar{\Delta}^2 - \Gamma^2 + 4\Omega^2\right)$. The imaginary part which is proportional to the damping rate Γ gives the exponentially decaying function to the dressed states populations.

5.6.2 Complete Population Transfer in STIRAP

For the purpose of population transfer, we start with all the populations in state $|a\rangle$ and wish to transfer it completely to $|b\rangle$. From Eq. 5.113, it is clear that this can be achieved if the populations remain in the state $|\Psi_3\rangle$ as the mixing angle evolves from $\theta(t_i) = 0$ at initial time t_i to $\theta(t_f) = \pi/2$ at final time $t_f = t_i + \tau$. Here, $\Omega_a = \Omega_p$ is from the *pump* laser while $\Omega_b = \Omega_S$ is from the *Stokes* laser. This gives the boundary conditions for the pulses evolutions as

$$\tan\theta(t_i) = \frac{\Omega_p(t_i)}{\Omega_S(t_i)} \to 0 \text{ and } \tan\theta(t_f) = \frac{\Omega_p(t_f)}{\Omega_S(t_f)} \to \infty \quad (5.118)$$

The relevent state vector for is the *adiabatic state* or *dark state*

$$|\Psi_3(t_i)\rangle = |a\rangle \to |\Psi_3(t_f)\rangle = -|b\rangle$$

which has zero light shift, $E_3 = 0$.

The *diabatic (non adiabatic)* states are

$$|\Psi_1(t_i)\rangle = \sin\varphi|b\rangle + \cos\varphi|e\rangle \rightarrow |\Psi_1(t_f)\rangle = \sin\varphi|a\rangle + \cos\varphi|e\rangle \quad (5.119)$$

$$|\Psi_2(t_i)\rangle = -\cos\varphi|b\rangle + \sin\varphi|e\rangle \rightarrow |\Psi_2(t_f)\rangle = -\cos\varphi|a\rangle + \sin\varphi|e\rangle \quad (5.120)$$

which contain the untargeted state $|e\rangle$. Any population in state $|e\rangle$ will have a finite probability of loss through spontaneous decay. In order to maximize the transfer efficiency, the state $|e\rangle$ should be a long living state (narrow linewidth) and the evolution during the population transfer should be made slow enough so that the populations remain in the adiabatic state and minimize populating in the diabatic states.

The adiabatic condition [264] occurs when the rate of change of the adiabatic state projected onto the diabatic states is small compared to the eigenvalues splitting, $|\langle\Psi_1|\frac{d}{dt}|\Psi_3\rangle| = \frac{d\theta}{dt}\sin\varphi << \frac{1}{2}\{\sqrt{\bar{\Delta}^2 + 4\Omega^2} - \bar{\Delta}\}$ or

$$(\frac{d\Omega_p}{dt}\Omega_S - \Omega_p\frac{d\Omega_S}{dt}) << \Omega^3\sqrt{(1+t^2)} \quad (5.121)$$

where $t = -x + \sqrt{1+x^2}$ and $x = \bar{\Delta}/2\Omega$.

When the Stokes and the pump pulses have the same time dependence, the pulses overlap and they can be related by a constant r, as $\Omega_p = r\Omega_S$. Hence, the left-hand-side of Eq. 5.121 vanishes and the adiabatic condition is fulfilled even any magnitude of Rabi frequency. This corresponds to a constant θ (from Eq. 5.117. For resonant case $\bar{\Delta} = 0$ or $\Omega >> \bar{\Delta}$, we can set $x \rightarrow 0$ or $t \rightarrow 1$ and Eq. 5.121 becomes

$$(\frac{d\Omega_p}{dt}\Omega_S - \Omega_p\frac{d\Omega_S}{dt}) << \sqrt{2}\Omega^3 \quad (5.122)$$

This adiabatic criteria is valid for continuous wave (CW) lasers. For real pulse, there is a slight modification due to phase fluctuation of the laser [287].

5.6.3 Simulation of STIRAP Dynamics

We also want to study how the population transfer dynamics and efficiency are affected by the decaying intermediate state, the impossibility of having exactly zero two-photon detuning due to finite Doppler width of the gas. It is also interesting to compute the transient light force from STIRAP. All these can be done appropriately by numerically solving the density matrix equations 5.26. In this section we present simulation results of the population transfer by STIRAP by numerically solving the density matrix equations 5.26 with quantization of the center of mass momentum.

For Gaussian pulse where the Stokes pulse precedes the pump pulse (*counter-intuitive* order), we can write

$$\Omega_p(t) = \Omega_{po}e^{-(t-\tau_p)^2/\sigma_p^2} \text{ and } \Omega_S(t) = \Omega_{So}e^{-(t-\tau_S)^2/\sigma_S^2} \quad (5.123)$$

where τ_S the peak time of Stokes pulse, $\tau_p = \tau_S + \tau_d$ the peak time of pump pulse and $\tau_d \doteq (\sigma_p + \sigma_S)\sqrt{\ln 2}$ is the time delay between the Stokes and pump pulses. The duration for the STIRAP process can be estimated as (see Figure 4.1)

$$\tau = (2.5 + \sqrt{\ln 2})(\sigma_p + \sigma_S) \simeq 3.33(\sigma_p + \sigma_S). \tag{5.124}$$

If we let the starting time and ending time of population transfer as $t_i = \tau_S$ and $t_f = \tau_p$ respectively, Eq. 5.118 can be written as

$$\tan\theta(t_i) = \frac{\Omega_{po} e^{-{t_d}^2/\sigma_p^2}}{\Omega_{So}} \to 0 \text{ and } \tan\theta(t_f) = \frac{\Omega_{po}}{\Omega_{So}} e^{{t_d}^2/\sigma_S^2} \to \infty \tag{5.125}$$

The transfer efficiency can be estimated from Eq. 5.125

$$\epsilon = |\langle 2|\Psi_3(t_f)\rangle|^2 = \sin^2\{\tan^{-1}(\frac{\Omega_{po}}{\Omega_{So}} e^{(\frac{\sigma_p}{\sigma_S}+1)^2 \ln 2})\} \tag{5.126}$$

Equation 5.126 shows that we can maximize the transfer efficiency by using large pump pulse area $\sim \Omega_{po}\sigma_p$. For $\sigma_p = \sigma_S$ we have $\tan\theta(t_i) = 0.062 \to 0$ and $\tan\theta(t_f) = 16 \to \infty$, with the transfer efficiency $\epsilon = 0.996\,11$.

For identical pulses ($\sigma_p = \sigma_S$) the adiabatic condition Eq. 5.122 gives the more exact criteria than the well-known one $\Omega T >> 1$ [265]

$$\frac{2\sqrt{2\ln 2}}{\sigma} << \frac{(\Omega_p^2 + \Omega_S^2)^{3/2}}{\Omega_p \Omega_S} \tag{5.127}$$

Based on the above theory, we simulate the STIRAP dynamics including the center of mass momentum using the density matrix equations (Eqs. 5.26) as shown in Figs. 5.8. The entire populations with a broad momentum distribution can be efficiently transferred (Fig. 5.8b) from an initial state $|a\rangle$ (Fig. 5.8c) to the final state $|b\rangle$(Fig. 5.8d) using the overlapping Gaussian pulses with unequal Rabi frequencies (Fig. 5.8a).

STIRAP Parameters with Gaussian pulses
$\omega_{ea} = 6.163\,7 \times 10^{15} s^{-1} = \omega_p$(pump frequency)
$\omega_{eb} = 4.851\,8 \times 10^{15} s^{-1} = \omega_S$(Stokes frequency)
$\Omega_S = 4.8846 \times 10^9 s^{-1}$(Stokes Rabi frequency)
$\Omega_p = 6.1057 \times 10^9 s^{-1}$(pump Rabi frequency)
$\tau = 5 \times 10^{-8} s$ (STIRAP duration)

5.6.4 Repeated Reversal of STIRAP

The molecules initially in an internal state (say $|g+\rangle$) can be given repeated momentum kicks for continuous deceleration (or acceleration) by employing repeated STIRAP processes. Although the system entropy S_S is invariant throughout this unitary process, the translational kinetic energy of the molecules can be substantially decreased (or increased).

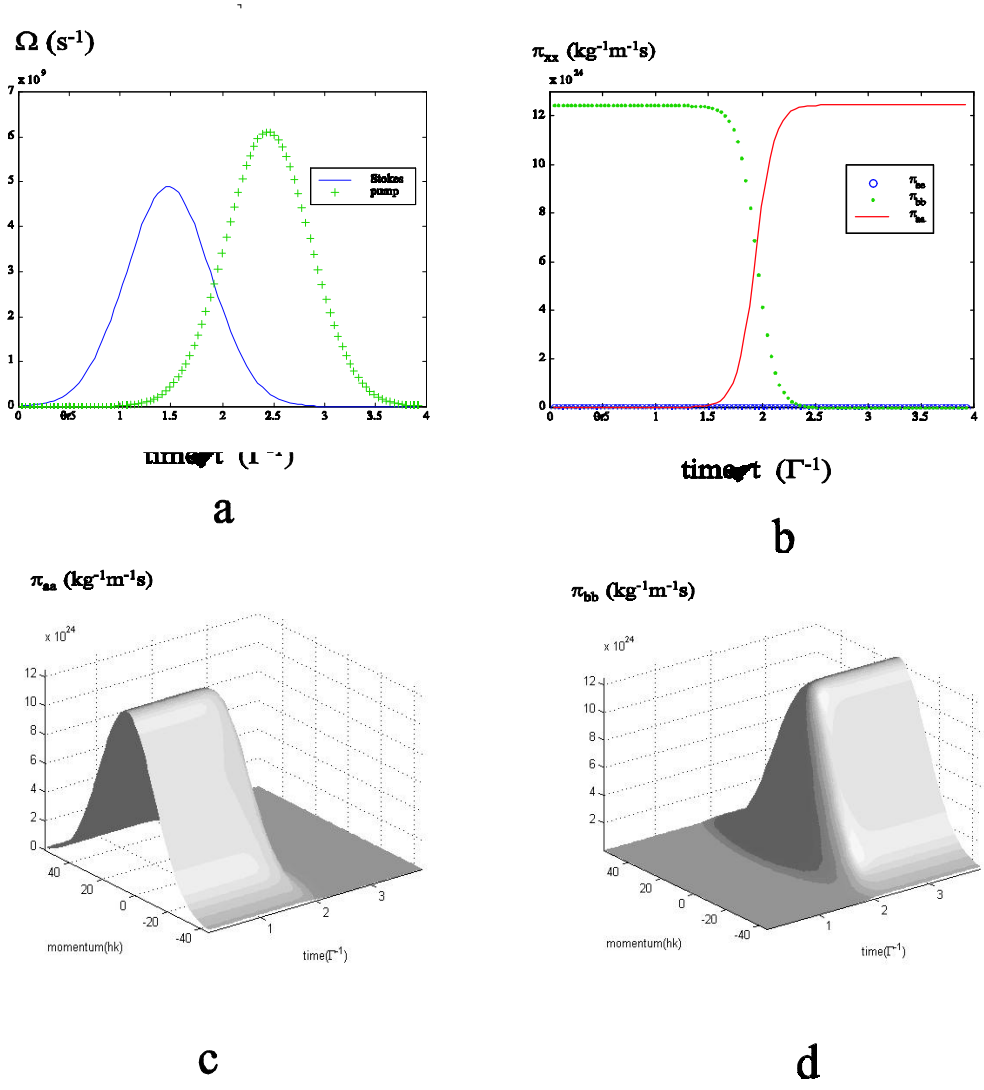

Figure 5.8: Dynamics of STIRAP a) time evolutions of the pulses (preceding Stokes pulse has lower peak), b) transient evolutions of the populations in initial state $\pi_{aa}(t)$ and final state $\pi_{aa}(t)$; and momentum-transient distributions in c) $\pi_{aa}(P,t)$ and d) $\pi_{bb}(P,t)$.

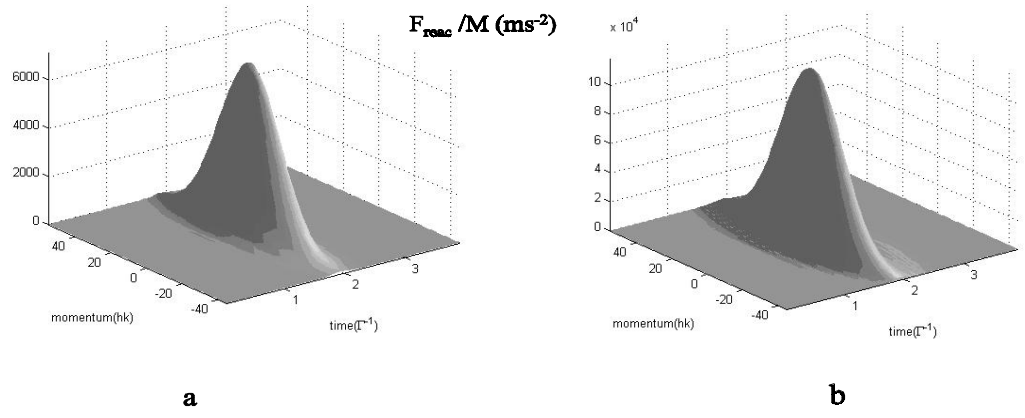

Figure 5.9: The transient and momentum distributions of the reactive light force for a) co-propagating pulses, b) counter-propagating pulses.

The *reactive optical light force* is responsible for the change in the kinetic energy and we have derived it in the previous Section. The force is simulated by using the numerical solutions of the Bloch equations (Eqs. 5.26) with the force equations, Eqs. 5.15-5.16 [1]. The results show a larger force for counter-propagating lasers(Fig 5.9b) corresponding to a large deceleration of $10^5 ms^{-2}$.

Each cycle in the deceleration process is composed of two STIRAP processes. The first STIRAP uses a pair of counter-propagating pulses to transfer the population from state $|g_+, P + \hbar k_{1+}\rangle$ to $|g_-, P - \hbar k_{1-}\rangle$, thus reducing the momentum of the population by $\Lambda_1 \doteq \hbar(k_{1-} + k_{1+})$. By reversing the directions and the counter-intuitive ordering of the pulses as shown in Fig. 5.10, the population in $|g_-, P - \hbar k_{1-}\rangle$ is transferred back to $|g_+, P - \hbar k_{1-} - \Lambda_2\rangle$, giving another momentum transfer of $\Lambda_2 \doteq \hbar(k_{2-} + k_{2+})$ as shown in Fig 5.11.Generally, the $n-th$ pair of pulses ($n \geq 1$) is defined as following. The σ^+ pulse couples states $|g_+, P_n - (-1)^n \alpha \hbar k_{n+}\rangle$ and $|e, P_n\rangle$ has the wavevector and the Rabi frequency with Gaussian profile

$$\mathbf{k}_{n+} = (-1)^n \alpha \hat{z} k_{n+} \tag{5.128}$$

$$\Omega_+(t) = \Omega_{+o} e^{-(t-t_{n+})^2/\sigma_+^2} \text{ with } t_{n+} = (2n-1)\tau/2 - (-1)^n \Delta t_{F+}/2 \tag{5.129}$$

The σ^- pulse couples states $|e, P_n\rangle$ and $|g_-, P_n + (-1)^n \alpha \hbar k_-\rangle$ has the wavevector and the Rabi frequency

$$\mathbf{k}_{n-} = -(-1)^n \alpha \hat{z} k_- \tag{5.130}$$

$$\Omega_- = \Omega_{-o} e^{-(t-t_{n-})^2/\sigma_-^2} \text{ with } t_{n-} = (2n-1)\tau/2 + (-1)^n \Delta t_{F-}/2 \tag{5.131}$$

[1] We use a symmetric momentum distribution, so Eq. 5.17 vanishes.

Figure 5.10: Two pairs of STIRAP pulses with opposite ordering. The directions of the second pair of pulses are reversed from the first one.

Figure 5.11: Momentum transfer during one cycle of STIRAP deceleration which is composed of two reversed STIRAP processes.

where $\{P_n\}$ is the momentum family of the coupled states, $\sigma_\pm$ are the temporal standard deviations, $\Delta t_{F\pm} = \sigma_\pm 2\sqrt{\ln 2}$ is the FWHM (full width at half maximum), $\tau = 2(\Delta t_{F+} + \Delta t_{F-}) = (\sigma_+ + \sigma_-)4\sqrt{\ln 2}$ is the period for each pair of the overlapping pulses, $t_d = (\sigma_+ + \sigma_-)\sqrt{\ln 2}$ is the pulses delay as shown in Fig. 4.1.

The parameter $\alpha = sgn(P_n)$ ensures that P_n is always parallel to the Stokes wavevector (stimulated emission) so as to reduce the momentum by $\hbar(k_{n-} + k_{n+})$ where $P_n = P_{n-1} - \alpha\hbar(k_{n-} + k_{(n-1)-})$ and $P_n = P_{n-1} - \alpha\hbar(k_{n+} + k_{(n-1),+})$ for even and odd n respectively. The momentum reduces from P_1 to $P_1 - \sum_{i=1}^{n} \alpha\hbar(k_{i-} + k_{i+})$ during the n-th cycle. If the Rabi frequency is much greater than the Doppler width $k_\pm \Delta P/M$ of the population, we can fix the laser frequencies to be the same for every cycle, $k_{n\pm} = k_\pm$. In each cycle, the molecules are decelerated by $\hbar(k_+ + k_-)$ of recoil momentum by the Stokes and pump photons.

The results from the analysis of the velocity selection and STIRAP processes are important and they are used in the proposed laser cooling schemes for molecules (in Ref. [1] and Chapter 6) which incorporates the STIRAP technique for decelerating the velocity selected molecules.

5.7 Momentum Squeezing

Unconfined gas at high temperature undergoes rapid expansion and lost into free space. In order to cool the gas, we need a a trap with sufficiently large depth and lifetime. Due to the practical limitation of the trap depth, the most energetic molecules can never be trapped. Besides, existing traps for molecules are often leaky, with short lifetime [65] compared to the magnetic-optical trap for atoms. It would be most convenient if the kinetic energy of the molecules can be substantially reduced fast enough before they spread out in space. Ammann and Christensen [15] have used a pulsed potential to rotate the phase space of an expanding gas. They called it delta-kick cooling although there is no dissipative mechanism involved in their scheme. Optimization of this cooling concept using harmonic potential has been proposed and demonstrated in one dimension by Myrskog et. al. [16]. Although these techniques involve purely unitary or coherent process which simply reduce the kinetic energy but do not change the phase space since there is no incoherent dissipative mechanism involved, yet they are called 'cooling' schemes.

We present the evolution of the quasi-phase space Wigner function and derive the conditions leading to either momentum squeezing [317] or momentum bunching, depending on the trap frequency and initial conditions. We start with a pulse of molecules with a narrow spatial extend but with a large momentum width. We let it expand in the center of the harmonic potential for a quarter of the trap oscillation period, after which the phase space of the molecules has been rotated to a narrow momentum width but spatially extended. The momentum squeezing effect can only occur under certain conditions, which we will derived. We use the conditions to progressive squeeze the momentum width by alternating

the trapping frequency.

5.7.1 Wigner Function in Harmonic Potential

We consider a molecular gas with a Gaussian distribution in one-dimensional spatial and momentum spaces, with a momentum (spatial) width σ_{po} (σ_{zo}) and mean momentum (position) $\bar{p}$ ($\bar{z}$). The initial quasi phase space (QPS) distribution of the molecules is described by the Wigner function

$$W_o(z,p) \doteq W(z,p,t=0) = e^{-(p-\bar{p})^2/\sigma_{po}^2} e^{-(z-\bar{z})^2/\sigma_{zo}^2} \tag{5.132}$$

The choice of a Gaussian distribution implies that the molecules are in thermal equilibrium, at least along the z axis. This enables rather convenient analytical calculations to illustrate the basic concept of momentum squeezing. We discuss its practical realization in the end of this section.

We consider a molecular gas in one dimensional harmonic trap potential $V(z) = \frac{1}{2}M\omega^2 z^2$, which is turned on at time $t = 0$, where M is the mass of a molecule and ω is the trap frequency. From the Hamiltonian $H = \frac{p^2}{2M} + V(z)$, we have the well-known classical differential equation for the Wigner function which describes the time evolution of the molecules in position and momentum spaces,

$$\frac{\partial}{\partial t}W(z,p,t) = -\frac{p}{M}\frac{\partial}{\partial z}W(z,p,t) + M\omega^2 z\frac{\partial}{\partial p}W(z,p,t) \tag{5.133}$$

with the characteristic equations: $\frac{dz}{dt} = \frac{p}{M}, \frac{dp}{dt} = -M\omega^2 z$.

The formal solution of the Wigner distribution is

$$W(z,p,t) = e^{\{-\frac{p}{M}\frac{\partial}{\partial z} + M\omega^2 z\frac{\partial}{\partial p}\}t} W_o(z,p) \tag{5.134}$$

By defining $q = M\omega x$ and replacing $p = C\sin\phi$, and $q = C\cos\phi$, Eq. 5.133 transforms into

$$\frac{\partial}{\partial t}W(\phi,t) = \omega\frac{\partial}{\partial \phi}W(\phi,t) \tag{5.135}$$

with the formal solution

$$W(\phi,t) = e^{\omega t\frac{\partial}{\partial\phi}} W_o(\phi) = W_o(\phi+\omega t) \tag{5.136}$$

where $\phi = \tan^{-1}\frac{p}{q}$ is the phase space angle and $C = \sqrt{p^2+q^2}$.

For the initial condition of Eq. 5.132, the Wigner function evolves as

$$\begin{aligned} W(z,p,t) &= e^{-(p\cos\omega t + zM\omega\sin\omega t - \bar{p})^2/\sigma_{po}^2} e^{-(-\frac{p}{M\omega}\sin\omega t + z\cos\omega t - \bar{z})^2/\sigma_{zo}^2} \\ &\equiv e^{-p^2/\sigma_p^2} e^{-z^2/\sigma_z^2} e^{-pz/\sigma_{pz}^2} F_{\bar{p},\bar{z}} \end{aligned} \tag{5.137}$$

where the time dependent widths are

$$\sigma_p(t) \doteq \{(\frac{\cos\omega t}{\sigma_{po}})^2 + (\frac{\sin\omega t}{M\omega\sigma_{zo}})^2\}^{-\frac{1}{2}} \tag{5.138}$$

$$\sigma_z(t) \doteq \{(\frac{M\omega\sin\omega t}{\sigma_{po}})^2 + (\frac{\cos\omega t}{\sigma_{zo}})^2\}^{-\frac{1}{2}} \tag{5.139}$$

$$\sigma_{pz} \doteq \{\sin 2\omega t(\frac{M\omega}{\sigma_{po}^2} - \frac{1}{M\omega\sigma_{zo}^2})\}^{-\frac{1}{2}} \tag{5.140}$$

and the parameters which depend on the initial mean position $\bar{z}$ and momentum $\bar{p}$ are

$$F_{\bar{p},\bar{z}} \doteq e^{-\bar{p}^2/\sigma_{po}^2} e^{-\bar{z}^2/\sigma_{zo}^2} e^{p/a_p} e^{z/a_z} \tag{5.141}$$

$$a_p \doteq \{\frac{2\bar{p}\cos\omega t}{\sigma_{po}^2} - \frac{2\bar{z}\sin\omega t}{M\omega\sigma_{po}^2}\}^{-1} \text{ and } a_z \doteq \{\frac{2\bar{p}M\omega\sin\omega t}{\sigma_{po}^2} + \frac{2\bar{z}\cos\omega t}{\sigma_{zo}^2}\}^{-1} \tag{5.142}$$

The QPS volume of Eq. 5.137 can be shown to be a constant $\int\int W(z,p,t)dzdp = \pi\sigma_z\sigma_p$ and $\int\int W^2(z,p,t)dzdp = \frac{1}{2}\pi\sigma_p\sigma_z$ during the time evolution in the harmonic potential. The Wigner function satisfies the normalization condition $\int\int W_n(z,p,t)dzdp = 1$, thus $W_n(z,p,t) = \frac{1}{\pi\sigma_z\sigma_p}W(z,p,t)$. The quantum mechanical property of the Wigner function is manifested by the inequality $\int\int W_n^2(z,p,t)dzdp \leq (2\pi\hbar)^{-1}$ [221]. From these, we have the minimum phase space relation

$$\sigma_z\sigma_p \geq \hbar \tag{5.143}$$

as the result of the quantum mechanical nature of the Wigner function.

The Renyi entropy [113] $S_R = Tr\{\rho^2\}$ which measures the purity of an ensemble is unchanged since

$$Tr\{\rho^2\} = 2\pi\hbar\int\int W_n^2(z,p,t)dzdp = \frac{\hbar}{\sigma_z\sigma_p} \leq 1. \tag{5.144}$$

The time evolutions of the average kinetic energy and potential energy of the molecules can be computed from the following,

$$\langle\hat{K}(t)\rangle = \int\int \frac{p^2}{2M}W_n(z,p,t)dzdp \tag{5.145}$$

$$\langle\hat{V}(t)\rangle = \int\int \frac{M\omega^2z^2}{2}W_n(z,p,t)dzdp \tag{5.146}$$

From Eq.5.136, we see that the Wigner function maintains its shape while it rotates in the phase space with angular velocity $\omega = d\phi/dt$. Thus, a Wigner function with a large initial momentum width can be reduced at the expense of increasing its spatial width by

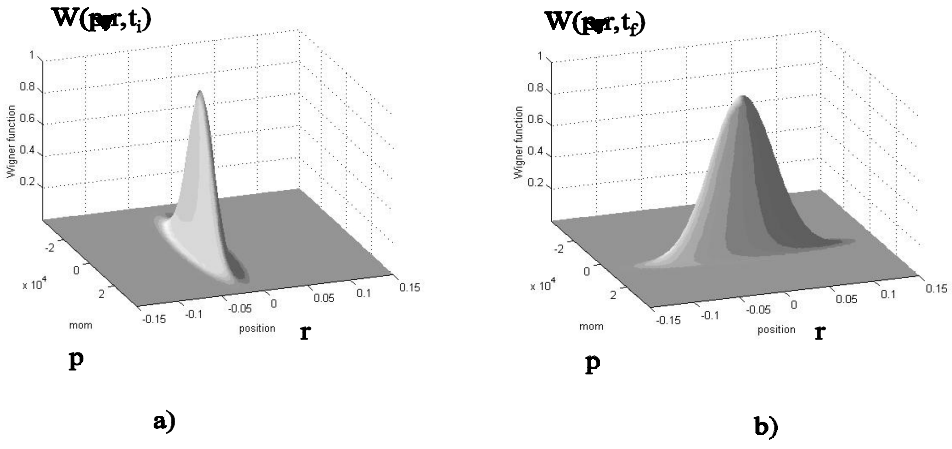

Figure 5.12: Momentum squeezing effect. Wigner function for a)initial narrow spatial width and large momentum width and b)final large spatial width and narrow momentum width.

performing a rotation of $\Delta\phi = \omega t = 90^o$ which corresponds to duration $t_f = \frac{\pi}{2\omega}$. At this time, the potential is switched off and from Eq. 5.137, the Wigner function becomes

$$W(z,p,t) = e^{-(zM\omega-\bar{p})^2/\sigma_{po}^2} e^{-(\frac{p}{M\omega}+\bar{z})^2/\sigma_{zo}^2} \tag{5.147}$$

with the respective momentum and spatial widths

$$\sigma_{pf} \doteq \sigma_p(t_f) = \sigma_{zo} M\omega \tag{5.148}$$

$$\sigma_{zf} \doteq \sigma_z(t_f) = \sigma_{po}/M\omega \tag{5.149}$$

while the mean momentum and position are respectively

$$\bar{p}_f = -\bar{z}M\omega \tag{5.150}$$

$$\bar{z}_f = \bar{p}/M\omega \tag{5.151}$$

Thus, after 90^o rotation in phase space, the QPS volume of the gas is unchanged $\sigma_{zf}\sigma_{pf} = \sigma_{zo}\sigma_{po}$.

5.7.2 Conditions for Momentum Squeezing/Bunching

We define a parameter

$$\chi \doteq \sigma_{pf}/\sigma_{po} = M\omega\sigma_{zo}/\sigma_{po} \tag{5.152}$$

which gives the *momentum squeezing* condition when $\chi < 1$ $(\sigma_{zo}/\sigma_{po} < 1/M\omega)$ and *momentum bunching* when $\chi > 1 (\sigma_{zo}/\sigma_{po} > 1/M\omega)$.

In principle, we can obtain arbitrarily narrow momentum but with large spatial width within the condition Eq. 5.143. However, in practice final spatial width $\sigma_{z\,\max} > \sigma_{zf}$

must be within the typical dimension of the trap size to ensure that the molecules do not traverse beyond the harmonic trapping potential. Besides, there is a minimum initial spatial width from effusive source of the gas. For an initial velocity width of $\Delta u_o = \sigma_{po}/M$, we have the practical momentum squeezing conditions

$$\omega\sigma_{zo} < \Delta u_o < \omega\sigma_{z\,\max} \tag{5.153}$$

If the squeezing condition of Eq. 5.153 is satisfied, a small initial position spread σ_{zo} leads to small final momentum spread σ_{pf}. Substantial kinetic energy has been transformed to the potential energy. We can show that at time t_f, the average kinetic energy, Eq. 5.145 is minimal while the potential energy, Eq. 5.146 is maximal. When the harmonic potential is switched off at this time, the potential energy is reduced to zero and we end up with the molecules with a lower kinetic energy. This can be understood since the faster molecule traverses a longer distance and converts more of its kinetic energy to potential energy than the slower one.

The momentum squeezing effect in the Wigner function from the initial distribution (Eq. 5.132) to final distribution (Eq. 5.147) with narrow momentum width is simulated in Fig. 5.12. Although the QPS volume and the entropy of the molecules are conserved in this unitary dynamics [109], the average kinetic energy is reduced at the expense of increasing the average potential energy. Since the Wigner function evolves continuously immediately before and after time t_f so does the density operator; and the entropy is unchanged by the sudden turn off of the potential.

5.7.3 Practical Considerations

We assume that the molecules can be prepared in a trapping state where they experience a harmonic potential, and in an untrapped state where they do not 'see' the potential. Figure 5.13 shows two methods for obtaining the initial distribution with a narrow spatial width. Buffer gas cooled molecules trapped in a magnetic field can be used as precursor. But, it is practically hard to switch the magnetic field in a timely and rapid manner. So, we do not alter the trapping field but instead uses lasers to switch the molecules between trapping and untrapping states (Fig. 5.13a). Spatially focused and overlapping STIRAP laser beams can be used to rapidly 'switching on' a spatially narrow pulse of molecules (width $\sigma_{zo} \approx 0.1mm$) by transferring the population into a trapping state of the harmonic potential. After time t_f, we transfer the molecules back to the untrapping state with another laser, with broader width. The dimension of the trapping potential sets the upper bound for the final spatial width of the momentum squeezed molecules as $\sigma_{z\,\max} \approx 10cm$. From inequality Eq. 5.153, we obtain the practical range for the trapping

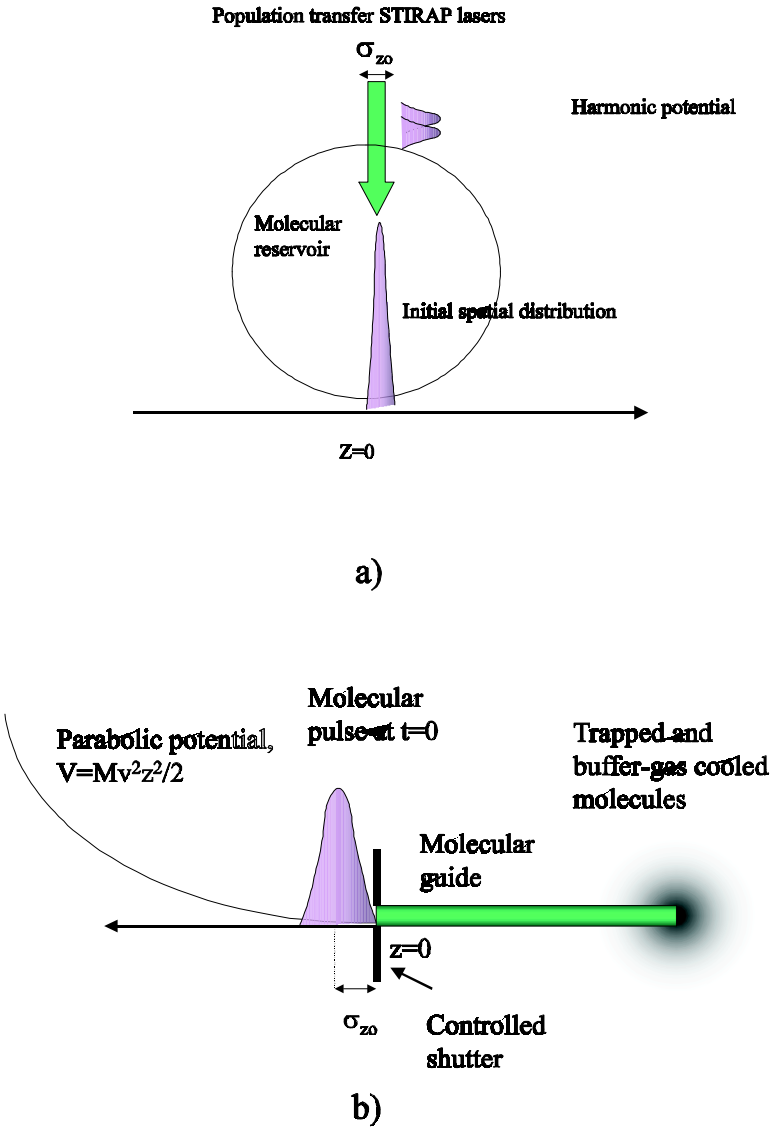

Figure 5.13: Methods of producing a spatially squeezed initial ensemble of molecular gas. a)using STIRAP b) using guides for molecules.

frequency $10^2 s^{-1} < \omega < 10^5 s^{-1}$. If we use $\omega = 500 s^{-1}$, we have $\sigma_{zf} = \frac{10 m s^{-1}}{500 s^{-1}} = 20mm$ and $\sigma_{pf}/M = 5cms^{-1}$. The momentum squeezing concept discussed above can be extended to 2 and 3 dimensions. A second method of producing narrow pulse of molecules is by using a magnetic guide [119] or hollow beam fiber [120] to release a pulse of molecules as shown in Fig. 5.13b.

5.7.4 Repeated Squeezing

We can repeat the squeezing process for another quarter period using a new trap frequency ω_2 with Eqs. 5.147 as the initial conditions,

$$W(z,p,t) = e^{-(zM\omega - \bar{p})^2/\sigma_{po}^2} e^{-(\frac{p}{M\omega} + \bar{z})^2/\sigma_{zo}^2} \tag{5.154}$$

Thus, the second squeezing process gives with the respective momentum and spatial widths $\sigma_{pf2} \doteq \sigma_{zf} M\omega_2 = \sigma_{po}\omega_2/\omega, \sigma_{zf2} \doteq \sigma_{pf}/M\omega_2 = \sigma_{zo}\omega/\omega_2$. We proceed with the third squeezing process using the trap frequency ω_3 and obtain $\sigma_{pf3} \doteq \sigma_{zf2} M\omega_3 = \sigma_{zo} M\omega_3\omega/\omega_2, \sigma_{zf3} \doteq \sigma_{pf2}/M\omega_3 = \sigma_{po}\omega_2/(M\omega_3\omega)$. The fourth squeezing process gives $\sigma_{pf4} \doteq \sigma_{zf3} M\omega_4 = \sigma_{po}\omega_4\omega_2/(\omega_3\omega)$ and $\sigma_{zf4} \doteq \sigma_{pf3}/M\omega_4 = \sigma_{zo}\omega_3\omega/\omega_2\omega_4$, and so on.

Generally, for $n \geqslant 0$ we can write

$$\sigma_{pf(2n+1)} \doteq \sigma_{zo} M \prod_{i=0}^{n} \omega_{(2i+1)} / \prod_{i=0}^{n} \omega_{(2i)} \tag{5.155}$$

$$\sigma_{pf(2n+2)} \doteq \sigma_{po} \prod_{i=0}^{n} \omega_{(2i+2)} / \prod_{i=0}^{n} \omega_{(2i+1)} \tag{5.156}$$

If we let all frequencies of the even processes the same as $\omega_{(2i+2)} = \omega_{even}$ and all frequencies of the odd processes the same as $\omega_{(2i+1)} = \omega_{odd}$ we have

$$\sigma_{pf(2n+2)} \doteq \sigma_{po} (\omega_{even}/\omega_{odd})^n \tag{5.157}$$

Provided that we instantaneously change between a large trap frequency ω_{odd} and a low trap frequency $\omega_{even} < \omega_{odd}$ for a large number of cycles $n \to \infty$, we obtain very narrow momentum width $\sigma_{pf(2n+2)} \to 0$. On the other hand, we can achieve vary narrow spatial compression of a large volume of gas by using $\omega_{even} > \omega_{odd}$. In the end of spatial compression, we obtain a dense hot gas with very large momentum width. By thermalizing the hot gas with buffer gas, entropy can be removed from the hot gas and we have a cold gas with thermal temperature around $0.05K$.

Chapter 6

Laser Cooling Schemes for Molecules

In this Chapter, we briefly discuss a few preliminary laser cooling schemes for molecules which are possible in principle. We do not elaborate on these schemes because of the difficulties of realizing these schemes from practical point of views. Following this, we elaborate on a more practical laser cooling scheme for molecules using the concepts of velocity selection, deceleration and spontaneous emission. The detailed theories of spontaneous emissions which been presented in Chapter 3, and the Raman velocity selection and STIRAP deceleration presented in Chapter 5 are applied to represent these concepts. The detailed scheme and laser parameters depend on the internal structures of the molecule. We apply the knowledge of molecular physics for diatomic molecules presented in Chapter 2 to estimate the cooling parameters for real hydroxyl (OH) molecules.

6.1 Preliminary Laser Cooling Schemes

In using laser for cooling the translational motion of molecules, we rely on three aspects: 1) *linear* momentum transfer between photons and molecules, 2) repetition of momentum reduction process 3) irreversibility. This is mediated by the absorption and emission processes where momentum and energy are conserved. The most probable and strongest radiative processes are through the dipole coupling.

From previous chapters, some important conclusions related to molecule-radiation processes should be emphasized. The presence of the additional rotational and vibrational motions in molecules lead to the more closely spaced rotational and vibrational energy levels in addition to the electronic levels present only in atoms. Thus, the molecule-radiation processes involve photons with lower frequencies (in infrared and microwave regime) in addition to the optical frequencies. The levels are not evenly spaced, so the dipole transitions involve many different frequencies of photons. That means, repeated laser pumping would require multi-frequency lasers.

Moreover, spontaneous emissions from an excited electronic state or fluorescence will distribute the populations to many rotational and vibrational levels. Spontaneous emissions from vibrational and rotational transitions are much slower than optical spontaneous emission. From Chapter 4, we found that the cooling rate is measured by the entropy production rate which is proportional to the spontaneous emission rate while the kinetic energy removal rate which is proportional to the light force. This means that rotational transitions within a vibronic state is too slow to be practically applicable, although it forms a closed two level system. In the following, we consider a few 'primitive' cooling schemes for heteronuclear diatomics.

6.1.1 Scheme 1-Electronic-Vibrational Transitions

In this scheme, we choose the ground states in the ground electronic state $|g_v\rangle = |X, \{v = 0, 1, 2, .., N\}, J = 1\rangle$ coupled to a single excited state in an excited electronic state $|e\rangle = |A, v' = 0, J' = 0\rangle$ by a number N of lasers to form a set of closed optical pumping cycles, where N depends on the Franck-Condon branching factors of a chosen molecule (see Fig. 6.1a). For some molecules where the internuclear distances at the minimum of the two electronic potentials almost coincide, only a few vibrational levels are occupied by spontaneous emissions (fluorescence) from $|e\rangle$. If the minimums are widely separated, the fluorescence may populate a large number of vibrational levels.

Since only one rotational level with $J = 1$ is occupied within each vibrational level, we only need N lasers with different frequencies given by

$$v_v = v_{AX} - \omega_e v(1 - x_e) + \omega_e x_e v^2 - 2B_e + 2\alpha_e(v + \frac{1}{2}) \tag{6.1}$$

If we choose $|\Sigma\rangle = |X\rangle$ and $|\Pi\rangle = |A\rangle$, the ground electronic state has $\Lambda = 0$, with $J \geq (\Omega = |0 + \Sigma|)$ and excited electronic state has $\Lambda' = 1$, with $J' \geq (\Omega' = |1 + \Sigma|)$ via selection rule $\Delta\Lambda = 1$. From angular momentum selection rule ($\Delta J = \pm 1$),we use an excited state with $J' = 0$ which decays spontaneously via dipole transition only to $J = 1$, (corresponding to P(1) line), this requires that $\Sigma = -1$, $S \geq 1$ (since $-S \leq \Sigma \leq S$). Thus, the state with $S = 0$ is unapplicable. We can use ${}^{3,5..}\Sigma_{0,1,2,3..}$ and ${}^{3,5}\Pi_{0,1,2,3..}$as the ground and excited states respectively.

Taking into account the possible transitions to magnetic sublevels with the selection rules $\Delta M_J = 0, \pm 1$ actually we need a total of 3N lasers, with σ^+, σ^- and linearly polarized for each frequency. The downward transitions via optical spontaneous emissions (fluorescence) populate three magnetic substates only $|\sum, v, J = 1, M = 0, \pm 1\rangle$ and a number of N vibrational states. Thus, the cooling scheme involves a total number of $3N + 1$ molecular states.

For heteronuclear diatomic molecules, the loss of populations to other states by vibrational-rotation spontaneous emissions may occur. This can be prevented since the Rabi frequencies of the optical pumping is typically $10^7 s^{-1} - 10^8 s^{-1}$, much larger than the

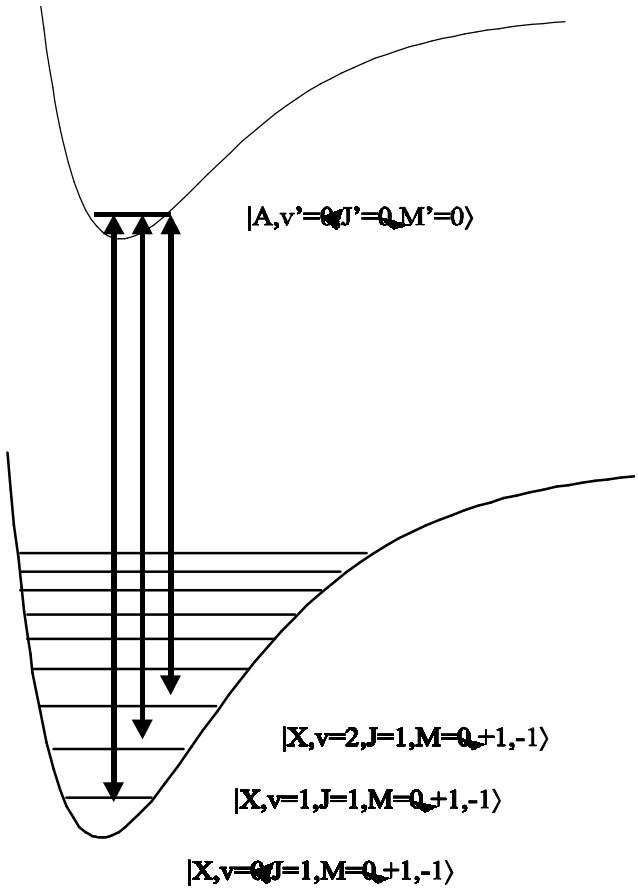

Figure 6.1: Preliminary laser cooling scheme 1 uses many optical lasers to pump the populations to the ground vibrational state in an excited electronic state.

infrared decay rate $10^2 s^{-1} - 10^3 s^{-1}$. For efficient Doppler cooling, low laser intensity is used. This also ensures that the laser of a particular frequency excites only the designated transition and avoid multiphoton processes [192]. The frequencies of the lasers are not exactly equally spaced due to the anharmonicity of the vibrational levels.

There are two challenges for this scheme. First, the requirement for many lasers poses a major practical difficulty. Only for molecules where the minimum potential curve of the electronic states almost coincide, it is possible to have a few vibrational states involved for cooling. Second, the cooling process requires thousands of repeated pumping cycle and the efficiency will drop even if a very small fraction of the populations fall into states which are not pumped up by laser. Thus, the cooling scheme requires precise data of the Franck-Condon population distribution. This scheme is similar to the proposal in Ref. [59].

6.1.2 Scheme 2-Vibrational-Rotational Transitions

We consider the pumping cycle between the three ground states $|g0,\pm\rangle \equiv |^1\Sigma, v = 0, J = 1, M = 0, \pm 1\rangle$ and one excited state $|^1\Sigma, v = 1, J = 0, M = 0\rangle$ within the ground electronic state. The four rovibrational states form a closed pumping cycle. Three infrared lasers with σ^+, σ^- and *linear* polarizations couple the ground states to the excited state (see Fig. 6.2). The direction of the *linear* polarized laser is orthogonal to the σ^+ and σ^- polarized lasers. However, parallel $\sigma^+ - \sigma^-$ and antiparallel $\sigma^+ - \sigma^-$ give different kinetic effects on the momentum distributions. For antiparallel $\sigma^+ - \sigma^-$ polarized lasers, half of the population form the dark trapping state of $|NC\rangle$ while the other half in the superposition of state $|C\rangle$ is pumped to $|g0\rangle$, which would be repumped back to $|g+\rangle$ and $|g-\rangle$ by the linearly polarized laser.

Alternatively, with a magnetic field the degeneracy in the ground level is lifted and we have four levels Λ system. Here, we can couple $|g_0\rangle$ to $|e\rangle$ using a linear polarized laser, and couple $|g_0\rangle \leftrightarrow |g_1\rangle$ and $|g_0\rangle \leftrightarrow |g_{-1}\rangle$ using $\sigma^+ - \sigma^-$ polarized masers to form a closed pumping cycle, similar to the scheme of Ref. [97]. The main practical difficulty of this scheme is the long cooling time due to the slow infrared spontaneous decay rate and more cooling cycles are required. The magnitude of the momentum transfer from infrared photon is about $10-50$ times smaller than optical photon during absorption. So, the scheme requires $10-50$ times more number of pumping cycles to effectively reduce the momentum of the molecules compared to using optical lasers. Besides, the infrared spontaneous emissions rate is typically 10^4 times slower than optical decay rate.

The scheme can be modified to provide larger momentum transfer if we use optical transitions. The direct one-photon rovibrational transitions can be replaced by the Λ scheme via an excited electronic state. Thus, larger momentum transfers from the two-photon optical transitions can be achieved. The chosen excited electronic states are restricted by the dipole selection rules given in Section 2.6.1.

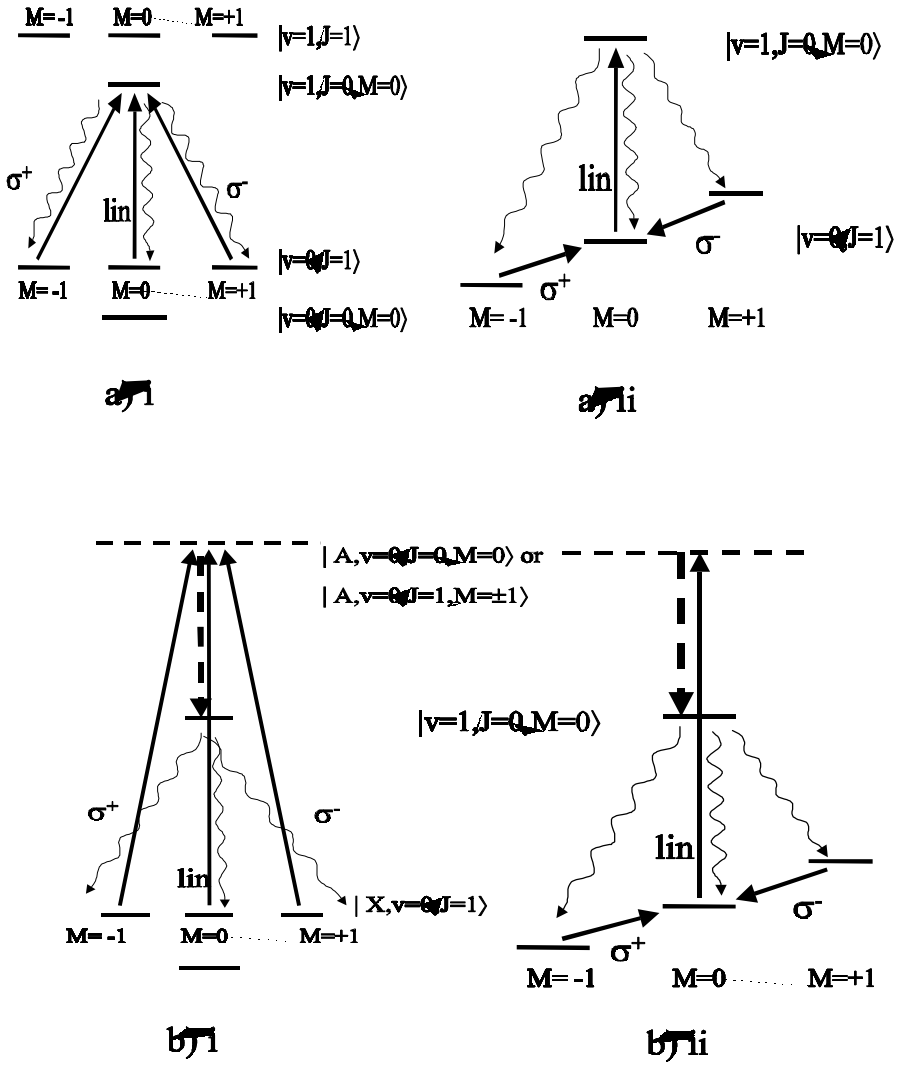

Figure 6.2: Preliminary cooling scheme 2 uses infrared vibrational-rotational transitions. a)i three degenerate ground states are coupled to a single excited state with three IR lasers with different polarizations and a single frequency. a)ii degeneracy is lifted and the levels are coupled by a single linearly polarized IR laser and two circularly polarized masers. b)i and b)ii are the corresponding modified schemes which provide larger momentum transfer. Optical two-photon transitions replace the one-photon infrared transitions. Only one additional Stokes laser is required.

6.2 Laser Cooling of Molecules by Zero Velocity Selection

We present a general laser cooling scheme using simple well-known techniques. The scheme overcomes the problem of closed pumping cycle and repeated spontaneous emissions. In Section 6.2.1, we outline the cooling idea, the steps and laser techniques. The initial setup and preparation of the precursor molecules for laser cooling are discussed in Section 6.2.2. The first cooling step (zero velocity selection) is elaborated in Section 6.2.3. We apply the optimum conditions for the zero velocity selection to estimate the operational parameters and cooling performance using real OH molecules. The spectroscopic data for OH molecule is available in quite detailed [178]. Similarly, the second step, STIRAP deceleration process is elaborated in Section 6.2.4 along with operational parameters *(in S.I. units)* and numerical estimates. The details of the accumulation process (third step) are presented in Section 6.2.5. We also estimate the overall cooling time and spatial drift, which may be of practical interests. The results of simulations with OH molecules using the density matrix equations are discussed. Finally, we present the modelling of the cooling process with analytical density matrix equations and compute the time evolutions of the internal and center of mass entropies.

6.2.1 New Laser Cooling Concept

Let us first describe the general idea (Fig. 6.3) behind the cooling concept, which need not necessarily use lasers. It is the repetition of a cooling cycle, each composed of three steps: *zero velocity selection, deceleration and accumulation.* In the first step, a narrow velocity width with *zero* mean velocity is selected from a translationally hot gas of molecules in a state $|g_i\rangle$ and coherently transferred to a decaying state $|d\rangle$. In order to repeatedly extract the narrow zero velocity population from $|g_i\rangle$ we need to fill up the population around the zero velocity after each zero velocity selection step. This is the purpose of the second step (deceleration). It can be done either by thermalization process, or momentum deceleration whereby the remaining population reservoir in $|g_i\rangle$ is translated in momentum space by an mount ΔP_{dec} roughly equal to the selected momentum width, ΔP_{vs}. This creates a finite population around zero momentum for the next cycle of zero velocity selection. Finally (third step), in order to repeatedly accumulate the narrow velocity populations, we need an irreversible process.

We shall demonstrate the applicability of the cooling concept by using simple laser pumping techniques on a levels scheme in OH molecules. Each *cooling cycle* is composed of a sequence of the three steps:1)zero velocity selection with Raman π-pulses [313], [314], 2) deceleration with STIRAP [265], and 3) accumulation by single optical spontaneous emission, as shown in Fig. 6.4. Although the laser techniques of this cooling scheme are similar to our previous work [1], there are two major differences in the way populations are selected, decelerated and accumulated. First, the velocity selection is performed around zero velocity instead of non-zero velocity. Second, we decelerate the initial (hot) population of

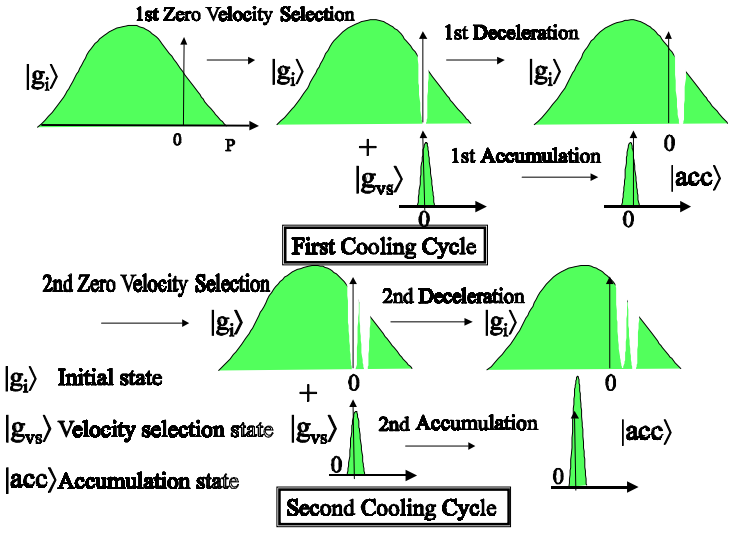

Figure 6.3: Idea of the new cooling concept based on zero velocity selection, deceleration and accumulation. The schematic shows the expected momentum distribution in the first two cycles of the cooling process.

gas instead of the narrow velocity selected population, by using only two STIRAP processes. Thus, the cooling time in each cycle is considerably shortened by the reduced number of STIRAP processes compared to the previous scheme. In our previous work, the velocity selection is *not* around zero velocity. Therefore, extensive deceleration is required to bring the mean momentum to zero in each cooling cycle by using many (hundreds) of STIRAP pulses. Thus, the present scheme has the advantage from the practical point of view. In this scheme, we also include the real numerical data of OH for the simulations.

6.2.2 Initial Setup

Before discussing each cooling step in details, we elaborate on the preparation of the initial precursor molecules in a proposed setup. We assume that a gas of molecules effused out slowly from a source has finite population around zero momentum, as shown in Fig. 6.6. The molecules occupy essentially a single molecular level $|g_i\rangle$ (but possibly in different magnetic substates). The initial density operator which includes the internal and the external center of mass (c.m.) states is written as

$$\hat{\rho}_{tot}(0) = \hat{\rho}_I(0) \otimes \hat{\rho}_{cm}(0) = |g_i\rangle\langle g_i| \otimes \sum_P W(P)|P\rangle\langle P| \tag{6.2}$$

where $W(P) = \frac{1}{\sqrt{\pi}\sigma_i} \exp\{-(P - \Delta P_i)^2/\sigma_i^2\}$ is the Gaussian momentum distribution, and $\Delta P_i = 2\sqrt{\ln 2}\sigma_i = \sqrt{2Mk_BT_i}$ is defined as the momentum width at half maximum with

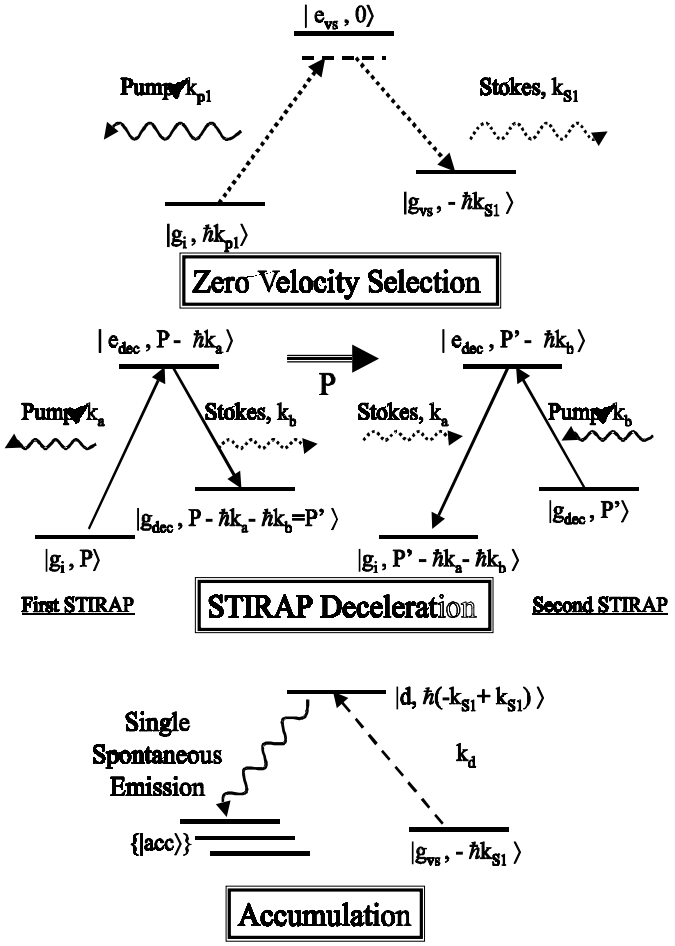

Figure 6.4: Internal and momentum states for the laser cooling scheme with Raman zero velocity selection, double STIRAP inversions for deceleration and single optical spontaneous emission for accumulation. Also shown are the wavevectors of the lasers, k_{p1}, k_{S1}, k_a, k_b, and k_d.

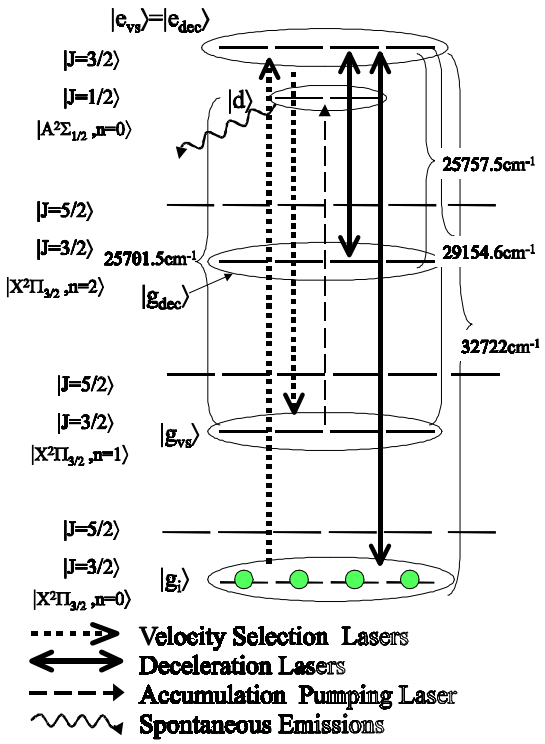

Figure 6.5: Relevent energy levels (in wavenumbers) and states of OH molecules for laser cooling. The group of magnetic substates are shown coupled by the cooling lasers for zero velocity selection, STIRAP deceleration and irreversible accumulation steps.

effective axial translational temperature T_i. The Stark deceleration of supersonic molecular beam [67] and buffer gas thermalization [64] techniques have produced cold molecules at about 0.05K with density of 10^7molecules/cm^3. These molecules are essentially in a single vibrational and rotational level in the ground electronic state, but may be in several magnetic quantum states. They can serve as the precursors for further cooling to temperature of μK or below using this laser cooling scheme.

Here, we use OH molecules as an example to study and demonstrate the feasibility of the laser cooling scheme. The necessary energy levels and states are shown in Fig.6.5. At close to thermal equilibrium temperature of $T_i = 1K$, only the states $|X^2\Pi_{3/2}, n = 0, J = \frac{3}{2}, \Omega = \pm\frac{3}{2}, M_J = \pm\frac{1}{2}, \pm\frac{3}{2}\rangle$ are appreciably populated [121], which can be designated as $|g_i\rangle$.

In the absence of trapping, the molecules undergo free spatial expansion beyond the laser interaction region and the entropy increases indefinitely as $k_B \ln(V/V_o)$ [293], where $V_o = Az_o$ is the initial gas volume. The phase-space density would hardly increase even if the momentum width is reduced by laser cooling. Trapping is required to fix the spatial density as we reduce the momentum width. But the molecules in $|\Omega = \pm\frac{3}{2}, M_J = \mp\frac{1}{2}, \mp\frac{3}{2}\rangle$ are low field seekers while those in $|\Omega = \pm\frac{3}{2}, M_J = \pm\frac{1}{2}, \pm\frac{3}{2}\rangle$ are high field seekers [121]. Electro-

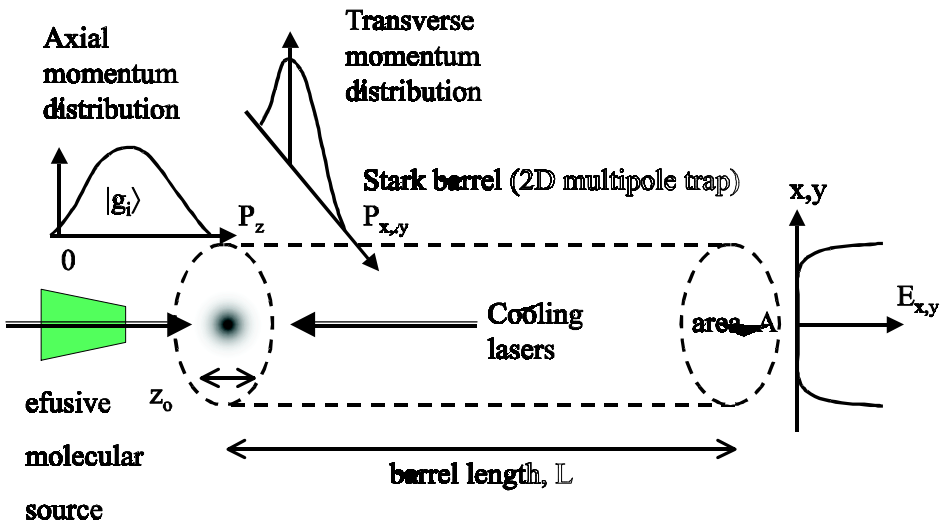

Figure 6.6: Proposed setup apparatus for the laser cooling scheme with initial momentum distribution, the Stark barrel for two dimensional trapping and the directions of the cooling lasers.

dynamic trap [310] can trap both low field and high field seekers simultaneously. Here, we are concerned with the trapping of the low field seekers only. We use the Stark barrel [312] which provides two-dimensional trapping for the molecules with transverse(radial) kinetic energy $\lesssim 1K$ in an essentially homogeneous field area A (Fig. 6.6). The axial momentum component of the molecules is reduced by the laser cooling process. There is no potential barrier or trapping potential along the axial direction to avoid any change in the axial momentum distribution during the laser cooling process. The fastest molecules are decelerated to zero axial velocity in the end of cooling, have maximum drift distance, $z_{\max}$. Thus, the length L of the barrel should be larger than $z_{\max}$ and we define $L \doteq z_o + z_{\max}$.

6.2.3 Step 1: Zero Velocity Selection

Raman velocity selective π-pulses technique is used to transfer a fraction of population with a narrow momentum width ΔP_{vs}, around *zero* momentum family (Fig. 6.4) from the 'hot reservoir' state $|g_i, \hbar k_{p1}\rangle$ to an empty state $|g_{vs}, -\hbar k_{S1}\rangle$ via the intermediate excited electronic state $|e_{vs}, 0\rangle$ in a three-level Λ system. The pump and Stokes lasers are counter-propagating, with wavevectors k_{p1} and k_{S1}, and the corresponding Rabi frequencies Ω_{p1} and Ω_{S1} respectively. Complete population transfer of the narrow momentum width ΔP_{vs} around P_{vs} occurs when 3 conditions are satisfied:

- Raman resonance

- Large one photon detuning
- π-pulse consition.

The theory of velocity selection has been presented in previous chapter. We use the results for the foregoing analysis.

The *effective temperature* associated with the velocity selected width $\Delta v_{vs} = \Delta P_{vs}/M$ is defined as $T_{vs} = M(\Delta v_{vs})^2/2k_B$. For the gas with distribution of Eq. 6.2, with initial velocity width Δv_i, we define the maximum velocity as $u_{\max} \doteq 2\Delta v_i = 2\sqrt{2k_BT_i/M}$. The total number of velocity selection cycles (which is the number of cooling cycles) can be predicted as

$$N_{cyc} = \frac{u_{\max}}{2\Delta v_{vs}} = \frac{\Delta v_i}{\Delta v_{vs}} = \frac{|\Delta_{vs}|(k_{p1} + k_{S1})}{0.6092 \times 8\Omega_{o1}^2}\sqrt{\frac{2k_BT_i}{M}} \tag{6.3}$$

If the pulse duration for each cycle is the same, we obtain the *total time* for velocity selection step in the cooling process

$$N_{cyc}\tau_1 = \frac{\pi|\Delta_{vs}|^2(k_{p1} + k_{S1})}{0.37 \times 8\Omega_{o1}^4}\sqrt{\frac{2k_BT_i}{M}} \tag{6.4}$$

In practice, it is desirable to have fast velocity selection process which requires short pulse duration and higher power lasers. However, shorter pulse duration leads to wider selected width and higher T_{vs}. An arbitrarily narrow velocity width corresponds to small Rabi frequency (Eq. 5.105), large number of cooling cycles (Eq. 6.3) and long total cooling time (Eq. 6.4). For optimal cooling, we should minimize the product of the cooling time $N_{cyc}\tau_1$and the effective temperature T_{vs}, which can be regarded as the 'merit' for velocity selection

$$N_{cyc}\tau_1 T_{vs} = \pi\sqrt{\frac{1}{2}Mk_BT_i}\frac{1}{(k_{p1} + k_{S1})} \tag{6.5}$$

The result Eq. 6.5 shows that levels scheme with large transition frequency enables the use of high frequency (optical or near UV) lasers are best suited for the velocity selection step.

Zero Velocity Selection Parameters for OH

The levels spacing between two lowest rovibrational states ($|v = 0, J = 1/2\rangle$ and $|v = 0, J = 3/2\rangle$) in the excited electronic state $|A^2\Sigma_{1/2}\rangle$ (Fig 6.5) is about $10^{13}s^{-1}$. If we apply a negative detuning of $\Delta = -10^{11}s^{-1}$ relative to the level $|v = 0, J = 3/2\rangle$, it is a

hundred times closer to $|v=0, J=1/2\rangle$ than $|v=0, J=3/2\rangle$. Thus, the velocity selection scheme can well be described by a three level Λ system since the lower level, $|v=0, J=1/2\rangle$ can be disregarded. The detuning is much larger than the typical Rabi frequency and the linewidth of the level, so the excited states are not populated during velocity selection.

The transition coefficients for transitions $(J=3/2, M=\pm 1/2 \leftrightarrow J=3/2, M=\pm 1/2)$ is $\alpha_{1/2}=\frac{1}{15}$ while for transitions $(J=3/2, M=\pm 3/2 \leftrightarrow J=3/2, M=\pm 3/2)$ is $\alpha_{3/2}=\frac{3}{5}$. Even though the coefficients are different, the π-pulse concept can still be applied to transfer the entire velocity selected populations from the four substates in $|g_i\rangle$ to $|g_{vs}\rangle$ because the ratio of the coefficients is an *odd* integer $\alpha_{3/2}/\alpha_{1/2}=9$. Since the laser pulse duration τ_1, the dipole moment d and laser fields $E_2(t)$ are the same for both substates. From the definition of Rabi frequency $\Omega_i \doteq dE_iC_i$, where C_i is related to the transition coefficient by $\alpha_i = C_iC_i^*$ and Eq. 5.97, we have $\frac{2n_1-1}{2n_2-1}=\frac{\alpha_1}{\alpha_2}=9$ which gives the complete population transfer for both substates for $n_{1/2}=1$ (corresponds to the πpulse) and $n_{3/2}=5$ (corresponds to 5π pulse) with $\tau_1 = |\Delta_{vs}|\pi/(0.6092\frac{1}{15}d^2E_{o1}^2)$.

This enables velocity selection from the four ground states $|g_i\rangle = |X^2\Pi_{3/2}, v=0, J=3/2, M=\pm 1/2, \pm 3/2\rangle$ to be performed concurrently to $|g_{vs}\rangle = |X^2\Pi_{3/2}, v=1, J=3/2, M=\pm 1/2, \pm 3/2\rangle$ which are essentially empty, via the intermediate excited states $|e_{vs}\rangle = |A^2\Sigma_{1/2}, v=0, J=3/2, M=\pm 1/2, \pm 3/2\rangle$, with the transition angular frequencies (in S.I. unit of s^{-1}) $\omega_{e_{vs},g_i} = 6.163\,7\times 10^{15}s^{-1}, \omega_{e_{vs}g_{vs}} = 5.491\,7\times 10^{15}s^{-1}$[177]. We need only two *linearly polarized* lasers, the pump and the Stokes to couple *parallel transitions states*. Suppose we fix the pump laser frequency at $\omega_{p1}=6.1636\times 10^{15}s^{-1}$(corresponds to $\Delta_p = \omega_{p1}-\omega_{e_{vs},g_i} = -10^{11}s^{-1}$), the Raman resonance condition (Eq. 5.88) gives the Stokes frequency $\omega_{S1}=5.4916\times 10^{15}s^{-1}$.

We select the momentum width of $\Delta P_{vs}=\hbar(k_{p1}+k_{S1})$ which corresponds to velocity width $\Delta v_{vs}=\Delta P_{vs}/M=14.5cms^{-1}$ and effective temperature $T_{vs}=\frac{1}{2}M(\Delta v_{vs})^2/k_B \approx 21\mu K$. From Eq. 5.105, the required Rabi frequency is $\Omega_{op1}=\Omega_{oS1}=3.4\times 10^8 s^{-1}$, which satisfies the condition $\Delta >> \Omega_{o1}, (\Gamma \approx 1.5\times 10^6 s^{-1})$ that avoids populating the excited state. From Eq. 5.104, we obtain the required pulse duration $\tau_1 = 4.45\mu s$. If we start from the temperature $T_i = 1K$ with velocity width $\Delta v_i \approx 31ms^{-1}$and maximum velocity of $u_{\max} \approx 62ms^{-1}$, we need about $N_{cyc} \approx 215$ cycles. The total velocity selection time required is $t_1 = N_{cyc}\tau_1 \approx 1ms$.

6.2.4 Step 2: Deceleration by STIRAP

This step is intended to create a finite population around zero momentum for the next cycle of zero velocity selection. In principle, non-optical deceleration technique can be applied [67]. However, STIRAP process is simple and provides rapid removal of kinetic energy with high deceleration/acceleration up to $10^5 ms^{-2}$. It has been demonstrated experimentally to be highly efficient for molecules, like Na_2 [285], NO [287] and SO_2 [286].

The remaining 'hot' population in $|g_i\rangle$ is transferred to the empty state $|g_{dec}\rangle$

through an excited state $|e_{dec}\rangle$, and back to $|g_i\rangle$. This corresponds to only two STIRAP processes. Each STIRAP process is accompanied by the photon momentum transfer of $\hbar(k_a+k_b)$ along the pump laser direction [282]. The momentum transfers can be tailored to decelerate the remaining population in $|g_i\rangle$ by roughly equal the selected momentum width $\Delta P_{dec} \gtrsim \Delta P_{vs}$. Although closed optical pumping cycle for *dissipation* is not possible in molecules, this step shows that it is possible to have a *closed pumping cycle for a coherent process*, particularly for removing the kinetic energy.

The STIRAP uses a pair of counter-propagating laser pulses, with frequencies ω_a and ω_b resonantly coupled to the transitions $|g_i\rangle \leftrightarrow |e_{dec}\rangle$ and $|g_{dec}\rangle \leftrightarrow |e_{dec}\rangle$ respectively. *Complete population transfer* from $|g_i\rangle$ to another state $|g_{dec}\rangle$ via an excited state $|e_{dec}\rangle$ can be achieved with three conditions:

- First, the Stokes pulse (with wavevector $k_{S2} = k_b$) overlaps in time with the pump pulse ($k_{p2} = k_b$) but always reaches the molecules before the pump pulse (*counter-intuitive order*). For the typical Gaussian pulse shape, the time dependent Rabi frequencies can be represented by

$$\begin{aligned} \Omega_{S2} &= \Omega_{S2o} \exp\{-(t-2.5\sigma_S)^2/\sigma_S^2\} \\ \Omega_{p2} &= \Omega_{p2o} \exp\{-(t-(2.5\sigma_p+\Upsilon))^2/\sigma_p^2\} \end{aligned} \tag{6.6}$$

where $\Omega_{p2o} \doteq \frac{1}{\hbar}E_{po}\langle g_i|\hat{d}|e_{dec}\rangle, \Omega_{S2o} \doteq \frac{1}{\hbar}E_{So}\langle e_{dec}|\hat{d}|g_{dec}\rangle$ are the pump and Stokes Rabi frequency amplitudes for STIRAP pulses and $\sigma_{p,S}$ are the pulses standard deviations and $\Upsilon = \sqrt{\ln 2}(\sigma_p + \sigma_S)$ is the temporal separation of the peaks which gives overlap at the half maxima of both pulses.

- The second condition is that the laser frequencies are tuned to resonant.
- Third, is the adiabatic criteria[281], $\Omega_{o2}\tau_2 >> 1$ which requires that the Rabi frequencies vary sufficiently slow, where $\Omega_{o2} \doteq \sqrt{\Omega_{p2o}^2 + \Omega_{S2o}^2}$ and $\tau_2 = (2.5+\sqrt{\ln 2})(\sigma_S+\sigma_p)$ is the interaction duration.

The second STIRAP process is applied by reversing the directions and counter-intuitive order of the laser pulses. The population in $|g_{dec}\rangle$ is transferred back to $|g_i\rangle$ while giving another $\hbar(k_a + k_b)$ of momentum transfer. Here, $k_{S2} = k_b$ and $k_{p2} = k_a$. Thus, the two STIRAP processes constitute 2 inversions which effectively transfer the population back to $|g_i\rangle$ and provide the total momentum transfer of $\Lambda_{dec} \doteq 2\hbar(k_a + k_b)$ to the entire reservoir population (see Fig. 6.4).

STIRAP Deceleration Parameters for OH

In order to maximize the cooling efficiency, the momentum transfer from the STIRAP deceleration step $\Delta P_{dec} = 2\hbar(k_a + k_b)$ (see Fig. 6.4) should be as close as possible

to $2\Delta P_{vs}$. This ensures that a maximum population is transferred to $|g_{vs}\rangle$ in each velocity selection step while leaving a minimum residual of population in $|g_i\rangle$ after the cooling process.

From previous section, $\Delta P_{vs} \approx \hbar(k_{p1} + k_{S1})$ and we should choose the state $|g_{dec}\rangle$ and $|e_{dec}\rangle$ such that $(k_a + k_b) \approx (k_{p1} + k_{S1})$. For convenience, we let $|e_{dec}\rangle = |e_{vs}\rangle$ so that $k_a \approx k_{p1}$(see Fig.6.5) and we require $k_b \approx k_{S1}$. This is fulfilled by choosing the states at a higher vibrational level as $|g_{dec}\rangle = |X^2\Pi_{3/2}, n_{dec} = 2, J = 3/2, M = \pm 1/2, \pm 3/2\rangle$. Since the states $|g_{dec}\rangle$ and $|g_{vs}\rangle$ are different, the deceleration step and accumulation step (pumping up $|g_{vs}\rangle$ to $|d\rangle$) can proceed simultaneously. For STIRAP with one-photon resonance, this gives $\omega_a = \omega_{e_{dec},gi} = 6.163\,7 \times 10^{15} s^{-1}$ and $\omega_b = \omega_{e_{dec},g_{dec}} = 4.851\,8 \times 10^{15} s^{-1}$. The Rabi frequency of the pulse can be large and contributes to the finite spectral width $\Delta\omega \approx \Omega_{o2}$ due to the light shift, but this should be much smaller than rotational level spacing $2\pi c B_e \approx 10^{12} s^{-1}$ to minimize off-resonant coupling with nearby rotational levels which may lead to imperfect transfer efficiency. Since *only two* STIRAP processes are required for step 2, even the transfer efficiency of 99% for each STIRAP process is sufficiently good.

Simulations of the STIRAP process using density matrix equations including spontaneous emissions but without center of mass momentum have been done in Ref. [289]. In our simulations of the STIRAP deceleration step, we have included both the spontaneous emissions from state $|e_{dec}\rangle$ and the quantization of the center of mass momentum. We obtain perfect transfer efficiency using a moderate peak Rabi frequency $\Omega_{p2o} = \Omega_{S2o} \approx 10^9 s^{-1}$ with the interaction time $t_2 \approx 10^{-7} s$ which corresponds to $\Omega_{o2}\tau_2 \approx 150$. The duration for step 2 is $2\tau_2 \approx 0.2\mu s$, which is close to the lifetime, $\Gamma \approx 0.69\mu s$ of the excited state but about 20 times shorter than each velocity selection cycle. The total STIRAP time for step 2 from all cycles is $t_2 = 2\tau_2 N_{cyc} \approx 0.043ms$, which is negligible compared to the time taken for step 1.

6.2.5 Step 3: Accumulation by Single Spontaneous Emission

In this step, the irreversible process is achieved via *single optical spontaneous emission*. The narrow width population with zero mean momentum in $|g_{vs}\rangle$ is transferred to a decaying (metastable) state $|d\rangle = |A^2\Sigma_{1/2}, n = 0, J = 1/2, M = \pm 1/2\rangle$ by alternating switching between the σ^+ polarized and σ^-polarized lasers of the same frequency $\omega_d = 4.8413 \times 10^{15} s^{-1}$. We use an excited electronic state which has much shorter natural decay lifetime than infrared transitions within the ground electronic states. The two pumping lasers must not be switched on simultaneously to avoid the creation of dark state population that will not be pumped up to $|d\rangle$. The transition coefficient for $(J = 3/2, M = \pm 3/2) \leftrightarrow (J = 1/2, M = \pm 1/2)$ transitions is $\alpha_1 = \frac{1}{2}$ and for $(J = 3/2, M = \pm 1/2) \leftrightarrow (J = 1/2, M = \mp 1/2)$ transitions is $\alpha_2 = \frac{1}{6}$. Even though the coefficients are different, the π-pulse concept is applicable because the ratio of the coefficients is an odd integer (see arguments for Step 2). We can rapidly transfer the population from $|g_{vs}\rangle$ to $|d\rangle$ by using the π-pulse with

Rabi frequency $\Omega_3 >> \Gamma$. Hence, we set the pulse duration as $\tau_3 = 0.1/\Gamma$ which gives $\Omega_3 = 10\pi\Gamma$. Subsequent optical spontaneous decays (fluorescence) populate a number of rotational and vibrational states within the ground electronic states $|X^2\Pi_{3/2}\rangle$ and $|X^2\Sigma_{1/2}\rangle$, designated as the *accumulation states* $\{|acc\rangle\}$. The decaying molecules are translationally cold and decoupled from the lasers. No repeated spontaneous emissions are required for these molecules. The irreversibility of spontaneous emission enables repeated accumulation of the molecules with narrow and zero mean momentum in a number of $\{|acc\rangle\}$ states in the end of each cooling cycle. It is this unique feature which makes translational laser cooling of molecules possible.

We set the sufficient duration for this step as $5\Gamma^{-1} \approx 3.5\mu s$. The total accumulation time is about $t_3 = N_{cyc}5\Gamma^{-1} \approx 0.75ms$. The spontaneous emissions lead to a momentum spread in the order of one photon recoil momentum, but this is negligible compared to the overall reduction of the initial momentum width. The actual momentum shift and variance are dependent on the laser intensity and the Franck-Condon branching factors. We take the final velocity width to be $\Delta v_f \approx \Delta v_{vs} + (\hbar k_{spe}/M) \approx 22cms^{-1}$.

6.2.6 Cooling Results and Parameters

In this section, we present the simulation results for the laser cooling process, estimate the total cooling time, spatial drift and the extend of cooling through effective temperature and spatial density.

We have simulated the cooling process by numerically integrating the density matrix elements equations Eqs. 5.26 which include both the spontaneous emissions (without recoil) from state $|e_{dec}\rangle$ and the quantization of the center of mass momentum. We have used real parameters of OH molecules, the Blackman pulse for velocity selection step and the Gaussian pulse for STIRAP deceleration. The populations distributions are shown in Fig. 6.7 for the first three cooling cycles. After the cooling process, there is a residual population in $|g_i\rangle$ (Fig. 6.8) due to the imperfect velocity selection profile. This may be overcomed by alternating the cooling cycles between zero velocity selection and finite velocity selection. The second velocity selection is at momentum family $\Lambda_{dec}/2 = \hbar(k_a + k_b)/2$ to clear up the residual population. Here, the velocity selection states in Fig (6.4) become $|g_i, \Lambda_{dec}/2 + \hbar k_{p1}\rangle$, $|e_{vs}, \Lambda_{dec}/2\rangle$ and $|g_{vs}, \Lambda_{dec}/2 - \hbar k_{S1} \approx 0\rangle$. The pumping laser to state $|d, P \approx 0\rangle$ is now made orthogonal to the cooling direction so as to impart no further momentum transfer.

The STIRAP deceleration (step 2) may proceed simultaneously with the spontaneous emission (step 3). Since the duration for STIRAP deceleration is usually shorter than the spontaneous emission lifetime, the sufficient duration for each cooling cycle is sum of the required durations for step 1 (velocity selection) and step 3 (the pumping and spontaneous emission), which is $t_{cyc} = \tau_1 + 5\Gamma^{-1} \approx 4.5\mu s + 3.5\mu s = 8\mu s$. The total cooling time from $N_{cyc} = 215$ cooling cycles is

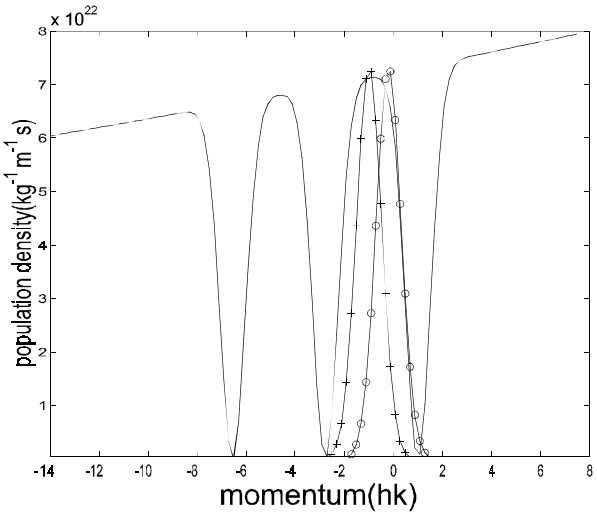

Figure 6.7: Populations of the states $|g_i\rangle$ (——), $|g_{vs}\rangle$ (–+–+–+–) and $|d\rangle$ (–o–o–o–) for OH molecules after the first three cooling cycles of zero velocity selection, double STIRAP deceleration and π-pulse pumping in the accumulation step. The population ρ_{vs} has been recoil-shifted by the pumping pulse to zero mean momentum. The wide momentum distribution of ρ_{gi} corresponds to the initial effective temperature of $T_i = 1K$.

$$t_{tot} = t_{cyc} N_{cyc} = (\tau_1 + 5\Gamma^{-1}) \frac{\Delta v_i}{\Delta v_{vs}} \approx 1.8ms. \tag{6.7}$$

The initial effective temperature of $T_i = 1K$ corresponds to $\Delta v_i \approx 31ms^{-1}$, $u_{\max} \approx 62ms^{-1}$and de Broglie wavelength $\Lambda_f \doteq h/(M\Delta v_i) \approx 0.75nm$. Using simple kinematics, we have the deceleration of the fastest molecules $a = u_{\max}/t_{tot} \approx 36800ms^{-2}$ and the maximum drift distance of the fastest molecules which is inversely proportional to the selected velocity width as

$$z_{\max} = u_{\max} t_{tot} - \frac{1}{2} a t_{tot}^2 = \frac{1}{2} u_{\max} t_{tot} = \Delta v_i t_{tot} \approx 5.3cm. \tag{6.8}$$

The final width of $\Delta v_f \approx 22cms^{-1}$ corresponds to effective final temperature $T_f = \frac{1}{2} M(\Delta v_f)^2/k_B \approx 50\mu K$ and de Broglie wavelength $\Lambda_f = h/(M\Delta v_f) \approx 0.1\mu m$. The cooled molecules can be confined in the axial direction by dipole force from the evanescent wave mirror[95].

We assume the initial spatial density is $\eta_o \approx 10^8 molecules/cm^3$ and gas volume $V_o = Az_o$ where $z_o \approx 1cm$ is the axial dimension of the gas. After laser cooling, the gas occupies the whole volume of the barrel $V_f = AL = V_o(L/z_o) \approx 2V_o$ where $L = z_o + z_{\max} \approx 6.3cm$ is the required barrel length, which is within experimental scale. The spatial density reduces only to $\eta_f = \eta_o z_o/L \approx 1.6 \times 10^7 molecules/cm^3$.

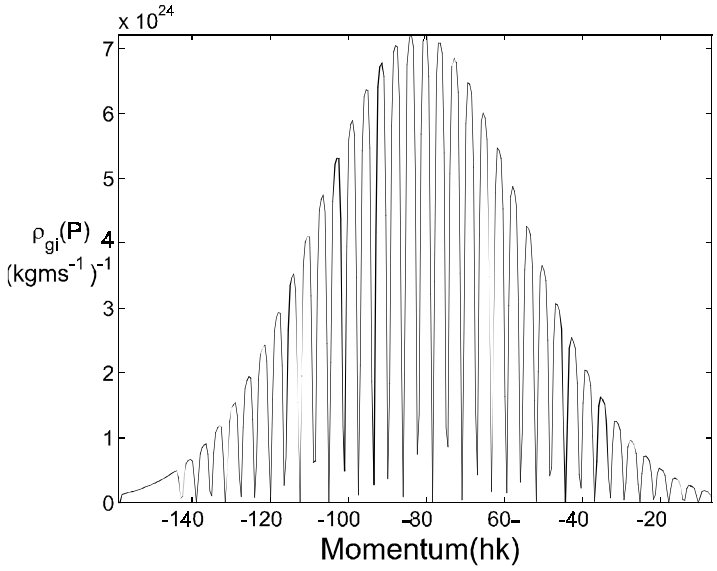

Figure 6.8: The remaining population ρ_{gi} after the cooling process for OH molecules with the initial effective temperature of $T_i = 0.1K$.(hk$\equiv \hbar(k_{S1} + k_{p1})/2$)

6.2.7 Entropy Modeling

Following the arguments in Ref. [1], we only need to evaluate the populations in order to compute the internal and external entropies during the cooling process. The transient populations of the quantum system can be modelled analytically throughout the cooling process. During step 1 of $N-th$ cycle the populations in states $|g_i\rangle$ and $|g_{vs}\rangle$ evolve as:

$$\begin{aligned}\rho_{g_i}(P,t_1)_{N:1} &= W(P)_{(P_o-(n-1)2\Lambda-\hbar k_{p1})} - \sum_{i=1}^{n} W(P_o)_{(i-1)2\Lambda} e^{-(P+(n-i)2\Lambda+\hbar k_{p1})^2/\sigma_{vs}^2} \\ &\quad -h_1(t_1) W(P_o)_{(n-1)2\Lambda} e^{-(P+\hbar k_{p1})^2/\sigma_{vs}^2} \qquad (6.9)\\ \rho_{vs}(P,t_1)_{N:1} &= h_1(t_1) W(P_o)_{(n-1)2\Lambda} e^{-(P-\hbar k_{S1})^2/\sigma_{vs}^2} \qquad (6.10)\end{aligned}$$

where $W(P)_{(x)} \doteq \frac{1}{Z} e^{-(P-x)^2/\sigma_o^2}, 0 \le t_1 \le \tau_1$, and τ_1 is the duration of the population transfer in step 1, $\Lambda = \hbar(k_a + k_b)$. The function $h_1(t_1) = \sin^2 \pi t/2\tau_1$ describes the time evolution of the populations.

There are two STIRAP processes or substeps 1 and 2 in the step 2, Only the populations in states $|g_i\rangle$ and $|g_{dec}\rangle$ change. During the first substep, the populations change as

$$\rho_{gi}(P,t_2)_{N:2(1)} = (1-h_2(t_2))\rho_{g_i}(P,\tau_1)_{N:1} \quad (6.11)$$

$$\rho_{dec}(P,t_2)_{N:2(1)} = h_2(t_2)\{W(P)_{(P_o-(n-1)2\Lambda-\Lambda-\hbar k_{p1})} - \sum_{i=1}^{n} W(P_o)_{(i-1)2\Lambda} e^{-(P+(n-i)2\Lambda-\Lambda+\hbar k_{p1})^2/\sigma_{vs}^2}\} \quad (6.12)$$

and during substep 2,

$$\rho_{dec}(P,t_2)_{N:2(2)} = (1-h_2(t_2))\rho_{g_i}(P,\tau_2)_{N:2(1)} \quad (6.13)$$

$$\rho_{gi}(P,t_2)_{N:2(2)} = h_2(t_2)\{W(P)_{(P_o-n2\Lambda-\hbar k_{p1})} - \sum_{i=1}^{n} W(P_o)_{(i-1)2\Lambda} e^{-(P+(n-i)2\Lambda-2\Lambda+\hbar k_{p1})^2/\sigma_{vs}^2}\} \quad (6.14)$$

The time interval for each substep is $0 \le t_2 \le \tau_2$, $h_2(t_2) = \sin^2 \pi t/2\tau_2$, τ_2 is the duration for one inversion and $\Lambda \doteq \hbar(k_a + k_b)$ is the total amount of momentum transfer provided by one STIRAP inversion process.

In the first stage of step 3, the narrow population in state $|g_{vs}\rangle$ is transferred to the decaying state $|d\rangle$ with a π-pulse of wavevector k_t and duration τ_t

$$\rho_{vs}(P,t_3)_{N:t} = (1-h_3(t_3))\rho_{vs}(P,\tau_1)_{N:1} \quad (6.15)$$

$$\rho_{dd}(P,t_3)_{N:t} = h_1(t_1)W(P_o)_{(n-1)2\Lambda} e^{-(P-\hbar k_{S1}+\hbar k_3)^2/\sigma_{vs}^2} \quad (6.16)$$

where $h_3(t_3) = \sin^2 \pi t/2\tau_3$, $0 \le t_3 \le \tau_3$ and τ_3 is the population transfer duration from $|g_{vs}\rangle$ to $|d\rangle$.

Finally, the population in $|d\rangle$ decays to many internal levels. Assuming that only a small branching ratio of the population from $|d\rangle$ decays back to $|g_{vs}\rangle$, the time evolution of the populations in step 3 is simply due to the spontaneous decays from $|d\rangle$ to M number of accumulation states $\{|acc_j\rangle, j = 1...M\}$ with the corresponding decay rates Γ_j. The populations dynamics can be modelled as

$$\rho_{dd}(P,t_d)_{N:d} = \rho_{dd}(P,\tau_3)_{N:t} e^{-\Gamma t_d} \quad (6.17)$$

$$\rho_{acc,j}(P,t_d)_{N:d} = \frac{F_j \sigma_{vs}}{\sigma_{acc,j}} e^{-(P-\hbar k_{S1}+\hbar k_t)^2/\sigma_{acc,j}^2} \{\sum_{i=1}^{n-1} W(P_o)_{(i-1)2\Lambda} + W(P_o)_{(n-1)2\Lambda}(1-e^{-\Gamma_j t_d})\} \quad (6.18)$$

where $0 \le t_d \le \tau_d$ is the time interval for step 3, τ_d is the duration for $|d\rangle$ to empty its populations to essentially zero (taken as $5/\Gamma$) whileF_j and Γ_j are the Franck-Condon factor and decay rate to level $|acc_j\rangle$ with $\sum_{j=1}^{M} F_j = 1$ and $\Gamma \doteq \sum_{j=1}^{M} \Gamma_j$. The accumulated momentum width σ_{acc} is slightly larger than σ_{vsel} due to the small momentum spread (about $0.5\hbar k_a$) from a single spontaneous emission. The normalization factor $\frac{\sigma_{vsel}}{\sigma_{acc}}$ in Eq. 6.18 ensures that $Tr_{tot}\{\hat{\rho}_{tot}\} = 1$ and can be estimated as $\sigma_{acc,j} \approx \sigma_{vsel} + 0.5\hbar k_j$ where $k_j \doteq (E_d - E_{acc,j})/\hbar c$.

The transient internal entropy $S_I(t)$ and external entropy $S_{cm}(t)$ throughout the cooling process can be computed using

$$S_I(t) \doteq -k_B \sum_a \rho_{aa}(t) \ln \rho_{aa}(t) \tag{6.19}$$

$$S_{cm}(t) \doteq -k_B \sum_{\mathbf{P}} f(\mathbf{P}, t) \ln f(\mathbf{P}, t) \tag{6.20}$$

where $\rho_{aa}(t) \doteq \int \rho_{aa}(P,t)dP$ and $f(\mathbf{P},t) \doteq \sum_a \rho_{aa}(P,t)$.

The results are shown in Figs. 6.9 for the first three cooling cycles. On overall, the center of mass entropy S_{cm} reduces (Fig. 6.9a) while the internal entropy S_I increases (Fig. 6.9b). The sum of the entropies $S_{cm} + S_I$ in the end of the third cycle is slightly greater than the initial sum, which agrees with the property of quantum entropy, Eq. 4.26. The reduction of S_{cm} during velocity selection, STIRAP decelerations and pumping are due to the predetermined laser directions intended to push the populations as close to zero mean values as possible. The slight increase in S_{cm} during free spontaneous emissions is due to the momentum spread.

The internal entropy S_I increases only during the velocity selection step and the spontaneous emission process. During STIRAP processes and the population transfer in step 3, there are no net change in the internal entropy although it has maximum values in the midst of the interactions. Figure 6.9c shows that the internal entropy increases as the number of the accumulation states increases. Of course, the number of internal states does not affect the external entropy.

6.2.8 Conclusions

We have presented a cooling scheme for molecules based on simple and well-establish quantum optical techniques: Raman π-pulse for zero velocity selection and STIRAP for deceleration. The kinetic energy of the molecules is rapidly removed by the fast internal transitions. The scheme requires only 2 pairs of lasers (for velocity selection and STIRAP) and an excitation laser (for accumulation step). This scheme requires a shorter cooling time than our previous scheme [1] as only two STIRAP inversions are required in each cooling cycle instead of many. We have derived an expression for predicting the selected momentum width. We also found that velocity selection from all Zeeman states in a single level can be performed simultaneously using a Raman π-pulse despite the different transition coefficients. The necessary theory for the cooling parameters is presented. Momentum distribution for the cooling process is simulated using the density matrix equations. The total cooling time and spatial drift for OH molecules are numerically estimated. We have modelled the evolution of the cooling process with analytical expressions for the populations from which we compute the transient external and internal entropies.

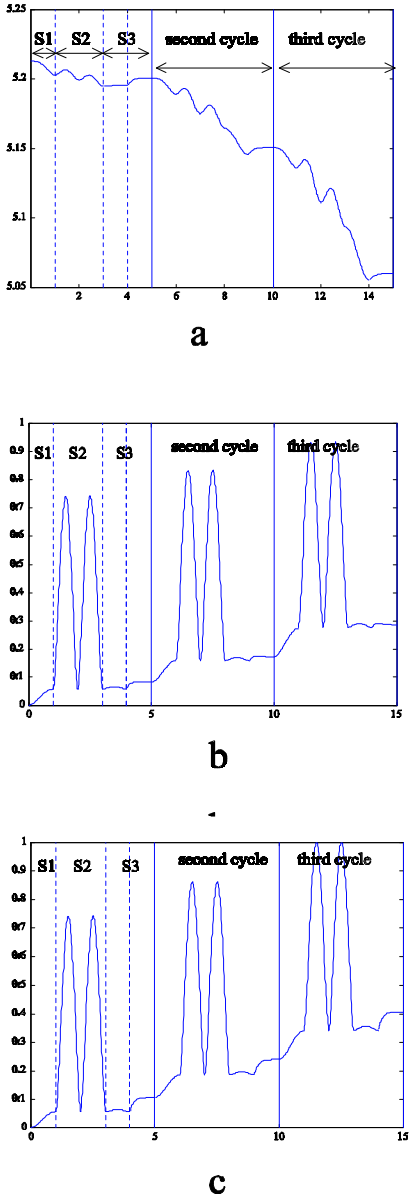

Figure 6.9: Evolutions of the entropies (normalized) S/k_B versus arbitrary unit: a)S_{cm}/k_B and b)S_I/k_B for the first three cooling cycles with 5 $|acc\rangle$ states, and c)S_I/k_B with 50 $|acc\rangle$ states. The Franck-Condon factors are $\ln m$, where m=1,2,...,N (number of $|acc\rangle$ states). Each cycle is partitioned with the vertical lines. The four processes:velocity selection, STIRAP inversions, pumping to the decaying state, and optical spontaneous emissions are partitioned with dotted lines.

Chapter 7

Conclusions

In conclusions, let us summarize the results which cover various aspects of physics related to laser cooling of molecules which encompass the fields of molecular physics, photon-molecule interactions, master equation with dissipation and quantum optical techniques. The results are then used to develop a laser scheme to cool the translational degree of dilute molecular gas down to temperature typically below microKelvin (paper [1]). Starting from Chapter 2, we used the non-relativistic Lagrangian formulation to derive the Hamiltonian in minimal coupling version for particles in static and electromagnetic fields. From this, we obtained the photon-diatomic molecule interactions and the expression for molecular dipole operator. Then, we derived the Hamiltonian in multipolar version through the gauge transformation. By coordinate transformation from space fixed frame to molecule-fixed frame, the c.m. kinetic energy is separated out from the free internal molecular Hamiltonian and the interaction Hamiltonian. By expansions of the polarization and magnetization, we derived the electric dipole, magnetic dipole and electric quadrupole interactions for diatomic molecules in terms of the quantized molecular center of mass canonical variables (position and momentum). We also obtained the Röntgen term which is proportional to the center of mass momentum and polarization. The commutation relations for the canonical center of mass variables, and the electronic and nuclear variables in molecular frame were also derived. Interactions between molecules like collisions, dipole-dipole interactions and van der Waals force have been neglected within the timescale of laser-molecules interaction period. From the free molecular Hamiltonian, we outlined a comprehensive review of the fundamentals of molecular spectra of diatomics. From the dipole interaction, we gave the dipole selection rules and also discussed the basis behind the additional parity selection rules. The Hamiltonian were used to study the effects of laser-molecule and radiation-molecule interactions on the center of mass momentum involving coherent and incoherent processes and for laser cooling schemes for a dilute molecular gas in subsequent chapters.

In Chapter 3, we have used the projection operator technique to derive general the master equation for particles in thermal and non–thermal radiation reservoir. We obtained the dissipative Liouvillean which depends on the laser interaction Hamiltonian which is

valid for arbitrary laser field strength. It provides the possibility of coherently controlling the spontaneous emission rate, an important mechanism required for laser cooling. As an example, we have used the Schrödinger equation to show how that the spontaneous emission rate can be controlled by applying multiple 2π-pulses in a V-scheme. It is a non-Markovian effect. This provides a possibility for enhancing the infrared decay process in the cooling Scheme 2 in Chapter 6. Formal solutions of the coupled Schrödinger equations for time independent field were obtained by Laplace transform method, which shows field dependent decay rate with non-exponential transient decay associated with the non-Markovian property. In the absence of driving fields, we have derived the dissipative Liouvillean for a multilevel molecule in thermal radiation with quantized momentum. It is used to derive the coupled equations which contain the effect of spontaneously generated coherences. The result is also used to study in detailed the momentum and transient dynamics of a two-level multi-ground state of a cold gas with undergoing spontaneous decay and coupled to a Markovian thermal reservoir at arbitrary temperature (paper [2]). In the paper, we have derived the momentum-convolutionless coupled equations for momentum Fourier transform of the populations. The cold gas regime enables the Röntgen term to be neglected. These equations were solved numerically and analytically for a specific internal scheme and for zero-temperature cases. The time and momentum evolutions of the populations were obtained by inverse Fourier transform. The momentum spread; and the transient center-of-mass and internal entropies across one momentum dimension were computed and compared for different internal schemes. For initial subrecoil momentum width, the $\sigma\pm$ transition displays a two-peak feature. The results well describe the momentum spread dynamics of cold gas in thermal radiation at early time and complement the results based on Fokker-Planck equation of Ref. [151]. The results of this paper apply to the momentum spread dynamics during the accumulation step in the laser cooling schemes in paper [1] and Chapter 6.

In Chapter 4, we established the appropriate quantities for measuring the extend of cooling. We invoked the concepts of quasi phase space Wigner function, entropy production rate and probability distribution and obtain analytical relations between these quantities. The external entropy production rate is found to be proportional to the rate of probability momentum density, and thus the decay rate. We showed that the von Neumann entropy is consistent with thermodynamics while the Renyi entropy is not. The Wigner function can change with time during unitary evolution. However, we showed that this does not change the Renyi entropy. We have shown that entropy can flow between the internal (molecular) and external (c.m.) degrees in a unitary process. This provides explanations to the transient evolutions of the external and internal entropies during velocity selection and deceleration steps in the cooling scheme described in Chapter 6 and paper [1].

In Chapter 5, we presented the analysis for coherent control of momentum through the quantum optical techniques of velocity selection and STIRAP. We started from the full Bloch equations and presented a systematic approximations to obtain the the analytical

solutions for CW lasers, Bloch vector equation, and expression for light force. We have derived the general relations for quantities that can be computed in a coherent process, like mean kinetic energy, mean light force and their relations to probability density and density matrix elements. Detailed theories of the Raman velocity selection and STIRAP techniques for coherently controlling the momentum of a gas were presented. We derived optimal operating conditions for efficient population transfer in Raman velocity selection and STIRAP. In particular we obtained expression for predicting the selected momentum width for a given Blackman pulse duration and Rabi frequency. These results were used in the simulations and modelling of the cooling process in Chapter 6. We also presented a simple technique for reducing the momentum width and kinetic energy in a harmonic potential using the concept of squeezing. The conditions which give either momentum squeezing or bunching were derived.

In Chapter 6, we discussed two preliminary laser cooling schemes for molecules which are theoretically possible but not feasible in practice. Following this, we presented a more feasible laser cooling scheme for molecules based on three concepts that can be realized using the quantum optical processes (elaborated in the preceding chapters):- Raman π-pulse for velocity selection, repeated STIRAP for deceleration, and a single spontaneous emission for irreversible accumulation. The first two are coherent manipulations of the external (center of mass momentum) and the internal quantum states of molecules, while the spontaneous emission is for dissipation. No closed pumping cycle nor repeated spontaneous emissions are required, so the scheme is applicable to cool a molecular gas. Detailed results were published in paper [1]. We also presented a modified scheme which has the advantage from practical point of views, although both use the same concepts. The scheme uses zero velocity selection (instead of non zero velocity selection) to create a fraction narrow momentum width population around zero momentum. So, no further deceleration is required. Besides, only two STIRAP cycles (instead of many) are required to decelerate the hot ensemble of gas in the initial state in order to create a finite population around zero velocity for next zero velocity selection cycle. Thus, the cooling time in each cycle is considerably shortened by the reduced number of STIRAP processes compared to the previous scheme. The cooling processes in both schemes can be modelled with analytical population density. This enables the simulations of the transient internal and external entropies throughout the cooling process. Simulations of the model show the significant reduction of the momentum width and the c.m entropy and thus demonstrate the cooling efficiency. Numerical estimates of the operational parameters using real OH molecular levels yield a reasonable cooling duration. This scheme should open up new possibilities for translational laser cooling of molecules, high-precision molecular spectroscopy and molecular interferometry. It serves to fulfill the aim of the thesis, to apply and develop quantum optical techniques for cooling of molecular gas.

Chapter 8

Appendices

This chapter has four appendices which contain detailed formalisms and derivations required for the calculations in the preceding chapters. Appendix I contains general expressions for the laser-molecule and radiation-molecule Hamiltonians in dipole couplings with quantized center of mass position. In the Appendix II, we present expressions for the photon wavector and field-vectors in terms of circular unit vectors, leading to the calculations of the angular dependent double product of the coupling constant. In Appendix III, we give the algebras for the center of mass operators in the interaction Hamiltonians which provide the center of mass momentum transfer, the Doppler and recoil frequency shifts. In the last Appendix IV, we present the derivation of the exact unitary evolution operator for a two level system in rotating wave approximation which includes the Röntgen term.

8.1 Appendix I: Explicit forms of Quantized Hamiltonians

In this appendix, the Hamiltonians of the internal molecular states, the center of mass kinetic energy, the radiation-molecule interaction and the laser-molecule interaction are explicitly expressed in terms of the quantized operators. The interaction Hamiltonians in both Schrödinger picture and interaction picture are given. The interactions are characterized by dipole coupling and complemented by the Röntgen term.

8.1.1 Radiation Fields in Schrödinger picture

The canonical quantizations of the vector potential $\mathbf{A}_\perp(\hat{\mathbf{r}})$ and the field conjugate $\Pi(\hat{\mathbf{r}})$ follow from the commutation relations $[\hat{r}_{iq}, \hat{p}_{jq'}] = i\hbar\delta_{qq'}\delta_{ij}$ for particles and $[\hat{A}_{jq}(\hat{\mathbf{r}}), \hat{\Pi}_{iq'}(\hat{\mathbf{r}}')] = i\hbar\delta^{\perp}_{qq'}(\hat{\mathbf{r}} - \hat{\mathbf{r}}')$ for fields where $q, q' \in x, y, z$ [188]. The fields are expressed in terms of the bosonic annihilation $\hat{a}_{\mathbf{k}\lambda}$ and creation $\hat{a}^{\dagger}_{\mathbf{k}\lambda}$ operators for the radiation Fock states and the center of mass position operator $\hat{\mathbf{r}}$.

$$\mathbf{A}(\hat{\mathbf{r}}) = \sum_{\mathbf{k},\lambda} \sqrt{\frac{\hbar}{2\varepsilon_o \omega_{\mathbf{k}\lambda} V}} (\hat{\varepsilon}_{\mathbf{k}\lambda} \hat{a}_{\mathbf{k}\lambda} e^{i\mathbf{k}\cdot\hat{\mathbf{r}}} + \hat{\varepsilon}^*_{\mathbf{k}\lambda} \hat{a}^\dagger_{\mathbf{k}\lambda} e^{-i\mathbf{k}\cdot\hat{\mathbf{r}}}) \tag{8.1}$$

$$\Pi(\hat{\mathbf{r}}) = -i \sum_{\mathbf{k},\lambda} \sqrt{\frac{\varepsilon_o \hbar \omega_{\mathbf{k}\lambda}}{2V}} (\hat{\varepsilon}_{\mathbf{k}\lambda} \hat{a}_{\mathbf{k}\lambda} e^{i\mathbf{k}\cdot\hat{\mathbf{r}}} - \hat{\varepsilon}^*_{\mathbf{k}\lambda} \hat{a}^\dagger_{\mathbf{k}\lambda} e^{-i\mathbf{k}\cdot\hat{\mathbf{r}}}) \tag{8.2}$$

$$\mathbf{B}(\hat{\mathbf{r}}) = \nabla \times \mathbf{A}_\perp(\hat{\mathbf{r}}) = i \sum_{\mathbf{k},\lambda} \sqrt{\frac{\hbar}{2\varepsilon_o \omega_{\mathbf{k}\lambda} V}} (\mathbf{k} \times \hat{\varepsilon}_{\mathbf{k}\lambda} \hat{a}_{\mathbf{k}\lambda} e^{i\mathbf{k}\cdot\hat{\mathbf{r}}} - \mathbf{k} \times \hat{\varepsilon}^*_{\mathbf{k}\lambda} \hat{a}^\dagger_{\mathbf{k}\lambda} e^{-i\mathbf{k}\cdot\hat{\mathbf{r}}}) \tag{8.3}$$

This fields commutation relation can be verified from Eqs. 8.1, 8.2 and the transversality relation $\sum_{\lambda=1,2} \epsilon_{\mathbf{k}\lambda q} \epsilon^*_{\mathbf{k}\lambda q'} = \delta_{qq'} - \kappa_q \kappa^*_{q'}$ which is equivalent to $\nabla \cdot \mathbf{A}(\hat{\mathbf{r}})$, as $\sum_{\mathbf{k}} \frac{i\hbar}{2V} 2 \sum_{\lambda=1,2} \epsilon_{\mathbf{k}\lambda q} \epsilon^*_{\mathbf{k}\lambda q'} = \frac{i\hbar}{V} \sum_{\mathbf{k}} (\delta_{qq'} - \kappa_q \kappa^*_{q'}) \to \frac{i\hbar}{V} \frac{V}{(2\pi)^3} \int d^3k (\delta_{qq'} - \kappa_q \kappa^*_{q'}) e^{i\mathbf{k}\cdot(\hat{\mathbf{r}} - \hat{\mathbf{r}}')} = i\hbar \delta^\perp_{qq'}(\hat{\mathbf{r}} - \hat{\mathbf{r}}')$.

When the $\hat{\mathbf{p}}$ and $\hat{\mathbf{r}}$ are quantized as canonical operators, it seems that $\mathbf{A}(\hat{\mathbf{r}}) \cdot \hat{\mathbf{p}} \neq \hat{\mathbf{p}} \cdot \mathbf{A}(\hat{\mathbf{r}})$ because $\hat{\mathbf{p}}$ does not commute with $e^{i\mathbf{k}\cdot\hat{\mathbf{r}}}$. But $[\hat{\mathbf{p}}\cdot, \mathbf{A}(\hat{\mathbf{r}})]|\mathbf{p}, n_{\mathbf{k},\lambda}, a\rangle = \sqrt{\frac{\hbar}{2\varepsilon_o \omega_{\mathbf{k}\lambda} V}} \{n_{\mathbf{k}\lambda} \hbar \mathbf{k} \cdot \hat{\varepsilon}_{\mathbf{k}\lambda} |\mathbf{p} + \hbar\mathbf{k}, n_{\mathbf{k},\lambda} - 1, a\rangle - (n_{\mathbf{k},\lambda} + 1) \hbar \mathbf{k} \cdot \hat{\varepsilon}^*_{\mathbf{k}\lambda} |\mathbf{p} - \hbar\mathbf{k}, n_{\mathbf{k},\lambda} + 1, a\rangle\}$ where $|a\rangle$ is the internal state. The Coulomb gauge $\nabla \cdot \mathbf{A}(\hat{\mathbf{r}}) = 0$ also means $\mathbf{k} \cdot \hat{\varepsilon}_{\mathbf{k}\lambda} = \mathbf{k} \cdot \hat{\varepsilon}^*_{\mathbf{k}\lambda} = 0$, or $\mathbf{A}(\hat{\mathbf{r}})$ is orthogonal to $\mathbf{k}$, so actually $\mathbf{A}(\hat{\mathbf{r}})$ commutes with $\hat{\mathbf{p}}$.

In minimal coupling formalism, the electric field of the radiation is the transverse electric field $\mathbf{E}_\perp(\hat{\mathbf{r}})$ defined as

$$\mathbf{E}_\perp(\hat{\mathbf{r}}) = -\frac{1}{\varepsilon_o} \Pi(\hat{\mathbf{r}}) = -\frac{\partial}{\partial t} \mathbf{A}(\hat{\mathbf{r}}, \mathbf{0}) = i \sum_{\mathbf{k},\lambda} \sqrt{\frac{\hbar \omega_{\mathbf{k}\lambda}}{2\varepsilon_o V}} (\hat{\varepsilon}_{\mathbf{k}\lambda} \hat{a}_{\mathbf{k}\lambda} e^{i\mathbf{k}\cdot\hat{\mathbf{r}}} - \hat{\varepsilon}^*_{\mathbf{k}\lambda} \hat{a}^\dagger_{\mathbf{k}\lambda} e^{-i\mathbf{k}\cdot\hat{\mathbf{r}}}) \tag{8.4}$$

However, in multipolar formalism, the physical electric field is $-\frac{1}{\varepsilon_o}\Pi(\hat{\mathbf{r}})$ and not $\mathbf{E}_\perp(\hat{\mathbf{r}})$[190].

8.1.2 Free Hamiltonian

The total field free Hamiltonian $H_o = H_{cm} + H_I + H_R$ is composed of the center of mass kinetic energy H_{cm}, the internal molecular energy H_I and the radiation H_R

$$H_{cm} = \frac{\hat{\mathbf{P}}^2}{2M} = \int d^3P \frac{\mathbf{P}^2}{2M} |\mathbf{P}\rangle\langle\mathbf{P}| \tag{8.5}$$

$$H_I = \sum_a \hbar\omega_a |a\rangle\langle a| \tag{8.6}$$

$$H_R = \sum_{\mathbf{k},\lambda} (\hat{a}^\dagger_{\mathbf{k}\lambda} \hat{a}_{\mathbf{k}\lambda} + \frac{1}{2}) \hbar \omega_{\mathbf{k}\lambda} \tag{8.7}$$

8.1.3 Laser Interaction in Schrödinger picture

The electric field of a laser can be described classically by a c-number through unitary transformation using the displacement operator [129] to project out a single mode quantized radiation field in coherent state [126], as shown by Mollow [128]. The equivalence of the c-number description and the quantum mechanical description was shown by Sudarshan [127]. The resultant electric field composed of the superpositions of laser fields can be written as

$$\mathbf{E}(\hat{\mathbf{R}},t)\equiv\sum_{L}(\mathbf{E}_{Lo}(\hat{\mathbf{R}})e^{-i\omega_L t}+\mathbf{E}^{*}_{Lo}(\hat{\mathbf{R}})e^{i\omega_L t}) \tag{8.8}$$

where $\mathbf{E}_{Lo}(\hat{\mathbf{R}})=\frac{1}{2}\hat{\varepsilon}_L E_{Lo}(\hat{\mathbf{R}})\exp(\mathbf{k}_L\cdot\hat{\mathbf{R}}+\phi_L)$, and $\hat{\varepsilon}_L,\mathbf{k}_L,\omega_L,\phi_L$ are the polarization unit vector, wavevector, frequency and phase of the laser respectively.

If we combine two lasers of arbitrary amplitudes and polarizations, we can define a real effective amplitude $E_{ef}(\hat{\mathbf{R}})$ and the position dependent polarization vector $\hat{\varepsilon}_{ef}(\hat{\mathbf{R}})$ as

$$\frac{1}{2}\{E_{1o}(\hat{\mathbf{R}})\hat{\varepsilon}_1 e^{i\mathbf{k}_1\cdot\hat{\mathbf{R}}}+E_{2o}(\hat{\mathbf{R}})\hat{\varepsilon}_2 e^{i\mathbf{k}_2\cdot\hat{\mathbf{R}}}\}\equiv E_{ef}(\hat{\mathbf{R}})\hat{\varepsilon}_{ef}(\hat{\mathbf{R}}) \tag{8.9}$$

Equation 8.9 can be generalized to more than two lasers. However, there are a few typical laser configurations:

- For a running continuous wave (CW), we have $\mathbf{E}(\hat{\mathbf{R}},t)\equiv\hat{\varepsilon}E_o(\hat{\mathbf{R}})\cos(\mathbf{k}\cdot\hat{\mathbf{R}}-\omega t+\phi)$
- For counter propagating waves with same frequencies and amplitudes, we have

$$\mathbf{E}(\hat{\mathbf{R}})\equiv E_o(\hat{\mathbf{R}})(\frac{1}{2}\hat{\varepsilon}_1 e^{i(\mathbf{k}\cdot\hat{\mathbf{R}}+\phi_1)}+\frac{1}{2}\hat{\varepsilon}_2 e^{i(-\mathbf{k}\cdot\hat{\mathbf{R}}+\phi_2)})e^{-i\omega t}+c.c.$$

- For standing wave (formed by counter propagating waves with *same polarizations*), $\hat{\varepsilon}_1=\hat{\varepsilon}_2$ and we have $\mathbf{E}(\hat{\mathbf{R}})=2\hat{\varepsilon}E_o(\hat{\mathbf{R}})\sin(\mathbf{k}_L\cdot\hat{\mathbf{R}}+\phi)\cos\omega t$.
- For lin⊥lin configuration (counter propagating waves with *orthogonal linear polarizations)*, $\hat{\varepsilon}_1=\hat{x},\hat{\varepsilon}_2=\hat{y}$, we have

$$\mathbf{E}(\hat{\mathbf{R}})\equiv\frac{1}{2}E_o(\hat{\mathbf{R}})((\hat{x}+\hat{y})\cos\mathbf{k}\cdot\hat{\mathbf{R}}+i(\hat{x}-\hat{y})\sin\mathbf{k}\cdot\hat{\mathbf{R}})e^{-i\omega t}+c.c.$$

- For $\sigma^+-\sigma^-$ configuration (counter propagating waves with *orthogonal circular polarizations)*, $\hat{\varepsilon}_1=\frac{1}{\sqrt{2}}(\hat{x}+i\hat{y}),\hat{\varepsilon}_2=\frac{1}{\sqrt{2}}(\hat{x}-i\hat{y})$ and we have

$$\mathbf{E}(\hat{\mathbf{R}})\equiv\frac{1}{2}E_o(\hat{\mathbf{R}})(\frac{1}{\sqrt{2}}(\hat{x}+i\hat{y})e^{i(\mathbf{k}\cdot\hat{\mathbf{R}}+\phi_1)}+\frac{1}{\sqrt{2}}(\hat{x}-i\hat{y})e^{i(-\mathbf{k}\cdot\hat{\mathbf{R}}+\phi_2)})e^{-i\omega t}+c.c. \tag{8.10}$$

The molecule-laser interaction can be described by the c-number corresponding to the coherent state of radiation [129]

$$\hat{V}_{SL}(\hat{\mathbf{R}},t) = -\hat{\mathbf{d}}\cdot\mathbf{E}(\hat{\mathbf{R}},t) = -\sum_L \frac{1}{2}E_{Lo}(\hat{\mathbf{R}})(\hat{\mathbf{d}}\cdot\hat{\varepsilon}_L e^{i(\mathbf{k}_L\cdot\hat{\mathbf{R}}-\omega_L t+\beta_L)} + \hat{\mathbf{d}}\cdot\hat{\varepsilon}_L^* e^{-i(\mathbf{k}_L\cdot\hat{\mathbf{R}}-\omega_L t+\beta_L)}) \tag{8.11}$$

By using Eqs. 8.43 and 8.45 with the subscript $\mathbf{k}\lambda$ being replaced by L, we can write

$$\begin{aligned}\hat{V}_{SL}(\hat{\mathbf{R}},t) &= -\sum_{L,a,b}\hbar\Omega_{Lab}(S_{ab}e^{i(\mathbf{k}_L\cdot\hat{\mathbf{R}}-\omega_L t)} + S_{ba}e^{-i(\mathbf{k}_L\cdot\hat{\mathbf{R}}-\omega_L t)}) \\ &= -\sum_{L,a,b<a}\hbar\Omega_{Lab}(S_{ba}^\dagger e^{i(\mathbf{k}_L\cdot\hat{\mathbf{R}}-\omega_L t)} + S_{ba}e^{-i(\mathbf{k}_L\cdot\hat{\mathbf{R}}-\omega_L t)}) \\ &\quad -\sum_{L,a,b>a}\hbar\Omega_{Lab}(S_{ba}e^{i(\mathbf{k}_L\cdot\hat{\mathbf{R}}-\omega_L t)} + S_{ba}^\dagger e^{-i(\mathbf{k}_L\cdot\hat{\mathbf{R}}-\omega_L t)})\end{aligned} \tag{8.12}$$

where we have removed the phase factor β_L by the redefinition $\epsilon_{Lq}^* e^{-i\beta_L} = \epsilon_{Lq}e^{i\beta_L} \to \epsilon_{Lq}$.

The Rabi frequency of the laser L which couples state $|a\rangle$ and $|b\rangle$ can be obtained with the help of Appendix II, Eq. 8.49 as

$$\hbar\Omega_{Lab} = \frac{1}{2}E_{Lo}(\hat{\mathbf{R}})\langle a|\hat{\mathbf{d}}\cdot\hat{\varepsilon}_{\mathbf{k}\lambda}|b\rangle = \frac{1}{2}E_{Lo}(\mathbf{R})d_{ab}\sum_{q=+,-,\mathbf{0}} C_{qab}\epsilon_{Lq} \tag{8.13}$$

$$S_{ab} = |a\rangle\langle b| = S_{ba}^\dagger \tag{8.14}$$

In the case of a single frequency laser with arbitrary configurations, Eq. 8.9 can be used to obtain the position dependent effective polarization component $\epsilon_{Lq}(\mathbf{R})$.

8.1.4 Radiation Interaction in Schrodinger picture

Similarly, we can write the molecule-radiation interaction as

$$\begin{aligned}\hat{V}_{SR}(\hat{\mathbf{R}},t) &= -\hat{\mathbf{d}}\cdot\mathbf{E}_\perp(\hat{\mathbf{R}}) = -\sum_{\mathbf{k}\lambda} i\sqrt{\frac{\hbar\omega_{\mathbf{k}\lambda}}{2\varepsilon_o V}}(\hat{a}_{\mathbf{k}\lambda}\hat{\mathbf{d}}\cdot\hat{\varepsilon}_{\mathbf{k}\lambda}e^{i(\mathbf{k}_\lambda\cdot\hat{\mathbf{R}}+\beta_{\mathbf{k}\lambda})} - \hat{a}_{\mathbf{k}\lambda}^\dagger\hat{\mathbf{d}}\cdot\hat{\varepsilon}_{\mathbf{k}\lambda}^* e^{-i(\mathbf{k}_{\mathbf{k}\lambda}\cdot\hat{\mathbf{R}}+\beta_{\mathbf{k}\lambda})}) \\ &= -\sum_{\mathbf{k}\lambda}\sum_{a,b<a}\hbar G_{ab\mathbf{k}\lambda}(\hat{a}_{\mathbf{k}\lambda}S_{ba}^\dagger e^{i(\mathbf{k}_\lambda\cdot\hat{\mathbf{R}})} + \hat{a}_{\mathbf{k}\lambda}^\dagger S_{ba}e^{-i(\mathbf{k}_{\mathbf{k}\lambda}\cdot\hat{\mathbf{R}})}) \\ &\quad -\sum_{\mathbf{k}\lambda}\sum_{a,b<a}\hbar G_{ab\mathbf{k}\lambda}(\hat{a}_{\mathbf{k}\lambda}S_{ba}e^{i(\mathbf{k}_\lambda\cdot\hat{\mathbf{R}})} + \hat{a}_{\mathbf{k}\lambda}^\dagger S_{ba}^\dagger e^{-i(\mathbf{k}_{\mathbf{k}\lambda}\cdot\hat{\mathbf{R}})})\end{aligned} \tag{8.15}$$

with

$$\hbar G_{ab\mathbf{k}\lambda} \doteq \sqrt{\frac{\hbar\omega_k}{2\varepsilon_o V}}\langle a|\hat{\mathbf{d}}\cdot\hat{\varepsilon}_{\mathbf{k}\lambda}|b\rangle = d_{ab}E_{\mathbf{k}\lambda}\sum_{q=+,-,\mathbf{0}}\epsilon_{\mathbf{k}\lambda q}C_{qab} \tag{8.16}$$

where it is always possible to choose $\beta_{\mathbf{k}\lambda}$ such that $-i\hat{\varepsilon}_{\mathbf{k}\lambda}^* e^{-i\beta_{\mathbf{k}\lambda}} \to \hat{\varepsilon}_{\mathbf{k}\lambda}$ is real.

8.1.5 Unitary Transformation to Interaction Picture

The field free Hamiltonian can be eliminated via unitary transformation from the Schrödinger picture to the interaction picture using the operator $\hat{U}(t) = \hat{U}_{cm}(t)\hat{U}_I(t)\hat{U}_R(t)$ with $\hat{U}_X(t) = e^{H_X t/i\hbar}$ and $X \in cm, I, R$.

The c.m. operator $\hat{U}_{cm}(t)$ transforms the operator $e^{\pm i\mathbf{k}\cdot\hat{\mathbf{R}}}$ as

$$\hat{U}^\dagger_{cm}(t)e^{i\mathbf{k}\cdot\hat{\mathbf{R}}}\hat{U}_{cm}(t) = e^{i\mathbf{k}\cdot\hat{\mathbf{R}}}e^{i\mathbf{k}\cdot\hat{\mathbf{P}}\frac{t}{M}}e^{i\frac{\hbar k^2}{2M}t} = e^{i\mathbf{k}\cdot(\hat{\mathbf{R}}+\hat{\mathbf{P}}\frac{t}{M})} = \hat{\pi}_{\mathbf{k}}(t) \tag{8.17}$$

Internal operator $\hat{U}_I(t)$ transforms the operator $|a\rangle\langle b|$ as

$$\hat{U}^\dagger_I(t)|a\rangle\langle b|\hat{U}_I(t) = |a\rangle\langle b|e^{i\omega_a t}e^{-i\omega_b t} \tag{8.18}$$

Radiation operator $\hat{U}_R(t)$ transforms the operator $\hat{a}_{\mathbf{k}\lambda}$ as

$$\hat{U}^\dagger_R(t)\hat{a}_{\mathbf{k}\lambda}\hat{U}_R(t) = \hat{a}_{\mathbf{k}\lambda}e^{-i\omega_{\mathbf{k}\lambda}t} \Leftrightarrow \hat{U}^\dagger_R(t)\hat{a}^\dagger_{\mathbf{k}\lambda}\hat{U}_R(t) = \hat{a}^\dagger_{\mathbf{k}\lambda}e^{i\omega_{\mathbf{k}\lambda}t} \tag{8.19}$$

In interaction picture, Eqs. 8.1 and 8.4 become

$$\mathbf{A}_\perp(\hat{\mathbf{R}},t) = \sum_{\mathbf{k},\lambda}\sqrt{\frac{\hbar}{2\varepsilon_o\omega_{\mathbf{k}\lambda}V}}(\hat{\varepsilon}_{\mathbf{k}\lambda}\hat{a}_{\mathbf{k}\lambda}e^{-i\omega_{\mathbf{k}\lambda}t}\hat{\pi}_{\mathbf{k}\lambda}(t) + \hat{\varepsilon}^*_{\mathbf{k}\lambda}\hat{a}^\dagger_{\mathbf{k}\lambda}e^{i\omega_{\mathbf{k}\lambda}t}\hat{\pi}^\dagger_{\mathbf{k}\lambda}(t)) \tag{8.20}$$

$$\mathbf{E}_\perp(\hat{\mathbf{R}},t) = -i\sum_{\mathbf{k},\lambda}\sqrt{\frac{\hbar\omega_{\mathbf{k}\lambda}}{2\varepsilon_o V}}(\hat{\varepsilon}_{\mathbf{k}\lambda}\hat{a}_{\mathbf{k}\lambda}e^{-i\omega_{\mathbf{k}\lambda}t}\hat{\pi}_{\mathbf{k}\lambda}(t) - \hat{\varepsilon}^*_{\mathbf{k}\lambda}\hat{a}^\dagger_{\mathbf{k}\lambda}e^{i\omega_{\mathbf{k}\lambda}t}\hat{\pi}^\dagger_{\mathbf{k}\lambda}(t)) \tag{8.21}$$

8.1.6 Laser Interaction in Interaction picture

The transformations of Eq. 8.12 using Eqs. 8.17-8.19 gives

$$\begin{aligned}\hat{V}^i_{SL}(\hat{\mathbf{R}},t) &= -\sum_{L,a,b<a}\hbar\Omega_{Lab}(S^\dagger_{ba}\hat{\pi}_L(t)e^{i(-\Delta_{abL}t)} + S_{ba}\hat{\pi}^\dagger_L(t)e^{i(\Delta_{abL}t)}) \\ &\quad -\sum_{L,a,b<a}\hbar\Omega_{Lab}(S_{ba}\hat{\pi}_L(t)e^{i(-\sigma_{abL}t)} + S^\dagger_{ba}\hat{\pi}^\dagger_L(t)e^{i(\sigma_{abL}t)}) \qquad (8.22)\\ &= -\hbar\sum_{L,a,b<a}(S^\dagger_{ba}\hat{F}_{Lab}(t) + S_{ba}\hat{F}^\dagger_{Lab}(t)) \qquad (8.23)\end{aligned}$$

where $\Delta_{abL} = \omega_L - |\omega_{oab}|, \sigma_{abL} = \omega_L + |\omega_{oab}|$ and $\hat{F}_{Lab}(t) = \Omega_{Lab}\{\hat{\pi}_L(t)e^{i(-\Delta_{abL}t)} + \hat{\pi}^\dagger_L(t)e^{i(\sigma_{abL}t)}\}$.

Alternatively, we can write

$$\begin{aligned}\hat{V}^i_{SL}(\hat{\mathbf{R}},t) &= -\sum_{L,a,b<a,\mathbf{P}'}\hbar\Omega_{Lab}(S^\dagger_{baL\mathbf{P}'}e^{-i\bar{\Delta}_{abL\mathbf{P}'}t} + S_{baL\mathbf{P}'}e^{i\bar{\Delta}_{abL\mathbf{P}'}t}) \\ &\quad -\sum_{L,a,b<a,\mathbf{P}'}\hbar\Omega_{Lab}(S^a_{baL\mathbf{P}'}e^{-i\bar{\sigma}_{abL\mathbf{P}'}t} + S^{a\dagger}_{baL\mathbf{P}'}e^{i\bar{\sigma}_{abL\mathbf{P}'}t}) \qquad (8.24)\end{aligned}$$

where

$$\begin{aligned} S_{baL\mathbf{P}'} &\doteq |b,\mathbf{P}'\rangle\langle a,\mathbf{P}'+\hbar\mathbf{k}_L| \quad , \quad S^a_{baL\mathbf{P}'} \doteq |a,\mathbf{P}'\rangle\langle b,\mathbf{P}'+\hbar\mathbf{k}_L|, \\ \bar{\Delta}_{abL\mathbf{P}'} &\doteq \Delta_{abL} - \omega^D_L(\mathbf{P}') - \omega^r_L \quad , \quad \bar{\sigma}_{abL\mathbf{P}'} \doteq \sigma_{abL} - \omega^D_L(\mathbf{P}') - \omega^r_L \\ \omega^D_L(\mathbf{P}') &\doteq \frac{\mathbf{k}_L\cdot\mathbf{P}}{M} \quad , \quad \omega^r_L \doteq \frac{\hbar k_L^2}{2M}. \end{aligned} \tag{8.25}$$

8.1.7 Radiation Interaction Hamiltonian (Interaction picture)

Similarly, the system-radiation interaction is

$$\begin{aligned} \hat{V}^i_{SR}(\hat{\mathbf{R}},t) &= -\sum_{\mathbf{k}\lambda}\sum_{a,b<a} \hbar g_{ab\mathbf{k}\lambda}(\hat{a}_{\mathbf{k}\lambda}S^\dagger_{ba}\hat{\pi}_{\mathbf{k}\lambda}(t)e^{-i\Delta_{ab\mathbf{k}\lambda}t} + \hat{a}^\dagger_{\mathbf{k}\lambda}S_{ba}\hat{\pi}^\dagger_{\mathbf{k}\lambda}(t)e^{i\Delta_{ab\mathbf{k}\lambda}t}) \\ &\quad -\sum_{\mathbf{k}\lambda}\sum_{a,b<a} \hbar g_{ab\mathbf{k}\lambda}(\hat{a}_{\mathbf{k}\lambda}S_{ba}\hat{\pi}_{\mathbf{k}\lambda}(t)e^{-i\sigma_{ab\mathbf{k}\lambda}t} + \hat{a}^\dagger_{\mathbf{k}\lambda}S^\dagger_{ba}\hat{\pi}^\dagger_{\mathbf{k}\lambda}(t)e^{i\sigma_{ab\mathbf{k}\lambda}t}) \quad (8.26) \\ &\equiv -\hbar\sum_{L,a,b<a}(S^\dagger_{ba}\hat{R}_{\mathbf{k}\lambda ab}(t) + S_{ba}\hat{R}^\dagger_{\mathbf{k}\lambda ab}(t)) \quad (8.27) \end{aligned}$$

where $\Delta_{abL} = \omega_{\mathbf{k}\lambda} - |\omega_{oab}|, \sigma_{abL} = \omega_{\mathbf{k}\lambda} + |\omega_{oab}|$ and $\hat{R}_{\mathbf{k}\lambda ab}(t) = g_{ab\mathbf{k}\lambda}\{\hat{a}_{\mathbf{k}\lambda}\hat{\pi}_{\mathbf{k}\lambda}(t)e^{-i\Delta_{ab\mathbf{k}\lambda}t} + \hat{a}^\dagger_{\mathbf{k}\lambda}\hat{\pi}^\dagger_{\mathbf{k}\lambda}(t)e^{i\sigma_{ab\mathbf{k}\lambda}t}\}$.

Alternatively, Eq. 8.22 can be rewritten as

$$\begin{aligned} \hat{V}^i_{SR}(\hat{\mathbf{R}},t) &= -\sum_{\mathbf{k}\lambda,a,b<a,\mathbf{P}'} \hbar g_{ab\mathbf{k}\lambda}(\hat{a}_{\mathbf{k}\lambda}S^\dagger_{ba\mathbf{k}\lambda\mathbf{P}'}e^{-i\bar{\Delta}_{ab\mathbf{k}\lambda\mathbf{P}'}t} + \hat{a}^\dagger_{\mathbf{k}\lambda}S_{ba\mathbf{k}\lambda\mathbf{P}'}e^{i\bar{\Delta}_{ab\mathbf{k}\lambda\mathbf{P}'}t}) \\ &\quad -\sum_{\mathbf{k}\lambda,a,b<a,\mathbf{P}'} \hbar g_{ab\mathbf{k}\lambda}(\hat{a}_{\mathbf{k}\lambda}S^a_{ba\mathbf{k}\lambda\mathbf{P}'}e^{-i\bar{\sigma}_{ab\mathbf{k}\lambda\mathbf{P}'}t} + \hat{a}^\dagger_{\mathbf{k}\lambda}S^{a\dagger}_{ba\mathbf{k}\lambda\mathbf{P}'}e^{i\bar{\sigma}_{ab\mathbf{k}\lambda\mathbf{P}'}t}) \quad (8.28) \end{aligned}$$

where

$$\begin{aligned} S_{ba\mathbf{k}\lambda\mathbf{P}'} &\doteq |b,\mathbf{P}'\rangle\langle a,\mathbf{P}'+\hbar\mathbf{k}_\lambda| \quad , \quad S^a_{ba\mathbf{k}\lambda\mathbf{P}'} \doteq |a,\mathbf{P}'\rangle\langle b,\mathbf{P}'+\hbar\mathbf{k}_\lambda|, \\ \bar{\Delta}_{ab\mathbf{k}\lambda\mathbf{P}'} &\doteq \Delta_{ab\mathbf{k}\lambda} - \omega^D_{\mathbf{k}\lambda}(\mathbf{P}') - \omega^r_{\mathbf{k}\lambda} \quad , \quad \bar{\sigma}_{ab\mathbf{k}\lambda\mathbf{P}'} \doteq \sigma_{ab\mathbf{k}\lambda} - \omega^D_{\mathbf{k}\lambda}(\mathbf{P}') - \omega^r_{\mathbf{k}\lambda} \\ \omega^D_{\mathbf{k}\lambda}(\mathbf{P}') &\doteq \frac{\mathbf{k}_\lambda\cdot\mathbf{P}}{M} \quad , \quad \omega^r_{\mathbf{k}\lambda} \doteq \frac{\hbar k_\lambda^2}{2M}. \end{aligned} \tag{8.29}$$

8.1.8 Interaction Hamiltonian with Röntgen term

In the radiation-particle, the center of mass momentum contributes to a correction Röntgen term in the interaction Hamiltonian. The Röntgen interaction term in dipole approximation has been derived in Ref. [236] and elaborated by Babiker[238]. The Röntgen term from the second line in Eq. 2.84 can be expressed in quantized radiation form using

Eq. 8.3 as

$$\begin{aligned}\hat{V}_{R\ddot{o}}(\hat{\mathbf{R}}) &= \frac{1}{2M}\{\hat{\mathbf{d}}\times\mathbf{B}(\hat{\mathbf{R}})\cdot\mathbf{P}+\mathbf{P}\cdot\hat{\mathbf{d}}\times\mathbf{B}(\hat{\mathbf{R}})\}\\ &= \frac{1}{2M}i\sum_{\mathbf{k},\lambda}\sqrt{\frac{\hbar}{2\varepsilon_o\omega_{\mathbf{k}\lambda}V}}(\hat{\mathbf{d}}\times\mathbf{k}\times\hat{\varepsilon}_{\mathbf{k}\lambda}\cdot\{e^{i\mathbf{k}\cdot\hat{\mathbf{R}}},\hat{\mathbf{P}}\}_+\hat{a}_{\mathbf{k}\lambda}-\hat{\mathbf{d}}\times\mathbf{k}\times\hat{\varepsilon}^*_{\mathbf{k}\lambda}\cdot\{e^{-i\mathbf{k}\cdot\hat{\mathbf{R}}},\mathbf{P}\}_+\hat{a}^\dagger_{\mathbf{k}\lambda})\end{aligned}$$

By using Eq. 8.75 and $\hat{\mathbf{d}}\times\mathbf{k}\times\hat{\varepsilon}_{\mathbf{k}\lambda}=\mathbf{k}(\hat{\mathbf{d}}\cdot\hat{\varepsilon}_{\mathbf{k}\lambda})-\hat{\varepsilon}_{\mathbf{k}\lambda}(\hat{\mathbf{d}}\cdot\mathbf{k})$, we have

$$\hat{V}_{R\ddot{o}}(\hat{\mathbf{R}}) = \sum_{\mathbf{k},\lambda}\sqrt{\frac{\hbar}{2\varepsilon_o\omega_{\mathbf{k}\lambda}V}}(\hat{a}_{\mathbf{k}\lambda}\hat{v}_{\mathbf{k}\lambda}e^{i\mathbf{k}\cdot\hat{\mathbf{R}}}+\hat{a}^\dagger_{\mathbf{k}\lambda}e^{-i\mathbf{k}\cdot\hat{\mathbf{R}}}\hat{v}_{\mathbf{k}\lambda}) \tag{8.30}$$

$$\hat{v}_{\mathbf{k}\lambda} = (\hat{\mathbf{d}}\cdot\hat{\varepsilon}_{\mathbf{k}\lambda})(\hat{\omega}^D_{\mathbf{k}\lambda}-\omega^r_{\mathbf{k}\lambda})-(\hat{\mathbf{d}}\cdot\hat{\kappa})\hat{\omega}_{\mathbf{k}\lambda\perp} \tag{8.31}$$

where $\omega^r_{\mathbf{k}\lambda}=\frac{\hbar k^2_{\boldsymbol{\lambda}}}{2M}$ is the recoil frequency, $\hat{\omega}^D_{\mathbf{k}\lambda}=\frac{\mathbf{k}_{\boldsymbol{\lambda}}\cdot\hat{\mathbf{P}}}{M}$ is the normal (*longitudinal)* Doppler shift operator and $\hat{\omega}_{\mathbf{k}\lambda\perp}=k_\lambda\frac{\hat{\varepsilon}_{\mathbf{k}\boldsymbol{\lambda}}\cdot\hat{\mathbf{P}}}{M}$ is the transverse Doppler shift operator from Röntgen term. The full expressions for the transverse dipole operator $\hat{\mathbf{d}}\cdot\hat{\varepsilon}_{\mathbf{k}\lambda}$ and the longitudinal dipole operator $\hat{\mathbf{d}}\cdot\hat{\kappa}$ are given in Appendix II, Eqs. 8.46 and 8.47. The interaction Hamiltonian which includes the Röntgen term in dipole approximation should be modified as

$$\begin{aligned}\hat{V}_{SR}(\hat{\mathbf{R}},t) &= -\hat{\mathbf{d}}\cdot\mathbf{E}_\perp+\frac{1}{2M}(\hat{\mathbf{d}}\times\mathbf{B}(\hat{\mathbf{R}})\cdot\hat{\mathbf{P}}+\hat{\mathbf{P}}\cdot\hat{\mathbf{d}}\times\mathbf{B}(\hat{\mathbf{R}}))\\ &= -\sum_{\mathbf{k}\lambda}\sum_{a,b<a}\hbar g_{ab\mathbf{k}\lambda}(S^\dagger_{ba}+S_{ba})(\hat{a}_{\mathbf{k}\lambda}\hat{\chi}_{ab\mathbf{k}\lambda}e^{i(\mathbf{k}_\lambda\cdot\hat{\mathbf{R}})}+\hat{a}^\dagger_{\mathbf{k}\lambda}e^{-i(\mathbf{k}_{\mathbf{k}\lambda}\cdot\hat{\mathbf{R}})}\hat{\chi}^*_{ab\mathbf{k}\lambda})\end{aligned} \tag{8.32}$$

$$\begin{aligned}\hat{\chi}_{ab\mathbf{k}\lambda}(\hat{\mathbf{P}}) &\doteq (\hat{e}_d\cdot\hat{\varepsilon}_{\mathbf{k}\lambda})(1-\hat{\kappa}\cdot\hat{\boldsymbol{\beta}}+\frac{\hbar k_{\boldsymbol{\lambda}}}{2Mc})+(\hat{e}_d\cdot\hat{\kappa})(\hat{\varepsilon}_{\mathbf{k}\lambda}\cdot\hat{\boldsymbol{\beta}})\\ &= (\hat{e}_d\times\hat{\boldsymbol{\beta}})\cdot(\hat{\kappa}\times\hat{\varepsilon}_{\mathbf{k}\lambda})+(\hat{e}_d\cdot\hat{\varepsilon}_{\mathbf{k}\lambda})(1+\frac{\hbar k_{\boldsymbol{\lambda}}}{2Mc})\\ &= \sum_{q=+,-,\mathbf{0}}C_{qab}\{\epsilon^*_{\mathbf{k}\lambda q}\frac{\hat{\omega}_{\mathbf{k}\lambda\parallel}(\hat{\mathbf{P}})}{\omega_{\mathbf{k}\lambda}}+\kappa^*_q\frac{\hat{\omega}_{\mathbf{k}\lambda\perp}(\hat{\mathbf{P}})}{\omega_{\mathbf{k}\lambda}}\}\end{aligned} \tag{8.33}$$

where $g_{ab\mathbf{k}\lambda}\doteq d_{ab}\sqrt{\frac{\hbar\omega_{k\lambda}}{2\varepsilon_oV}}$, $\hat{\boldsymbol{\beta}}\doteq\frac{\hat{\mathbf{P}}}{Mc}$ and $\hat{\omega}_{\mathbf{k}\lambda\parallel}(\hat{\mathbf{P}})\doteq\omega_{\mathbf{k}\lambda}-\frac{\mathbf{k}_{\boldsymbol{\lambda}}\cdot\hat{\mathbf{P}}}{M}+\frac{\hbar k^2_{\boldsymbol{\lambda}}}{2M}$ and $\hat{\omega}_{\mathbf{k}\lambda\perp}=k_\lambda\frac{\hat{\varepsilon}_{\mathbf{k}\boldsymbol{\lambda}}\cdot\hat{\mathbf{P}}}{M}$. We have used $(\hat{e}_d\cdot\hat{\kappa})(\hat{\varepsilon}_{\mathbf{k}\lambda}\cdot\hat{\boldsymbol{\beta}})-(\hat{e}_d\cdot\hat{\varepsilon}_{\mathbf{k}\lambda})(\hat{\kappa}\cdot\hat{\boldsymbol{\beta}})=(\hat{e}_d\times\hat{\boldsymbol{\beta}})\cdot(\hat{\kappa}\times\hat{\varepsilon}_{\mathbf{k}\lambda})$.

In interaction picture, the interaction Hamiltonian becomes

$$\hat{V}^i_{SR}(\hat{\mathbf{R}},t)=-\sum_{\mathbf{k}\lambda}\sum_{a,b<a}\hbar g_{ab\mathbf{k}\lambda}(S^\dagger_{ba}e^{i\omega_{ab}t}+S_{ba}e^{-i\omega_{ab}t})(\hat{a}_{\mathbf{k}\lambda}e^{-i\omega_{\mathbf{k}\lambda}t}\hat{\chi}_{ab\mathbf{k}\lambda}\hat{\pi}_{\mathbf{k}\lambda}(t)+\hat{a}^\dagger_{\mathbf{k}\lambda}e^{i\omega_{\mathbf{k}\lambda}t}\hat{\pi}^\dagger_{\mathbf{k}\lambda}(t)\hat{\eta}^*_{ab\mathbf{k}\lambda}) \tag{8.34}$$

8.2 Appendix II: Polarization Components of Radiation

In this Appendix, we present the fundamental formulas for fields vector and wave vector in terms of angular variables, the products of the dipole moment and field vector, and the evaluations the angular and frequency summations in the coupling of the free space radiation.

8.2.1 Field Vector and Wave Vector

We choose real field vectors $\hat{\varepsilon}_{\mathbf{k}1}, \hat{\varepsilon}_{\mathbf{k}2}$ and the wavevector $\mathbf{k}$ such that they form a right hand triad $\hat{\varepsilon}_1 \times \hat{\varepsilon}_2 \times \hat{\kappa} = 0$.

$$\begin{aligned} \mathbf{k} &= (\sin\theta\cos\varphi, \sin\theta\sin\varphi, \cos\theta) \\ \hat{\varepsilon}_{\mathbf{k}1} &= (\cos\theta\cos\varphi, \cos\theta\sin\varphi, -\sin\theta) \\ \hat{\varepsilon}_{\mathbf{k}2} &= (-\sin\varphi, \cos\varphi, 0) \end{aligned} \tag{8.35}$$

In matrix form, we have $\begin{pmatrix} \hat{\varepsilon}_{\mathbf{k}1} \\ \hat{\varepsilon}_{\mathbf{k}2} \\ \hat{\kappa} \end{pmatrix} = \begin{pmatrix} \cos\theta\cos\varphi & \cos\theta\sin\varphi & -\sin\theta \\ -\sin\varphi & \cos\varphi & 0 \\ \sin\theta\cos\varphi & \sin\theta\sin\varphi & \cos\theta \end{pmatrix} \begin{pmatrix} x \\ y \\ z \end{pmatrix}$.

8.2.2 Complex Unit Vectors ($\hat{e}_q$)

We define

$$\begin{aligned} \hat{e}_{\mathbf{0}} &= z \\ \hat{e}_+ &= \frac{1}{\sqrt{2}}(x+iy), \hat{e}_+^* = \frac{1}{\sqrt{2}}(x-iy) \\ \hat{e}_- &= \frac{1}{\sqrt{2}}(x-iy), \hat{e}_-^* = \frac{1}{\sqrt{2}}(x+iy) \end{aligned} \tag{8.36}$$

with the properties $\hat{e}_- = \hat{e}_+^*, \hat{e}_+ = \hat{e}_-^* \rightarrow \hat{e}_q = \hat{e}_{-q}^*$ and $\hat{e}_q \hat{e}_{q'}^* = \delta_{qq'}$.

In matrix form, we write $\begin{pmatrix} \hat{e}_+ \\ \hat{e}_- \\ \hat{e}_{\mathbf{0}} \end{pmatrix} = \frac{1}{\sqrt{2}} \begin{pmatrix} 1 & i & 0 \\ 1 & -i & 0 \\ 0 & 0 & \sqrt{2} \end{pmatrix} \begin{pmatrix} x \\ y \\ z \end{pmatrix}$ and $\begin{pmatrix} x \\ y \\ z \end{pmatrix} = \frac{1}{\sqrt{2}} \begin{pmatrix} 1 & 1 & 0 \\ -i & i & 0 \\ 0 & 0 & \sqrt{2} \end{pmatrix} \begin{pmatrix} \hat{e}_+ \\ \hat{e}_- \\ \hat{e}_{\mathbf{0}} \end{pmatrix} = \begin{pmatrix} \frac{1}{\sqrt{2}}(\hat{e}_+ + \hat{e}_-) \\ -\frac{1}{\sqrt{2}}i(\hat{e}_+ - \hat{e}_-) \\ \hat{e}_{\mathbf{0}} \end{pmatrix}$.

8.2.3 Field Vector and Wave Vector in Complex Unit Vectors

From Eqs. 8.35 and 8.36, we write the field and wavevectors in terms of complex unit vectors

$$\begin{pmatrix} \hat{\varepsilon}_{\mathbf{k}1} \\ \hat{\varepsilon}_{\mathbf{k}2} \\ \hat{\kappa} \end{pmatrix} = \frac{1}{\sqrt{2}} \begin{pmatrix} \epsilon_{\mathbf{k}1+} = e^{-i\varphi}\cos\theta & \epsilon_{\mathbf{k}1-} = e^{i\varphi}\cos\theta & \epsilon_{\mathbf{k}1,0} = -\sqrt{2}\sin\theta \\ \epsilon_{\mathbf{k}2+} = -ie^{-i\varphi} & \epsilon_{\mathbf{k}2-} = ie^{i\varphi} & \epsilon_{\mathbf{k}2,0} = 0 \\ \kappa_+ = e^{-i\varphi}\sin\theta & \kappa_- = e^{i\varphi}\sin\theta & \kappa_0 = \sqrt{2}\cos\theta \end{pmatrix} \begin{pmatrix} \hat{e}_+ \\ \hat{e}_- \\ \hat{e}_0 \end{pmatrix} \quad (8.37)$$

$$\hat{\varepsilon}_{\mathbf{k}\lambda} = \sum_{q=0,\pm1} \hat{e}_q \epsilon_{\mathbf{k}\lambda q} = \sum_{q=0,\pm1} \hat{e}_q^* \epsilon_{\mathbf{k}\lambda q}^* \quad (8.38)$$

$$\hat{\kappa} = \sum_{q=0,\pm1} \hat{e}_q \kappa_q = \sum_{q=+,-,0} \hat{e}_q^* \kappa_q^* \quad (8.39)$$

where $\lambda \in 1,2$ and the properties $\epsilon_{\mathbf{k}\lambda q}^* = \epsilon_{\mathbf{k}\lambda,-q}$, $\kappa_q^* = \kappa_{-q}$ and $\epsilon_{\mathbf{k}\lambda q} = \hat{e}_q^* \cdot \hat{\varepsilon}_{\mathbf{k}\lambda}$.

Using the tensor property $\hat{\varepsilon}_{\mathbf{k}1}\hat{\varepsilon}_{\mathbf{k}1} + \hat{\varepsilon}_{\mathbf{k}2}\hat{\varepsilon}_{\mathbf{k}2} + \hat{\kappa}\hat{\kappa} = I$ from Eq. 8.37, we obtain

$$\begin{aligned} \sum_{\lambda=1,2} \epsilon_{\mathbf{k}\lambda q}\epsilon_{\mathbf{k}\lambda q'}^* &= (\hat{e}_q \cdot \hat{\varepsilon}_{\mathbf{k}1})(\hat{e}_{q'}^* \cdot \hat{\varepsilon}_{\mathbf{k}1}^*) + (\hat{e}_q \cdot \hat{\varepsilon}_{\mathbf{k}2})(\hat{e}_{q'}^* \cdot \hat{\varepsilon}_{\mathbf{k}2}^*) \\ &= \hat{e}_q \cdot \{\hat{\varepsilon}_{\mathbf{k}1}\hat{\varepsilon}_{\mathbf{k}1}^* + \hat{\varepsilon}_{\mathbf{k}2}\hat{\varepsilon}_{\mathbf{k}2}^*\} \cdot \hat{e}_{q'}^* = \delta_{qq'} - \kappa_q\kappa_{q'}^* \quad (8.40) \\ \mathbf{a}\cdot\mathbf{b} - (\mathbf{a}\cdot\hat{\kappa})(\hat{\kappa}\cdot\mathbf{b}) &= (\mathbf{a}\cdot\hat{\varepsilon}_{\mathbf{k}1})(\hat{\varepsilon}_{\mathbf{k}1}\cdot\mathbf{b}) + (\mathbf{a}\cdot\hat{\varepsilon}_{\mathbf{k}2})(\hat{\varepsilon}_{\mathbf{k}2}\cdot\mathbf{b}) \quad (8.41) \end{aligned}$$

For $q \neq q'$, the φ integration of $\kappa_q\kappa_{q'}^*$ and $\sum_{\lambda=1,2} \epsilon_{\mathbf{k}\lambda q}\epsilon_{\mathbf{k}\lambda q'}^*$ are zero. For $q = q'$, we have

$$\sum_{\lambda=1,2} \epsilon_{\mathbf{k}\lambda q}\epsilon_{\mathbf{k}\lambda q}^* = 1 - \{\delta_{q0}\cos^2\theta + \delta_{q\pm}\frac{1}{2}\sin^2\theta\} = \{\delta_{q0}\sin^2\theta + \delta_{q\pm}(1 - \frac{1}{2}\sin^2\theta)\} \doteq N_q(\theta) \quad (8.42)$$

We can also evaluate $\sum_\lambda \hat{\varepsilon}_{\mathbf{k}\lambda} \cdot \hat{\varepsilon}_{\mathbf{k}\lambda}^* = \sum_\lambda \sum_{q=0,\pm1} \epsilon_{\mathbf{k}\lambda q}\epsilon_{\mathbf{k}\lambda q'}^* = \sin^2\theta + 2(1 - \frac{1}{2}\sin^2\theta) = 2$. The Coulomb gauge means that $\sum_{q=0,\pm1} \epsilon_{\mathbf{k}\lambda q}\kappa_{q'} = 0$.

8.2.4 Dipole Moment Operator for Molecules

The component of the dipole moment $\hat{\mathbf{d}}$ along the field unit vector $\hat{\varepsilon}_{\mathbf{k}\lambda}$ can be expressed as

$$\hat{\mathbf{d}}\cdot\hat{\varepsilon}_{\mathbf{k}\lambda} = \sum_{q=+,-,0} \epsilon_{\mathbf{k}\lambda q}\hat{d}_q^\dagger = \sum_{q=+,-,0} \epsilon_{\mathbf{k}\lambda q}\hat{d}_{-q} = \sum_{q=+,-,0} \epsilon_{\mathbf{k}\lambda q}^*\hat{d}_q = \sum_{q=+,-,0} \epsilon_{\mathbf{k}\lambda,-q}^*\hat{d}_{-q} \quad (8.43)$$

$$\hat{\mathbf{d}}\cdot\mathbf{k} = \sum_{q=+,-,0} \hat{d}_q\kappa_q^* = \sum_{q=+,-,0} \hat{d}_q^\dagger\kappa_q \quad (8.44)$$

where the q-component of the dipole operator $\hat{d}_q$ can be expressed in terms of the dipole components $\{\hat{d}_g\}$ in the rotating frame of the molecule

$$\hat{d}_q = \hat{d}_{-q}^\dagger = \sum_{g=0,+,-} \Phi_{qg}\hat{d}_g = \sum_{g=0,+,-} \sum_{a,b} S_{ab}d_{g(ab)}C_{qg(ab)} \quad (8.45)$$

where $S_{ab} = |a\rangle\langle b|$, $d_{g(ab)}$ is the reduced dipole moment and $C_{qg(ab)}$ contains all the dimensionless factors, for example the Clebsch-Gordan coefficient, the Honl-London factor and/or the Franck-Condon factor. The additional summation index 'g' is due to the existence of 3 components in molecule fixed frame. In the case of atoms, this does not exist and $\hat{d}_g \rightarrow \hat{d}_q$. Thus Eq. 8.43 becomes

$$\hat{\mathbf{d}}\cdot\hat{\varepsilon}_{\mathbf{k}\lambda} = \sum_{q=+,-,\mathbf{0}} \epsilon^*_{\mathbf{k}\lambda,q} \sum_{g=\mathbf{0},+,-} \sum_{a,b} S_{ab} d_{g(ab)} C_{qg(ab)} \tag{8.46}$$

$$\hat{\mathbf{d}}\cdot\hat{\kappa} = \sum_{q=+,-,\mathbf{0}} \kappa^*_{\mathbf{k}\lambda q} \sum_{g=\mathbf{0},+,-} \sum_{a,b} S_{ab} d_{g(ab)} C_{qg(ab)} \tag{8.47}$$

Alternatively, equation 8.43 can be rewritten as

$$\hat{\mathbf{d}}\cdot\hat{\varepsilon}_{\mathbf{k}\lambda} = \sum_{a,b} S_{ab} d_{ab\mathbf{k}\boldsymbol{\lambda}} \tag{8.48}$$

$$d_{ab\mathbf{k}\boldsymbol{\lambda}} = \langle a|\hat{\mathbf{d}}\cdot\hat{\varepsilon}_{\mathbf{k}\lambda}|b\rangle = \sum_{q,g=+,-,\mathbf{0}} \epsilon^*_{\mathbf{k}\lambda q} d_{g(ab)} C_{qg(ab)} \tag{8.49}$$

8.2.5 Mode Summation in Multipolar Coupling

The radiation coupling in multipolar version is expressed as

$$g_{ab\mathbf{k}\lambda} = d_{ab\mathbf{k}\boldsymbol{\lambda}} \sqrt{\frac{\omega_{k\boldsymbol{\lambda}}}{2\varepsilon_o V\hbar}} = \sqrt{\frac{\omega_{k\boldsymbol{\lambda}}}{2\varepsilon_o V\hbar}} \sum_{q,g=+,-,\mathbf{0}} \epsilon^*_{\mathbf{k}\lambda q} d_{g(ab)} C_{qg(ab)} \tag{8.50}$$

The mode summation involving the coupling constant can be evaluated by converting the discrete summation to integration

$$\sum_{\mathbf{k},\lambda} \rightarrow \sum_{\lambda} \int d\omega D_\lambda(\omega) \quad \text{with spectral density of states } D_\lambda(\omega) = \frac{V}{(2\pi c)^3}\omega^2 \int d\Omega_\lambda \tag{8.51}$$

thus giving

$$\sum_{\mathbf{k},\lambda} g_{ab\mathbf{k}\lambda} g_{cd\mathbf{k}\lambda} \ldots \rightarrow \sum_{\lambda} \int d\omega D_\lambda(\omega) g_{ab\mathbf{k}\lambda} g_{cd\mathbf{k}\lambda} \ldots = \sum_{\lambda} \int d\omega D_\lambda(\omega) \frac{\omega}{2\varepsilon_o V\hbar} (d_{ab\mathbf{k}\boldsymbol{\lambda}})(d_{cd\mathbf{k}\boldsymbol{\lambda}}) \ldots \tag{8.52}$$

where

$$(d_{ab\mathbf{k}\boldsymbol{\lambda}})(d_{cd\mathbf{k}\boldsymbol{\lambda}}) = \sum_{g,g'=+,-,\mathbf{0}} d_{g(ab)} d_{g'(cdb)} \sum_{q,q'=+,-,\mathbf{0}} \epsilon^*_{\mathbf{k}\lambda q} \epsilon_{\mathbf{k}\lambda q'} C_{qg(ab)} C_{-q'g'(cd)} \tag{8.53}$$

For polarization independent angular emission, $d\Omega_\lambda = d\Omega$ and for isotropic space $d\Omega \rightarrow \sin\theta d\theta d\phi$, we have

$$\sum_{\mathbf{k},\lambda} \rightarrow \sum_{\lambda} \frac{V}{(2\pi c)^3} \int_0^{\omega_c} \omega^2 d\omega \int d\Omega \quad \text{where} \quad \int d\Omega \equiv \int_0^{2\pi} d\phi \int_0^{\pi} d\theta \sin\theta \tag{8.54}$$

where ω_c is the cutoff-frequency. We combine Eqs. 8.52, 8.53 and 8.42 to obtain

$$\sum_{\mathbf{k},\lambda} g_{ab\mathbf{k}\lambda} g_{cd\mathbf{k}\lambda} \cdots = \sum_{g,g'=+,-,\mathbf{0}} \frac{d_{g(ab)} d_{g'(cd)}}{2\varepsilon_o \hbar (2\pi c)^3} \sum_{q=+,-,\mathbf{0}} C_{qg(ab)} C_{-qg'(cd)} \int_0^{\omega_c} d\omega \omega^3 \int d\Omega N_q(\theta) \ldots \tag{8.55}$$

Using $\int N_q(\theta) \sin\theta d\theta d\phi = \frac{8\pi}{3}$, we have

$$\sum_{\mathbf{k},\lambda} g_{ab\mathbf{k}\lambda} g_{cd\mathbf{k}\lambda} 2\pi\delta(\omega_{\mathbf{k}\lambda} - x) = \sum_{g,g'=+,-,\mathbf{0}} \frac{d_{g(ab)} d_{g'(cd)} x^3}{3\varepsilon_o \hbar \pi c^3} \sum_{q=+,-,\mathbf{0}} C_{qg(ab)} C_{-qg'(cd)} \tag{8.56}$$

For $ab \equiv cd$, Eq. 8.55 becomes

$$\sum_{\mathbf{k},\lambda} |g_{ab\mathbf{k}\lambda}|^2 \ldots = \Gamma_{ab} \frac{3}{16\pi^2} \int_0^{\omega_c} d\omega \frac{\omega^3}{\omega_{ab}^3} \int d\Omega N_q(\theta) \ldots \tag{8.57}$$

where $\Gamma_{ab} \doteq \sum_{g=+,-,\mathbf{0}} \frac{|d_{g(ab)}|^2 \omega_{ab}^3}{3\varepsilon_o \hbar \pi c^3} \sum_{q=+,-,\mathbf{0}} C_{qg(ab)} C_{-qg(ab)}$.

8.2.6 Mode Summation in Minimal Coupling

The minimal coupling version is expressed as

$$g_{ab\mathbf{k}\lambda} = \omega_{ab} d_{ab\mathbf{k}\boldsymbol{\lambda}} \sqrt{\frac{1}{2\varepsilon_o \omega_{k\boldsymbol{\lambda}} V\hbar}} = \omega_{ab} \sqrt{\frac{1}{2\varepsilon_o \omega_{k\boldsymbol{\lambda}} V\hbar}} \sum_{q,g=+,-,\mathbf{0}} \epsilon^*_{\mathbf{k}\lambda q} d_{g(ab)} C_{qg(ab)} \tag{8.58}$$

Thus, we have

$$\sum_{\mathbf{k},\lambda} g_{ab\mathbf{k}\lambda} g_{cd\mathbf{k}\lambda} \cdots = \sum_{g,g'=+,-,\mathbf{0}} \frac{d_{g(ab)} d_{g'(cd)} \omega_{ab} \omega_{cd}}{2\varepsilon_o \hbar (2\pi c)^3} \sum_{q=+,-,\mathbf{0}} C_{qg(ab)} C_{-qg'(cd)} \int_0^{\omega_c} d\omega \omega \int d\Omega N_q(\theta) \ldots \tag{8.59}$$

$$\sum_{\mathbf{k},\lambda} |g_{ab\mathbf{k}\lambda}|^2 \ldots = \Gamma_{ab} \frac{3}{16\pi^2} \int_0^{\omega_c} d\omega \frac{\omega}{\omega_o} \int d\Omega N_q(\theta) \ldots \tag{8.60}$$

From Eqs. 8.50 and 8.51, we find the summation of single $g_{ab\mathbf{k}\lambda}$

$$\sum_{\mathbf{k},\lambda} g_{ab\mathbf{k}\lambda} \cdots = \frac{V}{(2\pi c)^3} \sum_{\lambda} \int d\omega \omega^2 \int_0^{2\pi} d\phi \int_0^{\pi} d\theta \sin\theta \sqrt{\frac{\omega_{k\lambda}}{2\varepsilon_o V\hbar}} \sum_{q,g=+,-,\mathbf{0}} \epsilon^*_{\mathbf{k}\lambda q} d_{g(ab)} C_{qg(ab)} \cdots \tag{8.61}$$

From Eq. 8.37, we see that the angular integration of Eq. 8.61 vanishes except for $\epsilon_{\mathbf{k}\mathbf{1},\mathbf{0}} = -\sqrt{2}\sin\theta$.

8.3 Appendix III:Center of Mass Canonical Operators

We shall use the commutation relation of Eq. 2.58 to obtain the various operator relations for the center of mass variables

$$[\hat{R}_q, \hat{P}_{q'}] = i\hbar\delta_{qq'} \tag{8.62}$$

The quantized momentum and position operators are expressed as

$$\hat{\mathbf{P}} = -i\hbar\boldsymbol{\nabla}_R, \hat{\mathbf{R}} = i\hbar\boldsymbol{\nabla}_P \tag{8.63}$$

For discrete variables we have $f(\hat{\mathbf{P}})\,|\mathbf{P}_i\rangle = f(\mathbf{P}_i)\,|\mathbf{P}\rangle$ and $f(\hat{\mathbf{R}})\,|\mathbf{R}_i\rangle = f(\mathbf{R}_i)$. Since $\{|\mathbf{P}_i\rangle\}$ and $\{|\mathbf{R}_i\rangle\}$ form complete sets, we have the closure relations $\sum\limits_i |\mathbf{P}_i\rangle\langle\mathbf{P}_i| = 1$ and $\sum\limits_i |\mathbf{R}_i\rangle\langle\mathbf{R}_i| = 1$. From orthonormality $\langle\mathbf{P}_i|\,\mathbf{P}_j\rangle = \delta_{ij} = \sum\limits_k \langle\mathbf{P}_i|\,\mathbf{R}_k\rangle\langle\mathbf{R}_k|\,\mathbf{P}_j\rangle = \sum\limits_k e^{i(\mathbf{P}_i-\mathbf{P}_j)\cdot\mathbf{R}_k/\hbar}$ we have

$$\langle\mathbf{P}_i|\,\mathbf{R}_k\rangle = e^{i\mathbf{P}_i\cdot\mathbf{R}_k/\hbar} \tag{8.64}$$

For continuous variables we have $f(\hat{\mathbf{P}})\,|\mathbf{P}\rangle = f(\mathbf{P})\,|\mathbf{P}\rangle$ and $f(\hat{\mathbf{R}})\,|\mathbf{R}\rangle = f(\mathbf{R})\,|\mathbf{R}\rangle$. Since $\{|\mathbf{P}\rangle\}$ and $\{|\mathbf{R}\rangle\}$ form complete sets, we have the closure relations $\int d^3P\;|\mathbf{P}\rangle\langle\mathbf{P}| = 1$ and $\int d^3R\;|\mathbf{R}\rangle\langle\mathbf{R}| = 1$. From orthonormality

$$\langle\mathbf{P}|\,\mathbf{P}'\rangle = \delta(\mathbf{P}-\mathbf{P}') = \int \langle\mathbf{P}|\,\mathbf{R}\rangle\langle\mathbf{R}|\,\mathbf{P}'\rangle d^3R = \frac{1}{(2\pi\hbar)^3}\int e^{i(\mathbf{P}-\mathbf{P}')\cdot\mathbf{R}/\hbar}d^3R$$

we have

$$\langle\mathbf{R}|\,\mathbf{P}\rangle = \frac{1}{(2\pi\hbar)^{3/2}}e^{i\mathbf{P}\cdot\mathbf{R}/\hbar} = \psi_{\mathbf{P}}(\mathbf{R}) \tag{8.65}$$

Multiplying $\langle\mathbf{R}|\,\mathbf{P}\rangle$ with $|\mathbf{R}\rangle$ from left, integrating over R and using closure relation, we have

$$|\mathbf{P}\rangle = \frac{1}{(2\pi\hbar)^{3/2}}\int |\mathbf{R}\rangle e^{i\mathbf{P}\cdot\mathbf{R}/\hbar}d^3R \tag{8.66}$$

$$|\mathbf{R}\rangle = \frac{1}{(2\pi\hbar)^{3/2}}\int |\mathbf{P}\rangle e^{-i\mathbf{P}\cdot\mathbf{R}/\hbar}d^3P \tag{8.67}$$

where the momentum and position state vectors are related by Fourier transforms. In the following we use Eqs. 8.66 and 8.67 and obtain

$$\hat{\mathbf{R}}\,|\mathbf{P}\rangle = \frac{\mathbf{1}}{(2\pi\hbar)^{3/2}}\int \mathbf{R}\,|\mathbf{R}\rangle e^{i\mathbf{P}\cdot\mathbf{R}/\hbar}d^3R \tag{8.68}$$

$$\hat{\mathbf{P}}\,|\mathbf{R}\rangle = \frac{\mathbf{1}}{(2\pi\hbar)^{3/2}}\int \mathbf{P}\,|\mathbf{P}\rangle e^{-i\mathbf{P}\cdot\mathbf{R}/\hbar}d^3P \tag{8.69}$$

Similarly, we have $e^{\pm i\mathbf{k}\cdot\hat{\mathbf{R}}}|\mathbf{P}\rangle = \frac{1}{(2\pi\hbar)^{3/2}}\int e^{\pm i\mathbf{k}\cdot\hat{\mathbf{R}}}|\mathbf{R}\rangle e^{i\mathbf{P}\cdot\mathbf{R}/\hbar}d^3R = \frac{1}{(2\pi\hbar)^{3/2}}\int |\mathbf{R}\rangle e^{i(\mathbf{P}\pm\hbar\mathbf{k})\cdot\mathbf{R}/\hbar}d^3R$

$$e^{\pm i\mathbf{k}\cdot\hat{\mathbf{R}}}|\mathbf{P}\rangle = |\mathbf{P}\pm\hbar\mathbf{k}\rangle \rightarrow \langle\mathbf{P}|e^{\mp i\mathbf{k}\cdot\hat{\mathbf{R}}} = \langle\mathbf{P}\pm\hbar\mathbf{k}| \tag{8.70}$$

Also, $e^{\pm i\hat{\omega}_D t}|\mathbf{P}\rangle = e^{\pm i\omega_D t}|\mathbf{P}\rangle \rightarrow \langle\mathbf{P}|e^{\mp i\hat{\omega}_D t} = e^{\mp i\omega_D t}\langle\mathbf{P}|$.

Multiplying Eq. 8.70 with $\langle\mathbf{P}|$ and integrating, we have

$$e^{\pm i\mathbf{k}\cdot\hat{\mathbf{R}}} = \int d^3P|\mathbf{P}\pm\hbar\mathbf{k}\rangle\langle\mathbf{P}| = \int d^3P|\mathbf{P}\rangle\langle\mathbf{P}\mp\hbar\mathbf{k}| \tag{8.71}$$

For a state vector $|\Psi\rangle$ we can use the Taylor series $f(x+a) = e^{a\frac{\partial}{\partial x}}f(x)$ and write

$$\langle\mathbf{P}|\,e^{i\mathbf{k}\cdot\hat{\mathbf{R}}}\,|\Psi\rangle = \langle\mathbf{P}-\hbar\mathbf{k}\,|\Psi\rangle = \Psi(\mathbf{P}-\hbar\mathbf{k}) = e^{-\hbar\mathbf{k}\cdot\boldsymbol{\nabla}_P}\Psi(\mathbf{P}) = e^{i\mathbf{k}\cdot\hat{\mathbf{R}}}\Psi(\mathbf{P}) = e^{i\mathbf{k}\cdot\hat{\mathbf{R}}}\langle\mathbf{P}\,|\Psi\rangle \tag{8.72}$$

Using $[f(x),\hat{p}_x] = i\hbar\frac{\partial f(x)}{\partial x}$, $[x,f(p)] = i\hbar\frac{\partial f(x)}{\partial p}$, $e^{ik\hat{R}}\hat{P}e^{-ik\hat{R}} = \hat{P}+[ik\hat{R},\hat{P}]+\frac{1}{2!}[ik\hat{R},[ik\hat{R},\hat{P}]]+ ... = \hat{P}-\hbar k$ and $e^{ik\hat{R}}f(\hat{P})e^{-ik\hat{R}} = f(e^{ik\hat{R}}\hat{P}e^{-ik\hat{R}})$ we have

$$e^{i\mathbf{k}\cdot\hat{\mathbf{R}}}e^{i\mathbf{a}\cdot\hat{\mathbf{P}}}e^{-i\mathbf{k}\cdot\hat{\mathbf{R}}} = \exp\{i(e^{i\mathbf{k}\cdot\hat{\mathbf{R}}}\mathbf{a}\cdot\hat{\mathbf{P}}e^{-i\mathbf{k}\cdot\hat{\mathbf{R}}})\} = \exp\{i\mathbf{a}\cdot(\hat{\mathbf{P}}-\hbar\mathbf{k})\} \tag{8.73}$$

From $\hat{P}e^{i\mathbf{k}\cdot\hat{\mathbf{R}}} = \hat{P}+ik\cdot\hat{P}\hat{R}+\frac{1}{2}\hat{P}(ik\cdot\hat{R})^2+....$, and $e^{i\mathbf{k}\cdot\hat{\mathbf{R}}}\hat{P} = \hat{P}+ik\hat{R}\hat{P}+\frac{1}{2}(ik\cdot\hat{R})^2\hat{P}+.... = \hat{P}+ik(\hat{P}\hat{R}+i\hbar)-\frac{1}{2}k^2(\hat{P}\hat{R}^2+2i\hbar\hat{R})....$ we have

$$e^{\pm i\mathbf{k}\cdot\hat{\mathbf{R}}}\hat{\mathbf{P}} = (\hat{\mathbf{P}}\mp\hbar\mathbf{k})e^{\pm i\mathbf{k}\cdot\hat{\mathbf{R}}} \rightarrow \hat{\mathbf{P}}e^{\pm i\mathbf{k}\cdot\hat{\mathbf{R}}} = e^{\pm i\mathbf{k}\cdot\hat{\mathbf{R}}}(\hat{\mathbf{P}}\pm\hbar\mathbf{k}) \tag{8.74}$$

$$\{e^{i\mathbf{k}\cdot\hat{\mathbf{R}}},\hat{\mathbf{P}}\}_+ = (\mathbf{2}\hat{\mathbf{P}}-\hbar\mathbf{k})\mathbf{e}^{i\mathbf{k}\cdot\hat{\mathbf{R}}} = \mathbf{e}^{i\mathbf{k}\cdot\hat{\mathbf{R}}}(\mathbf{2}\hat{\mathbf{P}}+\hbar\mathbf{k}) \tag{8.75}$$

Equation 8.74 can be veritifed: LHS is $e^{\pm i\mathbf{k}\cdot\hat{\mathbf{R}}}\hat{\mathbf{P}}|\mathbf{P}\rangle = \mathbf{P}e^{\pm i\mathbf{k}\cdot\hat{\mathbf{R}}}|\mathbf{P}\rangle = \mathbf{P}|\mathbf{P}\pm\hbar\mathbf{k}\rangle$ →RHS is $(\hat{\mathbf{P}}\mp\hbar\mathbf{k})e^{\pm i\mathbf{k}\cdot\hat{\mathbf{R}}}|\mathbf{P}\rangle = (\hat{\mathbf{P}}\mp\hbar\mathbf{k})|\mathbf{P}\pm\hbar\mathbf{k}\rangle = \mathbf{P}|\mathbf{P}\pm\hbar\mathbf{k}\rangle$.

8.3.1 Time Dependent Center of Mass Operators

The center of mass operator in interaction picture is evaluated as

$$\hat{\pi}_{\mathbf{k}}(t) \doteq e^{i\frac{P^2}{2M\hbar}t}e^{i\mathbf{k}\cdot\hat{\mathbf{R}}}e^{-i\frac{P^2}{2M\hbar}t} = e^{i\mathbf{k}\cdot(\hat{\mathbf{R}}+\frac{t}{M}\hat{\mathbf{P}})} = e^{i\mathbf{k}\cdot\hat{\mathbf{R}}}e^{i\mathbf{k}\cdot\hat{\mathbf{P}}\frac{t}{M}}e^{i\frac{\hbar k^2}{2M}t} \tag{8.76}$$

$$= e^{i\mathbf{k}\cdot\hat{\mathbf{P}}\frac{t}{M}}e^{i\mathbf{k}\cdot\hat{\mathbf{R}}}e^{-i\frac{\hbar k^2}{2M}t} = e^{i\omega_r t}\sum_{\mathbf{P}'}\left|\mathbf{P}'+\hbar\mathbf{k}\right\rangle\langle\mathbf{P}'|e^{i\mathbf{k}\cdot\mathbf{P}'t/M} \tag{8.77}$$

$$\hat{\pi}_{\mathbf{k}}(t)\,|\mathbf{P}\rangle = |\mathbf{P}+\hbar\mathbf{k}\rangle\,e^{i\mathbf{k}\cdot\mathbf{P}\frac{t}{M}}e^{i\frac{\hbar k^2}{2M}t} \rightarrow \langle\mathbf{P}|\hat{\pi}^\dagger_{\mathbf{k}}(t) = \langle\mathbf{P}+\hbar\mathbf{k}|e^{-i\mathbf{k}\cdot\mathbf{P}\frac{t}{M}}e^{-i\frac{\hbar k^2}{2M}t} \tag{8.78}$$

$$\hat{\pi}^\dagger_{\mathbf{k}}(t) = e^{i\frac{P^2}{2M\hbar}t}e^{-i\mathbf{k}\cdot\hat{\mathbf{R}}}e^{-i\frac{P^2}{2M\hbar}t} \tag{8.79}$$

$$= e^{i\omega_r t}\sum_{\mathbf{P}'}\left|\mathbf{P}'-\hbar\mathbf{k}\right\rangle\langle\mathbf{P}'|e^{-i\mathbf{k}\cdot\mathbf{P}'\frac{t}{M}} = e^{-i\omega_r t}\sum_{\mathbf{P}'}\left|\mathbf{P}'\right\rangle\langle\mathbf{P}'+\hbar\mathbf{k}|e^{-i\mathbf{k}\cdot\mathbf{P}'\frac{t}{M}} \tag{8.80}$$

$$\hat{\pi}^\dagger_{\mathbf{k}}(t)\,|\mathbf{P}\rangle = |\mathbf{P}-\hbar\mathbf{k}\rangle\,e^{-i\mathbf{k}\cdot\mathbf{P}\frac{t}{M}}e^{i\frac{\hbar k^2}{2M}t} \rightarrow \langle\mathbf{P}|\hat{\pi}_{\mathbf{k}}(t) = \langle\mathbf{P}-\hbar\mathbf{k}|e^{i\mathbf{k}\cdot\mathbf{P}\frac{t}{M}}e^{-i\frac{\hbar k^2}{2M}t} \tag{8.81}$$

where $\hat{\pi}^\dagger_{\mathbf{k}}(t) = \hat{\pi}_{-\mathbf{k}}(t)$.

The time derivative of the c.m. operator is evaluated as $\frac{d\hat{\pi}_{\mathbf{k}}(t)}{dt} = \frac{d\hat{U}_E^+(t)}{dt} e^{i\mathbf{k}\cdot\hat{\mathbf{R}}} \hat{U}_E(t) + \hat{U}_E^+(t) e^{i\mathbf{k}\cdot\hat{\mathbf{R}}} \frac{d\hat{U}_E(t)}{dt} = \frac{1}{i\hbar}\hat{U}_E^+(t)[e^{i\mathbf{k}\cdot\hat{\mathbf{R}}}, H_E]\hat{U}_E(t) = i(\frac{\hat{\mathbf{P}}\cdot\mathbf{k}}{M} - \frac{\hbar\mathbf{k}^2}{2M})\hat{U}_E^+(t)e^{i\mathbf{k_L}\cdot\hat{\mathbf{R}}}\hat{U}_E(t)$

$$\frac{d\hat{\pi}_{\mathbf{k}}(t)}{dt} = i(\frac{\hat{\mathbf{P}}\cdot\mathbf{k}}{M} - \frac{\hbar k^2}{2M})\hat{\pi}_{\mathbf{k}}(t) = i\hat{\pi}_{\mathbf{k}}(t)(\frac{\hat{\mathbf{P}}\cdot\mathbf{k}}{M} + \frac{\hbar k^2}{2M}) \tag{8.82}$$

$$\frac{d\hat{\pi}^\dagger_{\mathbf{k}}(t)}{dt} = i(-\frac{\hat{\mathbf{P}}\cdot\mathbf{k}}{M} + \frac{\hbar k^2}{2M})\hat{\pi}^\dagger_{\mathbf{k}}(t) = -i\hat{\pi}^\dagger_{\mathbf{k}}(t)(\frac{\hat{\mathbf{P}}\cdot\mathbf{k}}{M} + \frac{\hbar k^2}{2M}) \tag{8.83}$$

Here, it is important to note that $\frac{d\hat{\pi}^\dagger_{\mathbf{k}}(t)}{dt} \neq (\frac{d\hat{\pi}_{\mathbf{k}}(t)}{dt})^\dagger$. Furthermore, can write $\hat{\pi}_{\mathbf{k}}(t) = \sqrt{\hat{\pi}_{\mathbf{k}}(t)}\sqrt{\hat{\pi}_{\mathbf{k}}(t)}$ and evaluate

$$\frac{d}{dt}\sqrt{\hat{\pi}_{\mathbf{k}}(t)} = \frac{d\hat{\pi}_{\mathbf{k}}(t)}{dt}\frac{1}{2\sqrt{\hat{\pi}_{\mathbf{k}}(t)}} = \frac{1}{2}i(\frac{\hat{\mathbf{P}}\cdot\mathbf{k}}{M} - \frac{\hbar k^2}{2M})\sqrt{\hat{\pi}_{\mathbf{k}}(t)} \tag{8.84a}$$

$$\frac{d}{dt}\sqrt{\hat{\pi}^\dagger_{\mathbf{k}}(t)} = \frac{d\hat{\pi}^\dagger_{\mathbf{k}}(t)}{dt}\frac{1}{2\sqrt{\hat{\pi}^\dagger_{\mathbf{k}}(t)}} = \frac{1}{2}i(-\frac{\hat{\mathbf{P}}\cdot\mathbf{k}}{M} + \frac{\hbar k^2}{2M})\sqrt{\hat{\pi}^\dagger_{\mathbf{k}}(t)} \tag{8.84b}$$

Next we use Eq. 8.74 and obtain

$$[\frac{\hat{\mathbf{P}}^2}{2M}, e^{\pm i\mathbf{k}\cdot\hat{\mathbf{R}}}] = (\pm\frac{\hbar\hat{\mathbf{P}}\cdot\mathbf{k}}{M} - \frac{\hbar^2\mathbf{k}^2}{2M})e^{\pm i\mathbf{k_L}\cdot\hat{\mathbf{R}}} \tag{8.85}$$

Since $[\frac{\hat{\mathbf{P}}^2}{2M}, \hat{\pi}_{\mathbf{k}}(t)] = \hat{U}^\dagger_{cm}(t)[\frac{\hat{\mathbf{P}}^2}{2M}, e^{i\mathbf{k_L}\cdot\hat{\mathbf{R}}}]\hat{U}_{cm}(t)$,we have

$$[\frac{\hat{\mathbf{P}}^2}{2M}, \hat{\pi}_{\pm\mathbf{k}}(t)] = (\pm\frac{\hbar\hat{\mathbf{P}}\cdot\mathbf{k}}{M} - \frac{\hbar^2\mathbf{k}^2}{2M})\hat{\pi}_{\pm\mathbf{k}}(t) \tag{8.86}$$

$$[\hat{\pi}^\dagger_{\mathbf{k}}(t), \frac{\hat{\mathbf{P}}^2}{2M}] = \hat{\pi}^\dagger_{\mathbf{k}}(t)(\frac{\hbar\hat{\mathbf{P}}\cdot\mathbf{k}}{M} - \frac{\hbar^2\mathbf{k}^2}{2M}) \tag{8.87}$$

8.3.2 Double operators product

The products of the c.m. operators which appear in the dissiptive Liouvillean in the master equation are obtained from Eqs. 8.77,8.80

$$\begin{aligned}
\hat{\pi}_{\mathbf{k}}(t)\hat{\pi}_{\mathbf{k}}(t') &= e^{i\omega_r(t-t')}\sum_{\mathbf{P}'}|\mathbf{P}'+\hbar\mathbf{k}\rangle\langle\mathbf{P}'-\hbar\mathbf{k}|e^{i\omega_{\mathbf{P}'}(t+t')} \\
\hat{\pi}^\dagger_{\mathbf{k}}(t)\hat{\pi}^\dagger_{\mathbf{k}}(t') &= e^{i\omega_r(t-t')}\sum_{\mathbf{P}'}|\mathbf{P}'-\hbar\mathbf{k}\rangle\langle\mathbf{P}'+\hbar\mathbf{k}|e^{-i\omega_{\mathbf{P}'}(t+t')} \\
\hat{\pi}_{\mathbf{k}}(t)\hat{\pi}^\dagger_{\mathbf{k}}(t') &= e^{i\omega_r(t-t')}\sum_{\mathbf{P}'}|\mathbf{P}'+\hbar\mathbf{k}\rangle\langle\mathbf{P}'+\hbar\mathbf{k}|e^{i\mathbf{k}\cdot\mathbf{P}'(t-t')/M} = e^{-i\omega_r\tau}\sum_{\mathbf{P}'}|\mathbf{P}'\rangle\langle\mathbf{P}'|e^{i\omega_{\mathbf{P}'}\tau} \\
\hat{\pi}^\dagger_{\mathbf{k}}(t)\hat{\pi}_{\mathbf{k}}(t') &= e^{-i\omega_r\tau}\sum_{\mathbf{P}'}|\mathbf{P}'\rangle\langle\mathbf{P}'|e^{-i\omega_{\mathbf{P}'}\tau}
\end{aligned} \tag{8.88}$$

8.4 Appendix IV: Solutions for Two-Level System with Quantized Center of Mass Momentum

In the case of time dependent Hamiltonian $V(t)$ in interaction picture, the evolution operator is given by

$$\begin{aligned}
\hat{U}(t,t_o) &= I+\sum_{n=1}^{\infty}\hat{U}^{(n)}(t,t_o)=T_{\leftarrow}\{e^{\frac{1}{i\hbar}\int_{t_o}^{t}dt'\hat{V}(t')}\} \\
\hat{U}^{(n)}(t,t_o) &= (\frac{1}{i\hbar})^n\int_{t_o}^{t}dt_1\int_{t_o}^{t_1}dt_2...\int_{t_o}^{t_{n-1}}dt_n\hat{V}(t_1)\hat{V}(t_2)...\hat{V}(t_n) \\
&= \frac{1}{n!}(\frac{1}{i\hbar})^n\int_{t_o}^{t}dt_1\int_{t_o}^{t}dt_2...\int_{t_o}^{t}dt_nT_{\leftarrow}\{\hat{V}(t_1)\hat{V}(t_2)...\hat{V}(t_n)\} \qquad (8.89)
\end{aligned}$$

In general, $\hat{U}(t,t_o)$ cannot be evaluated exactly. Even numerically, the evaluation of the infinite series is not possible. In this Section we derive the exact solutions for the quantum evolutions of the internal and external center of mass dynamics of *two-level system* driven by coherent laser fields. The center of mass with Röntgen effect [239] is included. Here, we show how $\hat{U}(t,t_o)$ can be evaluated precisely for arbitrary detuning in a two-level system within RWA. The Hamiltonian of the system can be written generally as $\hat{V}(t)=I\hat{a}(t)+\begin{pmatrix}\hat{b}(t) & \hat{f}(t)\\ \hat{f}^+(t) & -\hat{b}(t)\end{pmatrix}$ where $\hat{a}(t),\hat{b}(t),\hat{f}(t),\hat{f}^+(t)$ are arbitrary time dependent operators. We introduce the ansatz

$$\hat{U}(t)=e^{\frac{1}{i\hbar}\int_0^t\hat{a}(t')dt'}\begin{pmatrix}\hat{C}(t) & \hat{E}(t)\\ \hat{D}(t) & \hat{B}(t)\end{pmatrix} \qquad (8.90)$$

where we assume that the diagonal operator $\hat{a}(t)$ *commutes* with $\hat{b}(t),\hat{f}(t),\hat{f}^+(t)$. Using the equation for evolution operator $\frac{\partial}{\partial t}\hat{U}(t,t_o)=\frac{1}{i\hbar}\hat{V}(t)\hat{U}(t,t_o)$ we have the coupled equations to be solved

$$\begin{aligned}
\frac{\partial}{\partial t}\hat{B} &= \frac{1}{i\hbar}\{-\hat{b}\hat{B}+\hat{f}^+\hat{E}\} \\
\frac{\partial}{\partial t}\hat{C} &= \frac{1}{i\hbar}\{\hat{b}\hat{C}+\hat{f}\hat{D}\} \\
\frac{\partial}{\partial t}\hat{D} &= \frac{1}{i\hbar}\{-\hat{b}\hat{D}+\hat{f}^+\hat{C}\} \\
\frac{\partial}{\partial t}\hat{E} &= \frac{1}{i\hbar}\{\hat{b}\hat{E}+\hat{f}\hat{B}\} \qquad (8.91)
\end{aligned}$$

In interaction picture, $\hat{a}(t)=\hat{b}(t)=0$ and from Eqs. 8.91 we obtain the second order equation

$$\frac{\partial^2\hat{B}}{\partial t^2}=\frac{1}{\hat{f}\hat{f}^+}\frac{\partial\hat{f}^+}{\partial t}\hat{f}\frac{\partial\hat{B}}{\partial t}+\frac{1}{i\hbar}\frac{1}{i\hbar}\hat{f}^+\hat{f}\hat{B} \qquad (8.92)$$

with the boundary conditions from $\hat{U}^\dagger(t)\hat{U}(t) = I$

$$\hat{C}^\dagger\hat{C} + \hat{E}^\dagger\hat{E} = 1, \hat{B}^\dagger\hat{B} + \hat{D}^\dagger\hat{D} = 1, \hat{C}\hat{D}^\dagger + \hat{E}\hat{B}^\dagger = 0, \hat{D}\hat{C}^\dagger + \hat{B}\hat{E}^\dagger = 0 \tag{8.93}$$

The system-laser Hamiltonian in interaction picture can be written as

$$\begin{aligned}\hat{V}_{SL}(t) &= -\hbar(S^\dagger e^{i\omega_o t} + Se^{-i\omega_o t})\sum_L \frac{1}{2}\Omega_L(\hat{\chi}_L\hat{\pi}_L(t)e^{i(-\omega_L t)} + \hat{\pi}_L^\dagger(t)\hat{\chi}_L^\dagger e^{i(\omega_L t)}) \\ &\equiv \hat{f}(t)S^\dagger + \hat{f}^\dagger(t)S \end{aligned} \tag{8.94}$$

where

$$S \doteq |g\rangle\langle e| \tag{8.95}$$

$$\hat{f}(t) \doteq -\hbar\sum_L \frac{1}{2}\Omega_L(\hat{\chi}_L\hat{\pi}_L(t)e^{-i\Delta_L t} + \hat{\pi}_L^\dagger(t)\hat{\chi}_L^\dagger e^{i\sigma_L t}) \tag{8.96}$$

$$\hat{\chi}_L \doteq \sum_{q=+,-,\mathbf{0}} C_q\{\epsilon_{Lq}^*\frac{\omega_{\parallel,L}(\hat{\mathbf{P}})}{\omega_L} + \kappa_{Lq}^*\frac{\omega_{\perp,L}(\hat{\mathbf{P}})}{\omega_L}\} \tag{8.97}$$

$$\hat{\pi}_L(t) \doteq \hat{U}_{cm}^\dagger(t)e^{i\mathbf{k}_L\cdot\hat{\mathbf{R}}}\hat{U}_{cm}(t) = e^{i\mathbf{k}_L\cdot\hat{\mathbf{R}}}e^{i\hat{\omega}_D t}e^{i\omega_r t} \tag{8.98}$$

$$\Omega_L \doteq dE_L \tag{8.99}$$

The operator $\hat{\chi}_L$ includes the Röntgen effect. If this effect were neglected, $\hat{\chi}_L \to \sum_{q=+,-,\mathbf{0}} C_q\epsilon_{Lq}^*$ becomes a c-number. All other symbols are defined in Appendix I. In RWA, we have $\hat{f}(t) \to -\hbar\sum_L \frac{1}{2}\hat{\Omega}_L\hat{\chi}_L\hat{\pi}_L(t)e^{-i\Delta_L t}$. For a single frequency laser with *time independent* Rabi frequency, we can show $\frac{\partial\hat{f}(t)}{\partial t} = -\hat{f}(t)i\hat{\Delta}_L$ and $\hat{f}^+\hat{f} = \hat{f}\hat{f}^+ = \frac{1}{4}\hbar^2\Omega_L^2\ \hat{\chi}_L\hat{\chi}_L^\dagger$ by using the identity $\frac{d\hat{\pi}_\mathbf{k}(t)}{dt} = i\hat{\pi}_\mathbf{k}(t)(\frac{\hat{\mathbf{P}}\cdot\mathbf{k}}{M} + \frac{\hbar k^2}{2M})$ (from Appendix III), and Eq. 8.92 becomes

$$\frac{\partial^2\hat{B}}{\partial t^2} = i\hat{\Delta}_L\frac{\partial\hat{B}}{\partial t} - \frac{1}{4}\hat{\Omega}_L^2\hat{B} \tag{8.100}$$

where $\hat{\Delta}_L \doteq \Delta_L - \frac{\hat{\mathbf{P}}\cdot\mathbf{k}_L}{M} - \frac{\hbar\mathbf{k}_L^2}{2M}$ and $\hat{\Omega}_L \doteq \Omega_L\hat{\chi}_L$.

We note that $\hat{\Omega}_L^2$ commutes with $\hat{\Delta}_L$ so Eq. 8.100 can be solved for $\hat{B}$ using the Laplace transform method, giving

$$\hat{B} = \hat{B}_o' e^{i\hat{\Delta}_L t/2} i\frac{2}{\hat{R}}\sin\frac{1}{2}\hat{R}t + \hat{B}_o e^{i\hat{\Delta}_L t/2}\{-i\frac{\hat{\Delta}_L}{\hat{R}}\sin\frac{1}{2}\hat{R}t + \cos\frac{1}{2}\hat{R}t\} \tag{8.101}$$

where $\hat{R} \doteq \sqrt{\hat{\Delta}_L^2 + \hat{\Omega}_L^2}$and $\hat{B}_o' \doteq \frac{\partial\hat{B}(0)}{\partial t}$.

Similarly, we obtain

$$\hat{C} = \hat{C}'_o e^{-i\hat{\Delta}_L t/2} i\frac{2}{\hat{R}} \sin\frac{1}{2}\hat{R}t + \hat{C}_o e^{-i\hat{\Delta}_L t/2}\{i\frac{\hat{\Delta}_L}{\hat{R}}\sin\frac{1}{2}\hat{R}t + \cos\frac{1}{2}\hat{R}t\} \tag{8.102}$$

where $\hat{C}'_o \doteq \frac{\partial \hat{C}(0)}{\partial t}$.

Using $\frac{\partial}{\partial t}\hat{B} = \frac{1}{i\hbar}\hat{f}^+\hat{E}$ and Eq. 8.101 assuming $\hat{B}'_o = 0$, we obtain

$$\hat{E} = \frac{i\hbar\hat{f}}{\hat{f}\hat{f}^+}\frac{\partial \hat{B}}{\partial t} = i\hat{B}_o e^{-i\hat{\Delta}_L t/2}\frac{\hat{\Omega}_L\hat{\pi}_L(t)}{\hat{R}}\sin\frac{1}{2}\hat{R}t \tag{8.103}$$

Similarly, $\frac{\partial}{\partial t}\hat{C} = \frac{1}{i\hbar}\hat{f}\hat{D}$ and Eq. 8.102 gives

$$\hat{D} = \frac{i\hbar\hat{f}^+}{\hat{f}^+\hat{f}}\frac{\partial \hat{B}}{\partial t} = i\hat{C}_o e^{i\hat{\Delta}_L t/2}\frac{\hat{\pi}^\dagger_L(t)\hat{\Omega}^\dagger_L}{\hat{R}}\sin\frac{1}{2}\hat{R}t \tag{8.104}$$

From $\hat{U}(0) = \hat{U}^+(0) = I$, we have $\hat{C}_o = \hat{B}_o = 1$. The exact evolution operator for $\hat{V}(t) = \hat{f}(t)S^\dagger + \hat{f}^+(t)S$ including the c.m. quantization and Röntgen effect through $\hat{\chi}_L$ with finite detuning in RWA is

$$\hat{U}(t) = \begin{pmatrix} e^{-i\hat{\Delta}_L t/2}\{i\frac{\hat{\Delta}_L}{\hat{R}}\sin\frac{1}{2}\hat{R}t + \cos\frac{1}{2}\hat{R}t\} & ie^{-i\hat{\Delta}_L t/2}\frac{\Omega_L}{\hat{R}}\hat{\chi}_L\hat{\pi}_L(t)\sin\frac{1}{2}\hat{R}t \\ ie^{i\hat{\Delta}_L t/2}\frac{\Omega_L}{\hat{R}}\hat{\pi}^\dagger_L(t)\hat{\chi}^\dagger_L\sin\frac{1}{2}\hat{R}t & e^{i\hat{\Delta}_L t/2}\{-i\frac{\hat{\Delta}_L}{\hat{R}}\sin\frac{1}{2}\hat{R}t + \cos\frac{1}{2}\hat{R}t\} \end{pmatrix} \tag{8.105}$$

$$\hat{U}^\dagger(t) = \begin{pmatrix} e^{i\hat{\Delta}_L t/2}\{-i\frac{\hat{\Delta}_L}{\hat{R}}\sin\frac{1}{2}\hat{R}t + \cos\frac{1}{2}\hat{R}t\} & -ie^{-i\hat{\Delta}_L t/2}\frac{\Omega_L}{\hat{R}}\hat{\chi}_L\hat{\pi}_L(t)\sin\frac{1}{2}\hat{R}t \\ -ie^{i\hat{\Delta}_L t/2}\frac{\Omega_L}{\hat{R}}\hat{\pi}^\dagger_L(t)\hat{\chi}^\dagger_L\sin\frac{1}{2}\hat{R}t & e^{-i\hat{\Delta}_L t/2}\{i\frac{\hat{\Delta}_L}{\hat{R}}\sin\frac{1}{2}\hat{R}t + \cos\frac{1}{2}\hat{R}t\} \end{pmatrix} \tag{8.106}$$

A state vector evolves as $|\Psi(\mathbf{P},t)\rangle = \hat{U}(t)\begin{pmatrix} \sum_{\mathbf{P}} C_e(\mathbf{P},0)|\mathbf{P}\rangle \\ \sum_{\mathbf{P}} C_g(\mathbf{P},0)|\mathbf{P}\rangle \end{pmatrix} =$

$$\begin{pmatrix} \sum C_e(\mathbf{P},0)e^{-i\bar{\Delta}_L t/2}\{i\frac{\bar{\Delta}_L}{R}\sin\frac{1}{2}Rt + \cos\frac{1}{2}Rt\}|\mathbf{P}\rangle + \sum C_g(\mathbf{P},0)ie^{-i\Delta_L t/2}e^{i\frac{\hbar\mathbf{k}_L^2}{2M}t}\frac{\Omega_{L+}}{R_+}\sin\frac{1}{2}Rt|\mathbf{P}+\hbar\mathbf{k}_L\rangle \\ \sum C_e(\mathbf{P},0)ie^{i\Delta_L t/2}e^{-i\frac{\hbar\mathbf{k}_L^2}{2M}t}\frac{\Omega_{L-}}{R_-}\sin\frac{1}{2}Rt|\mathbf{P}-\hbar\mathbf{k}_L\rangle + \sum C_g(\mathbf{P},0)e^{i\bar{\Delta}_L t/2}\{-i\frac{\bar{\Delta}_L}{R}\sin\frac{1}{2}Rt + \cos\frac{1}{2}Rt\}|\mathbf{P}\rangle \end{pmatrix} \tag{8.107}$$

where $R^\pm \doteq \sqrt{\Delta^2_{L\pm} + \Omega^2_{L\pm}}$, $\Delta_{L\pm} \doteq \Delta_L - \frac{(\mathbf{P}\pm\hbar\mathbf{k}_L)\cdot\mathbf{k}_L}{M} - \frac{\hbar\mathbf{k}_L^2}{2M}$, $\bar{\Delta}_L \doteq \Delta_L - \frac{\mathbf{P}\cdot\mathbf{k}_L}{M} - \frac{\hbar\mathbf{k}_L^2}{2M}$ and $\Omega_{L\pm} \doteq dE_L \sum_{q=+,-,\mathbf{0}} C_q\{\epsilon^*_{Lq}\frac{\omega_{\parallel,L}(\mathbf{P}\pm\hbar\mathbf{k}_L)}{\omega_L} + \kappa^*_{Lq}\frac{\omega_{\perp,L}(\mathbf{P}\pm\hbar\mathbf{k}_L)}{\omega_L}\}$.

8.4.1 Resonant Case

For resonant case $\hat{\Delta}_L = 0$, and neglecting the c.m. operators, we have

$$\hat{U}(t) = \begin{pmatrix} \cos\frac{1}{2}\Omega_L t & i\sin\frac{1}{2}\Omega_L t \\ i\sin\frac{1}{2}\Omega_L t & \cos\frac{1}{2}\Omega_L t \end{pmatrix} = e^{i\frac{1}{2}\Omega_L t(|e\rangle\langle g|+|g\rangle\langle e|)} \tag{8.108}$$

A $n\pi/2$ pulse is defined as $\Omega_L t_{n\pi/2} = n\pi/2$. Thus, generally the state vector is written as $|\Psi(t_{n\pi/2})\rangle = e^{iS_1 n\pi/4}|\Psi(0)\rangle$ where $S_1 \doteq |e\rangle\langle g| + |g\rangle\langle e|$. For an initial state vector $|\Psi(0)\rangle = \begin{pmatrix} C_e \\ C_g \end{pmatrix}$,we have $|\Psi(t_{\pi/2})\rangle = \frac{1}{\sqrt{2}}\begin{pmatrix} C_e + iC_g \\ iC_e + C_g \end{pmatrix}$ for $\pi/2$ pulse, $|\Psi(t_\pi)\rangle = i\begin{pmatrix} C_g \\ C_e \end{pmatrix}$ for π pulse, $|\Psi(t_{3\pi/2})\rangle = \frac{1}{\sqrt{2}}\begin{pmatrix} -C_e + iC_g \\ iC_e - C_g \end{pmatrix}$ for $3\pi/2$ pulse and $|\Psi(t_{2\pi})\rangle = -\begin{pmatrix} C_e \\ C_g \end{pmatrix}$ for 2π pulse.

As expected, the π pulse provides population inversion, 2π pulse shifts the phase by π thus changing the coefficients to negative and $\pi/2$ pulse creates entanglement between the excited and ground states.

Bibliography

[1] C. H. Raymond Ooi, Karl-Peter Marzlin and Jürgen Audretsch, Laser Cooling of Molecules via Single Spontaneous Emission, Eur. Phys. J. D 00227-7 (2002).

[2] C. H. Raymond Ooi, Karl-Peter Marzlin, and Jürgen Audretsch, Momentum spread of spontaneously decaying cold gas in thermal radiation, Phys. Rev. A **66**, 063413 (2002).

Applications

[3] Carl E. Wieman, David E. Pritchard and David J. Wineland, Atom cooling, trapping, and quantum manipulation, Rev. Mod. Phys. **71**, S253 (1999).

[4] P. Berman (editor), *Atom Interferometry*, (Academic Press, New York, 1997).

[5] Fouad G. Major, *The quantum beat : the physical principles of atomic clocks*, (New York ; Berlin ; Heidelberg: Springer, 1998).

[6] Immanuel Bloch, Theodor W. Hänsch, and Tilman Esslinger, Atom Laser with a cw Output Coupler, Phys. Rev. Lett. **82**, 3008 (1999).

[7] Stenholm, S., Theoretical foundations of laser spectroscopy, Phys. Rep., Phys. Lett. 43C, 151 (1978).

[8] Adams, C., M. Sigel, and J. Mlynek, Atom Optics, Phys. Rep. **240**, 143 (1994).

[9] D. V. Strekalov, Andrey Turlapov, A. Kumarakrishnan, and Tycho Sleator, Periodic structures generated in a cloud of cold atoms, Phys. Rev. A **66**, 023601 (2002).

[10] Ben Dahan, M., E. Peik, J. Reichel, Y. Castin, and C. Salomon, Bloch Oscillations of Atoms in an Optical Potential, Phys. Rev. Lett. **76**, 4508 (1996).

[11] H. F. Hess, Evaporative cooling of magnetically trapped and compressed spin-polarized hydrogen, Phys. Rev. B **34**, 3476 (1986); N. Masuhara, J. M. Doyle, J. C. Sandberg, D. Kleppner, and T. J. Greytak, Evaporative Cooling of Spin-Polarized Atomic Hydrogen, Phys. Rev. Lett. **61**, 935 (1988).

[12] Anderson, M. H., J. R. Ensher, M. R. Matthews, C. E. Wieman, and E. A. Cornell, Observation of Bose-Einstein condensation in a dilute atomic vapor below 200nanoKelvin, Science **269**, 198 (1995); D. S. Durfee, D. M. Kurn, and W. Ketterle, Bose-Einstein condensation in a gas of sodium atoms, Phys. Rev. Lett. **75**, 3969(1995).

[13] M. D. Barrett, J. A. Sauer, and M. S. Chapman, All-Optical Formation of an Atomic Bose-Einstein Condensate, Phys. Rev. Lett. **87**, 10404 (2001).

[14] Ben Dahan, M., E. Peik, J. Reichel, Y. Castin, and C. Salomon, Phys. Rev. Lett. **76**, 4508, (1996).

Atom optics

[15] H. Ammann and N. Christensen, Delta Kick Cooling: A New Method for Cooling Atoms , Phys. Rev. Lett. **78**, 2088 (1997).

[16] S. H. Myrskog, J. K. Fox, H. S. Moon, J. B. Kim, and A. M. Steinberg, Modified delta-kick cooling using magnetic field gradients, Phys. Rev. A **61**, 053412 (2000).

[17] E. Marechal, R. Long, T. Miossec, J.-L. Bossennec, R. Barbe, J.-C. Keller, and O. Gorceix, Atomic spatial coherence monitoring and engineering with magnetic fields, Phys. Rev. A **62**,053603 (2000).

[18] E. Marechal, R. Long, J.-L. Bossennec, R. Barbe, J.-C. Keller, and O. Gorceix, Cold-cesium-atom spin-polarization interferometry, Phys. Rev. A **60**, 3197 (1999).

[19] Stefan Bernet, Markus K. Oberthaler, Roland Abfalterer, Jörg Schmiedmayer, and Anton Zeilinger, Coherent Frequency Shift of Atomic Matter Waves , Phys. Rev. Lett. **77**, 5160 (1996).

[20] S. Bernet, R. Abfalterer, C. Keller, M. K. Oberthaler, J. Schmiedmayer, and A. Zeilinger, Matter waves in time-modulated complex light potentials , Phys. Rev. A **62**, 023606 (2000).

[21] Immanuel Bloch, Michael Köhl, Markus Greiner, Theodor W. Hänsch, and Tilman Esslinger, Optics with an Atom Laser Beam , Phys. Rev. Lett. **87,** 030401 (2001).

Collisions

[22] John L. Bohn, Molecular spin relaxation in cold atom-molecule scattering, Phys. Rev. A **61**, 40702(R) (2000).

[23] Brian Stewart et al, Quasiresonant vibration-rotation transfer in ultracold atom-diatom collisions, Phys. Rev. Lett. **73**, 2563 (1994).

[24] R. C. Forrey, Quasiresonant energy transfer in ultracold atom-diatom collisions, Phys. Rev. A **63**, 51403 (2001).

Cooling Reviews for Atoms

[25] R. P. Hudson, *Principles and applications of magnetic cooling* (North Holland, Amsterdam, 1972).

[26] S. N. Fisher, A. M. Guénault, C. J. Kennedy, G. R. Pickett, Phys. Rev. Lett. **69**, 1073 (1992).

[27] Richard Epstein et al, Observation of laser-induced fluorescent cooling of a solid, Nature **377**, 500 (1995).

[28] Ya. B. Zeldovich, Cooling with the aid of high frequency energy, ZhETF Pis. Red 19, 120, 1973.

[29] Letokhov, V., 1968, Narrowing of the Doppler width in a standing light wave, JETP Lett. **7**, 272 (1968).

[30] Hänsch, T., and A. Schawlow, Cooling of gases by laser radiation, Opt. Commun. **13**, 68 (1975).

[31] D. J. Wineland, R. E. Drullinger, and F. L. Walls, Radiation-pressure cooling of bound resonant absorbers, Phys. Rev. Lett. **40**, 1639-1642 (1978).

[32] Claude N. Cohen-Tannoudji, Manipulating atoms with photons, Rev. Mod. Phys. **70**, 707-719 (1998); Laser cooling and trapping of neutral atoms: theory, C. Cohen-Tannoudji, Phys. Rep., 219, 153 (1992); C. Cohen-Tannoudji and W. D. Phillips, New mechanisms for laser cooling, Physics Today, 33 (Oct. 1990).

[33] William D. Phillips, Laser cooling and trapping of neutral atoms, Rev. Mod. Phys. **70**, 721-741 (1998); W. D. Phillips and H. F. Metcalf, Cooling and trapping atoms, Sci. Am., 256, 36 (1987).W. D. Phillips, P. L. Gould and P. D. Lett, Cooling, stopping, and trapping atoms, Science, 239, 877 (1988).

[34] S. Chu, Laser Manipulation of atoms and particles, Science, 253, 861 (1991); S. Chu, Laser trapping of neutral particles, Sci. Am., 266, 70 (1992).

[35] *Special issue on Laser Cooling and Trapping of Atoms*, edited by S. Chu and C. Wieman, J. Opt. Soc. Am. B **6** (11), 1989.

[36] C. Cohen-Tannoudji, Atomic motion in laser light, in *Fundamental Systems in Quantum Optics*, Les Houches 1990, Session LIII, edited by J. Dalibard, J.M. Raimond, and J. Zinn-Justin, (North-Holland, Amsterdam, 1992).

[37] H. Metcalf, and P. van der Straten, Phys. Rep. **244**, 203 (1994); W. D. Phillips and H. F. Metcalf, Cooling and trapping atoms, Sci. Am., **256**, 36 (1987).

[38] S. Stenholm, Semiclassical theory of laser cooling, Rev. Mod. Phys. **58**, 699 (1986); S. Stenholm, Laser cooling and trapping, Eur. J. Phys., **9**, 242 (1988).

[39] W. D. Phillips, Laser cooling and trapping of neutral atoms, in *Laser Manipulation of Atoms and Ions* (Proceedings of the International School of Physics Enrico Fermi, Course CXVIII, 1992), edited by E. Arimondo.

[40] Karl-Peter. Marzlin, Manipulation and interaction of ultra-cold atoms with light, Habilitation thesis, University of Konstanz (2000).

Cooling Schemes for Atoms

[41] Castin, Y., K. Berg-Sorensen, J. Dalibard, and K. Molmer, Two-dimensional Sisyphus cooling, Phys. Rev. A **50**, 5092(1994).

[42] Ertmer, W., R. Blatt, J. Hall, and M. Zhu, 1985, Laser manipulation of atomic beam velocities: Demonstration of stopped atoms and velocity reversal, Phys. Rev. Lett. **54**, 996.

[43] Hoffnagle, J., Proposal for continuous white light cooling of an atom beam, Opt. Lett. **13**, 102 (1988).

[44] W. Ketterle, A. Martin, M. A. Joffe, and D. E. Pritchard, Slowing and cooling atoms in isotropic light, Phys. Rev. Lett. **69**, 2483 (1992).

[45] Lett, P. D., R. N. Watts, C. I. Westbrook, W. D. Phillips, P. L. Gould, and H. J. Metcalf, Observation of atoms laser cooled below the Doppler limit, Phys. Rev. Lett. **61**, 169 (1988); Gould, and H. J. Metcalf, 1989, Observations of atoms laser-cooled below the Doppler limit, in Atomic Physics II, edited by S. Haroche, J. C. Gray, and G. Grynberg (World Scientific, Singapore).

[46] Y. Castin, H. Wallis, and J. Dalibard, Limit of Doppler cooling, J. Opt. Soc. Am. B **6**, (1989).

[47] Aspect, A., E. Arimondo, R. Kaiser, N. Vansteenkiste, and C. Cohen-Tannoudji, Laser cooling below the one-photon recoil energy by velocity-selective coherent population trapping: theoretical analysis, J. Opt. Soc. Am. B **6**, 2112 (1989).

[48] Dalibard, J., and C. Cohen-Tannoudji, Laser cooling below the Doppler limit by polarization gradients: simple theoretical models, J. Opt. Soc. Am. B **6**, 2023 (1989).

[49] P. Marte, R. Dum, R. Taib and P. Zoller, M. S. Shariar, and M. Prentiss, Polarization gradient assisted subrecoil cooling: Quantum calculations in one dimension, Phys. Rev. A **49**, 4826 (1994).

[50] E. A. Curtis, C. W. Oates, and L. Hollberg, Quenched narrow-line laser cooling of ^{40}Ca to near the photon recoil limit, Phys. Rev. A **64**, 031403(R), (2001).

[51] A. Aspect, J. Dalibard, A. Heidmann, C. Salomon and C. Cohen-Tannoudji, Cooling atoms with stimulated emission , Phys. Rev. Lett. **57**, 1688 (1986)

[52] J. Lawall, S. Kulin, B. Saubamea, N. Bigelow, M. Leduc, and C. Cohen-Tannoudji, Three-dimensional laser cooling of helium beyond the single-photon recoil limit, Phys. Rev. Lett. **75**, 4195 (1995).

[53] T. Zaugg, P. Meystre and G. Lenz, M. Wilkens, Theory of adiabatic cooling in cavities, Phys. Rev. A **49**, 3011 (1994).

[54] J. Chen, J. G. Story, J. J. Tollett and R. G. Hulet, Adiabatic cooling of atoms by an intense standing wave, Phys. Rev. Lett. **69**, 130 (1992).

[55] P. W. H. Pinkse, A Mosk, M. Weidemuller, N. W. Reynolds, T. W. Hijmans, and J. T. M. Walraven, Adiabatically changing the phase-space density of a trapped Bose gas, Phys. Rev. Lett. **78**, 990 (1997).

[56] Kastberg, A., W. D. Phillips, S. L. Rolston, R. J. C. Spreeuw, and P. S. Jessen, Adiabatic cooling of cesium to 700nK in an optical lattice, Phys. Rev. Lett. **74**, 1542 (1995).

[57] Setija, I. D., H. G. C. Werij, O. J. Luiten, M. W. Reynolds, T. W. Hijmans, and J. T. M. Walraven, Optical cooling of atomic hydrogen in a magnetic trap, Phys. Rev. Lett. **70**, 2257 (1994).

[58] G. Nienhuis, P. van ders Straten, Operator description of laser cooling below the Doppler limit, Phys. Rev. A **44,** 462 (1991).

Cooling Schemes for Molecules

[59] J. T. Bahns, W. C .Stwalley, and P. L. Gould, Laser cooling of molecules: A sequential scheme for rotation, translation and vibration, J. Chem. Phys. **104**, 9689 (1996).

[60] V. Vuletic and S. Chu, Phys. Rev. Lett. **84,** 3787 (2000); Vladan Vuletic, Hilton W. Chan, and Adam T. Black, Three-dimensional cavity Doppler cooling and cavity sideband cooling by coherent scattering ,Phys. Rev. A **64,** 33405 (2001).

[61] P. Horak, G. Hechenblaikner, K.M. Gheri, H. Stecher, and H. Ritsch, Cavity-Induced Atom Cooling in the Strong Coupling Regime, Phys. Rev. Lett. **79**, 4974 (1997).

[62] Y. B. Band and P. S. Julienne, Ultracold-molecule production by laser-cooled atom photoassociation , Phys. Rev. A **51**, R4317 (1995); D. Comparat, A. Crubellier, O. Dulieu, F. Masnou-Seeuws et P. Pillet, Formation of cold Cs2 molecules through

photoassociation, A. Fioretti, Phys. Rev. Lett. **80**, 4402 (1998); C. M. Dion, C. Drag, O. Dulieu, B. Laburthe Tolra, F. Masnou-Seeuws and P. Pillet, Resonant coupling in the formation of ultracold ground state molecules via photoassociation, Phys. Rev. Lett. **86**, 2253 (2001).

[63] Jinha Kim, Bretislav Friedrich, Daniel P. Katz, David Patterson, Jonathan D. Weinstein, Robert DeCarvalho, and John M. Doyle, Buffer-Gas Loading and Magnetic Trapping of Atomic Europium, Phys. Rev. Lett. **78**, 3665 (1997); Jonathan D. Weinstein, Robert DeCarvalho, Jinha Kim, David Patterson, Bretislav Friedrich, and John M. Doyle, Magnetic Trapping of Atomic Chromium, Phys. Rev. A **57**, R3173 (1998).

[64] J. Doyle, B. Friedrich, Jinha Kim, and David Patterson, Buffer-gas loading of atoms and molecules into a magnetic trap, Phys. Rev. A **52**, R2515 (1995).

[65] J. D. Weinstein, R. deCarvalho, T. Guillet, B. Friedrich, and J. Doyle, Nature (London) 395, 148 (1998); R. deCarvalho, J. M. Doyle, B. Friedrich, T. Guillet, J. Kim, D. Patterson, and J. D. Weinstein, Buffer-gas loaded magnetic traps for atoms and molecules: A primer, Eur. Phys. J. D **7**, 289 (1999).

[66] Hendrick L. Bethlem, Giel Berden, André J. A. van Roij, Floris M. H. Crompvoets, and Gerard Meijer, Trapping neutral molecules in a travelling potential well , Phys. Rev. Lett. **84**, 5744 (2000).

[67] J. A. Maddi, T. P. Dinneen, and H. Gould, Slowing and cooling molecules and neutral atoms by time-varying electric field gradients , Phys. Rev. A **60,** 3882 (1999); H. L. Bethlem, G. Berden, and G. Meijer, Decelerating neutral dipolar molecules , Phys. Rev. Lett. **83**, 1558 (1999); Hendrick L. Bethlem, Giel Berden, André J. A. van Roij, Floris M. H. Crompvoets, and Gerard Meijer, Trapping neutral molecules in a travelling potential well , Phys. Rev. Lett. **84**, 5744 (2000).

[68] Hendrick L. Bethlem, Giel Berden, Floris M. H. Crompvoets, Rienk T. Jongma, Andre J. A. van Roij and Gerard Meijer, Electrostatic Trapping of Ammonia Molecules, Nature **406**, 491 (2000).

[69] Martin Weitz, Frequency independent laser cooling of atoms and molecules, Europhys. Lett. **49**, 302 (2000).

[70] S. A. Rangwala. T. Junglen, T. Rieger, P.W.H. Pinkse, and G. Rempe, A continuous source of translationally cold dipolar molecules, arXiv:physics/0209041 v1 2002.

[71] S. G. Schirmer, Laser cooling of internal molecular degrees of freedom for vibrationally hot molecules, Phys. Rev. A **63,** 13407 (2000).

[72] Allon Bartana and Ronnie Kosloff, Laser cooling of molecular internal degrees of freedoms by a series of shaped pulse, J. Chem. Phys. **99,**196 (1993).

[73] Allon Bartana and Ronnie Kosloff, Laser cooling of internal degrees of freedom. II , J. Chem Phys. **106,** 1435 (1997).

[74] A. Bartana, R. Kosloff and D. J. Tannor, Laser Cooling of Molecules by Dynamically Trapped States, Chem. Phys., in press (2001), published on-line on March 14, 2001.

[75] Bretislav Friedrich, Slowing of supersonically cooled atoms and molecules by time-varying nonresonant induced dipole forces, Phys. Rev. A **61,** 25403 (2000).

[76] R. C. Forrey, Cooling and trapping of molecules in highly excited rotational states, Phys. Rev. A **63,** 51403 (2001).

[77] Jing Li, John T. Bahns, William C. Stwalley, Scheme for state selective formation of highly rotationally excited diatomic molecules, J. Chem Phys. **112**, 6255 (2000).

Deflections and Stern Gerlach

[78] E. Arimondo, A. Bambini, and S. Stenholm, Quasiclassical theory of laser-induced atomic-beam dispersion , Phys. Rev. A **24**, 898 (1981).

[79] S. Glasgow, P. Meystre, M. Wilkens, E. M. Wright, Theory of atomic beam splitter based on velocity-tuned resonances, Phys. Rev. A **43,** 2455 (1991).

[80] P. Domokos, T. Kiss, and J. Janszky, Selecting molecules in the vibrational and rotational ground state by deflection, Eur. Phys. J. D **14**, 49-53 (2001).

[81] T. Sleator, T. Pfau, V. Balykin, O. Carnal and J. Mlynek, Experimental deomonstration of the optical Stern-Gerlach effect, Phys. Rev. Lett. **68**, 1996 (1992).

[82] C. Salomon, J. Dalibard, A. Aspect, H. Metcalf and C. Cohen-Tannoudji, Channeling Atoms in a Laser Standing Wave, Phys. Rev. Lett. **59**, 1659 (1987).

[83] Peter J. Martin, Phillip L. Gould, Bruce G. Oldaker, Andrew H. Miklich, and David E. Pritchard, Diffraction of atoms moving through a standing light waves, Phys. Rev. A **36**, 2495 (1987).

[84] Robert M. Hill and Thomas F. Gallagher, Deflection of CsF molecules by resonant inhomogeneous electric fields , Phys. Rev. A **12**, 452 (1975).

[85] H. Stapelfeldt, Hirofumi Sakai, E. Constant, and P. B. Corkum, Deflection of Neutral Molecules using the Nonresonant Dipole Force, Phys. Rev. Lett. **79**, 2787 (1997).

Decay Dynamics and Non-Markovian

[86] K. Wodkiewicz, and J. H. Eberly, Markovian and non-Markovian behaviour in two-level atom fluorescence, Annals of Physics **101**, 574 (1976).

[87] L. Fonda, G. C. Ghirardi, and A. Rimini, Decay theory of unstable quantum system, Rep. Prog. Phys. **41**, 587 (1978).

[88] A. M. Lane, Decay at early times, Phys. Lett. **99**A, 359 (1983).

[89] P.L. Knight, and P.W. Milonni, Long time deviations from exponential decay in atomic spontaneous emission theory, Phys. Lett. A **56**, 275 (1976).

[90] K. Unnikrishnan, Short and long time decay laws and the energy distribution of a decaying state, Phys. Rev. A **60**, 41 (1999).

[91] L. A. Khalfin, Decay theory of quasi-stationary state, JETP **6**, 1953 (1958).

[92] J. R. Brinati, Non-Markovian analysis of coherence in a driven two-level atom, Phys. Rev. A **50**, 3304 (1994).

Dipole Force Trap

[93] R. Grimm, M. Weidemuller, and Yu. B. Ovchinnikov, Optical dipole traps for neutral atoms, Adv. At., Mol., Opt. Phys. **42**, 95 (2000).

[94] Bjorkholm, J., R. Freeman, A. Ashkin, and D. Pearson, Observation of focusing on neutral atoms by the dipole forces of resonance-radiation pressure, Phys. Rev. Lett. **41**, 1361(1978).

[95] R. J. Cook and R. K. Hill, Opt. Commun. **43**, 258 (1982); V.I. Balykin, V.S. Letokhov, Yu.B. Ovchinnikov, and A.I. Sidorov, JETP Lett. **45**, 353(1987).

[96] J. Söding, R. Grimm, Yu.B. Ovchinikov, Gravitational laser trap for atoms with evanescent-wave cooling, Opt. Comm. **119**, 652 (1995).

[97] K.-P. Marzlin and J. Audretsch, Gravito-optical trapping of three-level atoms, Phys Rev. A **53**, 4352 (1996).

[98] T. Takekoshi, B. M. Patterson, and R. J. Knize, Observation of optically trapped cold Cesium molecules, Phys. Rev. Lett. **81**, 5105 (1998).

[99] A. Mosk, S. Jochim, H. Moritz, Th. Elsässera, M. Weidemüller and R. Grimm, arXiv:physics/0105009 v2 17 Jul 2001.

[100] H. Engler, T. Weber, M. Mudrich, R. Grimm, and M. Weidemüller, Very long storage times and evaporative cooling of cesium atoms in a quasi-electrostatic trap, Phys. Rev. A **62**, 031402(R), (2000).

[101] R. J. C. Spreeuw et. al., Demonstration of neutral atom trapping with microwaves, Phys. Rev. Lett. **72**, 3162 (1994).

Dipole Force Compression to High Density

[102] Tetsuya Ido, Yoshitomo Isoya, and Hidetoshi Katori, Optical-dipole trapping of Sr atoms at a high phase-space density, Phys. Rev. A **61**, 061403(R), (2000).

[103] N. Friedman, L. Khaykovich, R. Ozeri, and N. Davidson, Compression of cold atoms to very high densities in a rotating-beam blue-detuned optical trap, Phys. Rev. A **61**, 31403 (2000).

[104] Dian-Jiun Han, Steffen Wolf, Steven Oliver, Colin McCormick, Marshall T. DePue, and David S. Weiss , 3D Raman Sideband Cooling of Cesium Atoms at High Density, Phys. Rev. Lett. **85**, 724 (2000).

Electromagnetic Induced Transparency

[105] E. Arimondo, Nonabsorbing Atomic coherences by coherent two-photon transitions in three-level optical pumping, Lettere Al Nuovo Cimento **17**, 333 (1976).

[106] Olga Kocharovskaya, Amplication and lasing without inversion, Phys. Rep. **219**, 175 (1992).

[107] Marlan O. Scully, From lasers and masers to phaseonium and phasers, Phys. Rep. **219**, 191 (1992).

Entropy and Dissipation

[108] Kerson Huang, *Statistical Mechanics* (John-Wiley and Sons, New York, 1987)p. 64.

[109] W. Ketterle and D. E. Pritchard, Atom cooling by time-dependent potentials, Phys. Rev. A **46**, 4051 (1992)

[110] G. Lindblad, Comm. Maths. Phys. **48**, 119, 1973.

[111] G. Lindblad, *Non-Equilibrium Entropy and Irreversibility*, (Reidel, Dordrecht, 1983).

[112] J. von Neumann, Gött. Nachr. **273** (1927).

[113] A. Renyi, Rev. Int. Stat. Inst. 33, 1 (1965).

[114] A. Wehrl, General properties of entropy, Rev. Mod. Phys. **50**, 221 (1978).

[115] H. Araki and E. H. Lieb, Commun. Math. Phys. **18**, 160 (1970).

[116] S. M. Barnett, and S. J. D. Pheonix, Entropy as a measure of quantum optical correlation, Phys. Rev. A **40**, 2404 (1989).

[117] Martin E. Carrera-Patino and R. Stephen Berry, Entropy production in stopping atoms with laser light, Phys. Rev. A **34**, 4728 (1986).

[118] S. J. van Enk and G. Nienhuis, Entropy production and kinetic effects of light, Phys. Rev. A **46**, 1438 (1992).

Guides for Atoms

[119] B. K. Teo and G. Raithel, Loading mechanism for atomic guides, Phys. Rev. A **63**, 31402 (2001).

[120] Jianping Yi, Yifu Zhu and Yuzhu Wang, Evanescent light-wave atomic funnel: A tandem hollow-fiber, hollow-beam approach, Phys. Rev. A **57**, 1957 (1998); Jianping Yi, Yifu Zhu and Yuzhu Wang, Atom guiding and cooling in a dark hollow laser beam, Phys. Rev. A **58**, 509 (1998).

[121] Toby D. Hain, Michael A. Weibel, Kyle M. Backstrand, and Thomas J. Curtiss, Rotational state selection and orientation of OH and OD radicals by electric hexapole beam-focusing, J. Phys. Chem. A **101**, 7675 (1997).

[122] Toby D. Hain, Robert M. Moision, and Thomas J. Curtiss, Hexapole state-selection and orientation of asymmetric top molecules: CH_2F_2, J. Chem. Phys. **111**, 6797 (1999).

[123] B. Ghafarri, J. M. Gerton, W.I. McAlexander, K. E. Strecker, D. M. Homan, and R. G. Hulet, Laser-free slow atom source, Phys. Rev. A **60**, 3878 (1999).

[124] P.W. Harland, Wang-Ping Hu, Claire Vallance, Spatial deorientation of upper-Stark-state-selected supersonic beams of CH_3F, CH_3Cl, CH_3Br, and CH_3I, Phys. Rev. A **60**, 3138 (1999).

[125] Roger. W. Anderson, Tracks of symmetric top molecules in hexapole electric fields, J. Phys. Chem. A **101**, 7664 (1997).

Laser

[126] R. Loudon, *The Quantum Theory of Light* (Clarendon, Oxford, 1983).

[127] Sudarshan, Equivalence of semiclassical and quantum mechanical description of statistical light beams, Phys. Rev. Lett. **10**, 276 (1963).

[128] B. R. Mollow, Pure-state analysis of resonant light scattering: Radiative damping, saturation and multiphoton effects, Phys. Rev. A **12**, 1919 (1975).

[129] R. Glauber, Coherent and incoherent states of the radiation field, Phys. Rev. **131**, 2767 (1963).

Master Equations

[130] Zwanzig: Ensemble Method in the Theory of Irreversibility, J. Chem. Phys. **33**, 1338 (1960).

[131] Nakajima, S., Prog. Theor. Phys. **20**, 948 (1958).

[132] F. Bloch, Generalized theory of relaxation, Phys. Rev. **105**, 1206 (1957); R. K. Wangness and F. Bloch, The Dynamical Theory of Nuclear Induction, Phys. Rev. **89**, 728 (1956).

[133] P. N. Argyres and P. L. Kelley, Theory of spin resonance and relaxation, Phys. Rev. **134**, 98 (1964).

[134] G. S. Agarwal, in *Quantum Statistical Theories of Spontaneous Emission and Their Relation to Other Approaches*, edited by G. Hohler, Springer Tracts in Modern Physics, Vol. 70 (Springer, Berlin, 1974).

[135] G. S. Agarwal, Master Equation Approach to Spontaneous Emission, Phys. Rev. A **2**, 2038 (1970).

[136] G. S. Agarwal, Master Equation Approach to Spontaneous Emission, II. Emission from a System of Harmonic Oscillators Phys. Rev. A **3**, 1783 (1971).

[137] G. S. Agarwal, in *Master Equation Methods in Quantum Optics, Progress in Optics* XI, edited by E. Wolf, 1, (North-Holland, Amsterdam, 1973).

[138] W.H. Louisell, *Quantum Statistical Properties of Radiation* (Wiley, New York, 1973).

[139] Carmichael, H.J., *An Open Systems Approach to Quantum Optics*, (Berlin: Springer, 1993).

[140] C. W. Gardiner, *Quantum Noise* (Springer-Verlag, New York, 1991).

[141] J. Javanainen, Density-matrix equations and photon recoil for multistate atoms, Phys. Rev. A **44**, 5857 (1991).

[142] R. H. Dicke, Coherence in spontaneous radiation processes, Phys. Rev. **93**, 99 (1954).

[143] R. H. Lehmberg, Radiation from an N-atom system. 1: General Fromalism, Phys. Rev. A **2**, 883 (1970).

[144] P. W. Milonni and P. L. Knight, Retardation in the resonant interaction of two identical atoms', Phys. Rev. A **10**, 1096 (1974).

Master Equation with Strong Fields

[145] Dalibard, J., and C. Cohen-Tannoudji, Dressed-atom approach to atomic motion in laser light: the dipole force revisited, J. Opt. Soc. Am. B **2**, 1707 (1985).

[146] O. Kocharovskaya, S.-Y. Zhu, M.O. Scully, P. Mandel, and Y.V. Radeonychev, Generalization of the Maxwell-Bloch equations to the case of strong atom-field coupling, Phys. Rev. A **49**, 4928 (1994).

[147] Olga Kocharovskaya, Paul Mandel, and M. O. Scully, Atomic Coherence via Modified Spontaneous Relaxation of Driven Three-Level Atoms, Phys. Rev. Lett. **74**, 2451 (1995).

[148] Olga Kocharovskaya, Y. V. Radeonychev, Paul Mandel, and M. O. Scully, Field-dependent relaxation effects in a three-level system driven by a strong coherent field, Phys. Rev. A **60**, 3091 (1999).

[149] C. R. Stroud, Jr., Quantum-electrodynamic treatment of spontaneous emission in the presence of applied field, Phys. Rev. A **3**, 1044 (1971).

[150] Anna Kowalewska-kudeaszyk and Ryszard Tanas, Generalized master equation for a two-level atom in a strong field and tailored reservoirs, J. Mod. Opt. **48**, 347 (2001).

[151] Cohen-Tannoudji, C., J. Dupont-Roc, and G. Grynberg, 1992, *Atom-Photon Interactions: Basic Processes and Applications* (Wiley, New York).

[152] K.V. Krutitsky, K.-P. Marzlin, and J. Audretsch, Ultracold Bose atoms in intense laser fields: intensity- and density-dependent effects, Laser Physics **12**, 121-126 (2002).

[153] Dalibard, J., and C. Cohen-Tannoudji, Atomic motion in laser light: connection between semiclassical and quantum descriptions, J. Opt. Soc. Am. B **2**, 1707 (1985).

Manipulation of Molecules with Intense Pulses

[154] A. H. Zewail, Physics Today, **33**, 27 (1980).

[155] S. Stenholm, Laser-Induced Processes in Molecular Systems, *Quantum Optics VI* (Springer Proceedings in Physics V77), p. 313.

[156] Dudley Herschbach, Chemical physics: molecular clouds, clusters, and corrals, Rev. Mod. Phys. **71,** S411 (1999).

[157] Andreea Boca and Bretislav Friedrich, Fine structure, alignment, and orientation of ^{32}S ^{16}O and ^{16}O^{18}O molecules in congruent electric and magnetic fields, J. Chem Phys. **112**, 3609 (2000).

[158] Bretislav Friedrich and Dudley Herschbach, Alignment and trapping of molecules in intense laser fields, Phys. Rev. Lett. **74**, 4623 (1995).

[159] Hirofumi Sakai, C. P. Safvan and Jakob Juul Larsen, Karen Marie Hilligsøe, Kasper Hald, and Henrik Stapelfeldt, Controlling the alignment of neutral molecules by a strong laser field, J. Chem. Phys. **110**, 10235 (1999).

[160] Jakob Juul Larsen, Kasper Hald, Nis Bjerre, and Henrik Stapelfeldt, Tamar Seideman, Three Dimensional Alignment of Molecules Using Elliptically Polarized Laser Fields, Phys. Rev. Lett. **85**, 2470 (2000).

[161] Joanna Karczmarek, James Wright, Paul Corkum and Misha Ivanov, Optical Centrifuge for Molecules, Phys. Rev. Lett. **82**, 3420 (1999).

[162] T. Seideman, Manipulating external degrees of freedom with intense light: Laser focusing and trapping of molecules, J. Chem. Phys. **106**, 2881 (1997).

[163] Tamar Seideman, Shaping molecular beam with intense light, J. Chem. Phys. **107**, 10420 (1997).

[164] Tamar Seideman, Molecular optics in an intense laser light: A route to nanoscale material design, Phys. Rev. A **56**, R17 (1997).

Mechanical Effect of Radiation

[165] Askaryan, G. A., Effects of the gradient of a strong electromagnetic beam on electrons and atoms, Sov. Phys. JETP **15**, 1088 (1962).

[166] Letokhov, V., V. Minogin, and B. Pavlik, Cooling and trapping atoms and molecules by a resonant laser field, Opt. Commun. **19**, 72 (1976); Letokhov, V. S., and V. G. Minogin, Laser radiation pressure on free atoms, Phys. Rep. **73**,1 (1981); V. G. Minogin, Atomic scattering by a resonant standing laser wave, Opt. Comm. **19**, 72 (1976); Letokhov, V. S., V. G. Minogin, and B. D. Pavlik, Cooling and capture of atoms and molecules by a resonant light field, Sov. Phys. JETP **45**, 698 (1977); V. G. Minogin and O.T. Serimaa, Resonant light pressure forces in a strong standing laser wave, Opt. Comm. **19**, 72 (1976).

[167] D. J. Wineland and W. M. Itano, Laser cooling of atoms, Phys. Rev. A **20**, 1521 (1979).

[168] Ashkin, A. Atomic-beam deflection by resonance-radiation pressure, Phys. Rev. Lett. **25**, 1321(1970); Ashkin, A., Trapping of atoms by resonance radiation pressure, Phys. Rev. Lett. **40**, 729 (1978); Gordon, J. P., and A. Ashkin, Motion of atoms in a radiation field, Phys. Rev. A **21**, 1606 (1980).

[169] Cohen-Tannoudji, C., Atomic motion in laser light, in *Fundamental Systems in Quantum Optics*, edited by J. Dalibard, J.-M. Raimond, and J. Zinn-Justin (North-Holland, Amsterdam), p. 1 (1992).

[170] Javanainen, J., and S. Stenholm, Broad band resonant light pressure I: Basic equations, Appl. Phys. **21**, 35 (1980); Javanainen, J., and S. Stenholm, Broad band resonant light pressure II: Cooling of gases, Appl. Phys. **21**, 163 (1980).

Molecule Theory

[171] G. Herzberg, *Molecular Spectra and Molecular Structure: I.Spectra of Diatomic Molecules*, 2nd ed. (Van Nostrand, Princeton, NJ, 1950).

[172] H. Lefebvre-Brion and R. W. Field, *Perturbations in the Spectra of Di-atomic Molecules* (Academic, New York, 1986).

[173] Jeffrey I. Steinfeld, *Molecules and Radiation: An introduction to modern spectroscopy*, (Harper & Row, New York 1974).

[174] Linus Pauling and Edgar Bright Wilson, *Introduction to Quantum Mechanics : with applications to chemistry* (New York: MacGraw-Hill, 1935).

[175] Harold W. Kroto, *Molecular rotation spectra* (London: Wiley, 1975).

[176] R. N. Zare, *Angular Momentum* (Wiley, New York, 1988).

[177] Aleksander A. Radzig and Boris M. Smirnov, *Reference data on atoms, molecules and ions*, (Springer series in chemical physics ; 31), Springer-Verlag Berlin Heidelberg 1985.

[178] Masataska Mizushima, Molecular parameters of OH free radical, Phys. Rev. A **5**, 143 (1972).

Molecular Hamiltonian

[179] M. Born and K. Huang, *Dynamical Theory of Crystal Lattices* (Oxford University Press, New York, 1956).

[180] Alexander I. Pegarkov, Resonant interactions of diatomic molecules with intense laser fields: time-independent multi-channel Green function theory and application to experiment, Phys. Rep. **336**, 255 (2000).

[181] Alan Carrington, Electron resonance of gaseous diatomic molecules, Adv. Chem. Phy. **18**, 149 (1970).

[182] B.J. Howard and R.E. Moss, The molecular Hamiltonian II. Linear Molecules, Molecular Phys. **20**, 147 (1971).

[183] W. Kolos and L. Wolniewicz, Nonadiabatic theory for diatomic molecules and its application to the hydrogen molecule, Rev. Mod. Phys. **35**, 473 (1963).

[184] B. R. Bunker, The electronic isotope shift in diatomic molecules and the partial breakdown of the Born-Oppenheimer approximation, J. Mol. Spect. **28**, 422 (1968).

Multipolar and Minimal Coupling Hamiltonians

[185] W. Heitler, *The Quantum Theory of Radiation* (Clarendon, Oxford, England, 1954).

[186] C. Cohen-Tannoudji, J. Dupont-Roc, and G. Grynberg, *Photons and Atoms* (Wiley, New York, 1989).

[187] Craig and T. Thirunamachandran, *Molecular Quantum Electrodynamics* (Academic Press, London, 1984).

[188] E. A. Power, *Introductory Quantum Electrodynamics* (Longman, London, 1964).

[189] J. D. Jackson, *Classical Electrodynamics* (John Wiley & Sons. Inc., New York, 1962).

[190] E. A. Power and S. Zienau, Coulomb gauge in non-relativistic quantum electrodynamics and the shape of spectral lines, Philos. Trans. R. Soc. London, Ser. A **251**, 427 (1959).

[191] R. G. Wooley, Molecular Quantum Electrodynamics, Proc. R. Soc. London, Ser. A **321**, 557 (1971).

[192] E. A. Power, in *Multiphoton Processes*, edited by J. H. Eberly and P. Lambropoulos (Wiley, New York, 1978).

[193] E. A. Power and T. Thirunamachandran, Mathematika **18**, 240 (1971).

[194] M. Babiker, E. A. Power and T. Thirunamachandran, On a generalization of the Power-Zienau-Woolley transformation in quantum electrodynamics and atomic field equations, Proc. R. Soc. London A **338**, 235 (1974).

[195] M. Babiker and R. Loudon, Derivation of the Power-Zienau-Woolley Hamiltonian in quantum electrodynamics by gauge transformation, Proc. R. Soc. London, Ser. A **385**, 439 (1983).

[196] E. A. Power and T. Thirunamachandran, The multipolar Hamiltonian in radiation theory, Proc. R. Soc. London, Ser. A **372**, 265 (1980).

[197] D. P. Craig and T. Thirunamachandran, *Molecular Quantum Electrodynamics* (Academic, London, 1984).

[198] G. Compagno, R. Passante, and F. Persico, *Atom-Field Interactions and Dressed Atoms* (Cambridge, London, 1995).

[199] P.W. Milonni, Semiclassical and quantum electrodynamical approaches to non-relativistic radiation theory, Phys. Rep. **25**, 1 (1976).

[200] J. R. Ackerhalt and P.W. Milonni, Interaction Hamiltonian in quantum optics, J. Opt. Soc. Am. B **1**, 117 (1983).

[201] W. P. Healy, *Non-relativistic quantum electrodynamics* (Academic Press, New York, 1982).

[202] W. P. Healy, Centre of mass motion in non-relativistic quantum electrodynamcis, J. Phys. A **10**, 279 (1976).

[203] H. E. Moses, Exact electromagnetic matrix elements and exact selection rules for hydrogen atoms, Lett. al Nuovo Cimento **4**, 51 (1972); H. E. Moses, Photon wave functions and the exact electromagnetic matrix elements for hydrogen atoms, Phys. Rev. A **8**, 1710 (1973).

[204] H. A. Bethe, The electromagetic shift of energy levels, Phys. Rev. **72**, 339 (1947).

[205] Karl-Peter Marzlin, Dipole coupling af atoms and light in gravitational fields, Phys. Rev. A **51**, 625 (1995).

[206] A.O. Barut (editor), *Quantum electrodynamics and quantum optics*: NATO ASI (Plenum Press, New York, 1984) p.431.

Optical lattice

[207] R. J. C. Spreeuw, and C. I. Westbrook, Observation of quantized motion of Rb atoms in an optical field, Phys. Rev. Lett. **69**, 49 (1992).

[208] Louis, B., P. Verkerk, J.-Y. Courtois, C. Salomon, and G. Grynberg, Quantized atomic motion in 1D cesium molasses with magnetic field, Europhys. Lett. **21**, 13 (1993).

[209] G. Grynberg, B. Lounis, P. Verkerk, J. Y. Courtois and C. Salomon, Quantized motion of cold cesium atoms in two- and three-dimensional optical potentials, Phys. Rev. Lett. **70**, 2249 (1993).

[210] A. Hemmerich T.W. Hänsch, Two-dimesional atomic crystal bound by light, Phys. Rev. Lett. **70**, 410 (1993).

[211] D. Jaksch, C. Bruder, J. I. Cirac, C. W. Gardiner, and P. Zoller, Cold Bosonic Atoms in Optical Lattices, Phys. Rev. Lett. **81**, 3108 (1998).

[212] Qian Niu, Xian-Geng Zhao, G. A. Georgakis and M. G. Raizen, Atomic Landau-Zener Tunneling and Wannier-Stark Ladders in Optical Potentials, Phys. Rev. Lett. **76**, 4504 (1996).

[213] M. Olshanii and David Weiss, Producing Bose condensates using optical lattices, Phys. Rev. Lett **89**, 090404 (2002).

[214] S. Potting, M. Cramer, C.H. Schwalb, H. Pu, and P. Meystre, Coherent acceleration of Bose-Einstein condensates, Phys. Rev. A **64**, 023604 (2001).

[215] Raithel, G., G. Birkl, A. Kastberg, W. D. Phillips, and S. L. Rolston, Cooling and localization dynamics in optical lattices, Phys. Rev. Lett. **78**, 630 (1997); Raithel, G., G. Birkl, W. D. Phillips, and S. L. Rolston, Compression and parametric driving of atoms in optical lattices, Phys. Rev. Lett. **78**, 2928 (1997).

[216] S. Lukman Winoto, Marshall T. DePue, Nathan E. Bramall, and David S. Weiss, Laser cooling at high density in deep far-detuned optical lattices, Phys. Rev. A **59**, R19 (1999).

Quantum Optics and Quantum Electrodynamics

[217] Peter W. Milloni, *The Quantum Vacuum : an introduction to quantum electrodynamics* (Boston: Academic Press, 1995).

[218] R. R. Puri, *Mathematical Methods of Quantum Optics*, (Springer Series in Optical Sciences 79. Springer-Verlag, New York, 2001).

[219] M.O. Scully, and M.S. Zubairy, *Quantum Optics* (Cambridge University Press, Cambridge, 1997).

[220] Stephen M. Barnett and Paul M. Radmore, *Methods in Theoretical Quantum Optics* (Oxford: Clarendon Press, 1997).

[221] Wolfgang P. Schleich, *Quantum Optics in Phase Space*, (Wiley-Vch, Berlin, 2001), Chap. 3.

[222] L. Allen and J. U. Eberly, *Optical Resonance and Two-Level Atoms* (Wiley-Interscience, New York, 1975).

[223] R. P. Feynman, F. L. Vernon and R. W. Hellwarth, Geometrical representation of the Schrödinger equation for solving maser problems, J. App. Phys. **28,** 49 (1957).

[224] A. S. Davydov, *Quantum mechanics*; edited by D. ter Haar (Oxford ; New York : Pergamon Press, 1976, 2d ed).

[225] H. Risken, *The Fokker Planck Equation* (Springer, Heidelberg, 1984).

[226] W. Louisell, Solutions of the Damped Oscillator Fokker-Planck Equation, IEEE J. Quan. Electron. **3**, 348 (1967).

Resonance Fluorescence and Photon Statistics

[227] R. J. Cook, Photon statistics in resonance fluorescence from laser deflection of an atomic beam, Opt. Comm. **35**, 347 (1980); D. Lenstra, Photon number statistics in resonance fluorescence, Phys. Rev. A **26**, 3369 (1982).

[228] S. Stenholm, Distribution of photons and atomic momentum in resonance fluorescence, Phys. Rev. A **27**, 2513 (1983).

[229] Mollow, B. R., Power spectrum of light scattered by two-level systems, Phys. Rev. **188**, 1969 (1969).

[230] L. M. Narducci, M. O. Scully, G.-L. Oppo, P. Ru, and J. R. Tredicce, Spontaneous emission and absorption properties of a driven three-level systems, Phys. Rev. A **42**, 1630 (1990).

[231] Fu-li Li and Shi-Yao Zhu, Resonance fluorescence quenching and spectral line narrowing via quantum interference in a four-level atom driven by two coherent fields, Phys. Rev. A. **59**, 2330 (1999).

[232] H. R. Xia, C. Y. Ye, and S. Y. Zhu, Experimental observation of spontaneous emission cancellation, Phys. Rev. Lett. **77,** 1032 (1996).

[233] C. Cohen-Tannoudji, and Serge Reynaud, Dressed-atom description of resonance fluorescence and absorption spectra of a multi-level atom in an intense laser beam, J. Phys. B **10**, 345 (1977).

Röntgen Term Effect

[234] Martin Wilkens, Spurious velocity dependence of free-space spontaneous emission, Phys. Rev. A **47**, 671 (1993).

[235] Martin Wilkens, Significane of Röntgen current in quantum optics: Spontaneous emission of moving atoms, Phys. Rev. A **47**, 671 (1993).

[236] C. Baxter, M. Babiker and R. Loudon, Canonical approach to photon pressure, Phys. Rev. A **47**, 1278 (1993).

[237] C. Baxter, Center-of-mass motion of an N-particle atom or ion and the Thomas-Reiche-Kuhn sum rule, Phys. Rev. A **50**, 587 (1994).

[238] M. Babiker, Theory of momentum changes in atomic transition due to irradiation with resonant light, J. Phys. B **17**, 4877 (4877).

[239] L. G. Boussiakou, C. R. Bennett and M. Babiker, Quantum theory of spontaneous emission by real moving atoms, Phys. Rev. Lett. **89**, 123001 (2002).

[240] K. Rzazewski and W. Zakowicz, Spontaneous emission by an extended wavepacket, J. Phys. B **25**, L319, 1992.

[241] Wolfgang Pauli, *Theory of relativity* (London: Pergamon Press, 1958).

Spontaneous Emission with Entanglement

[242] G. S. Agarwal and Sunish Menon, Quantum interferences and the question of thermodynamic equilibrium, Phys. Rev. A **63**, 23818 (2001).

[243] A. K. Patnaik and G. S. Agarwal, Cavity-induced coherence effects in spontaneous emissions from preselection of polarization, Phys. Rev. A **59**, 3015 (1999).

[244] J. Javanainen, Effect of state superposition created by spontaneous emission on laser-driven transitions, Europhys. Lett. **17**, 407 (1992).

[245] L. Jakobczyk, Entangling two-level atoms by spontaneous emission, arXiv:quant-ph/0204140 (2002).

Spontaneous Emissions Rate Control

[246] G. S. Agarwal, M.O. Scully, and H. Walther, Accelerating decay by multiple 2p pulses, Phys. Rev. A **63**, 044101 (2001).

[247] Maciej Janowicz, Non-Markovian decay of an atom coupled to a reservoir: Modification by frequency modulation, Phys. Rev. A **61**, 25802 (2000).

[248] G. S. Agarwal, Control of decoherence and relaxation by frequency modulation of a heat bath, Phys. Rev. A **61**, 013809 (1999).

[249] Jörg Evers and Christoph H. Keitel, Spontaneous emission suppression on arbitrary atomic transitions, Phys. Rev. Lett. **89**, 163601 (2002).

[250] P. R. Berman, Analysis of dynamical suppression of spontaneous emission, Phys. Rev. A **58**, 4886 (1998).

[251] A. G. Kofman and G. Kurizki, Universal Dynamical Control of Quantum Mechanical Decay: Modulation of the Coupling to the Continuum, Phys. Rev. Lett. **87**, 270405 (2001).

[252] P. Facchi and S. Pascazio, Spontaneous emission and lifetime modification caused by an intense electromagnetic field, Phys. Rev. A **62**, 023804 (2000).

[253] Alexander D. Panov, General equation for Zeno-like effects in spontaneous exponential decay, arXiv:quant-ph/9909079 (1999).

[254] David J. Tannor and Allon Bartana, On the interplay of control fields and spontaneous emission in laser cooling, J. Phys. Chem. **103**, 10359 (1999).

[255] D. Vitali and P. Tombesi, Using parity kicks for decoherence control, Phys. Rev. A **59**, 4178 (1999).

[256] Lorenza Viola and Seth Lloyd, Dynamical suppression of decoherence in two-state quantum systems, Phys. Rev. A **58**, 2733 (1998).

Spontaneous Emissions in Structured Reservoir

[257] P. Lambropoulos, Fundamental quantum optics in structured reservoir, Rep. Prog. Phys. **63**, 456 (2000).

[258] A. G. Kofman, G. Kurizki and B. Sherman, Spontaneous and induced atomic decay in photonic band structures, J. Mod. Opt. **41**, 353 (1994).

[259] C. M. Cornelius and Jonathan P. Dowling, Modification of Planck blackbody radiation by photonic band-gap structures, Phys. Rev. A **59**, 4736 (1999).

[260] Jonathan P. Dowling and Charles M. Bowden, Atomic emission rates in inhomogeneous media with applications to photonic band structures, Phys. Rev. A **46**, 612 (1992).

[261] Mesfin Woldeyohannes and Sajeev John, Coherent control of spontaneous emission near a photonic band edge:A qubit for quantum computation, Phys. Rev. A **60**, 5046 (1999).

STIRAP and Population Transfer

[262] G. M. Moy, J. J. Hope, and C. M. Savage, Atom laser based on Raman transitions, Phys. Rev. A **55**, 3631 (1997).

[263] Oreg, J., F. T. Hioe, and J. H. Eberly, Adiabatic following in multilevel systems, Phys. Rev. A **29**, 690697 (1984).

[264] Messiah, A., *Quantum Mechanics* (North-Holland/Elsevier Science, New York, 1962).

[265] K. Bergmann, H. Theuer, and B. W. Shore, Coherent population transfer among quantum states of atoms and molecules, Rev. Mod Phys **70**, 1003 (1998).

[266] S. Kallush and Y. B. Band, Phys. Rev. A **61**, R41401 (2000); V.S. Malinovsky and J. L. Krause, Efficiency and robustness of coherent population transfer with intense, chirped laser pulses, Phys. Rev. A **63**, 43415 (2001); V.S. Malinovsky and J.L. Krause, General theory of population transfer by adiabatic rapid passage with intense, chirped laser pulses, Eur. Phys. J. D **14**, 147 (2001).

[267] T. A. Laine, and S. Stenholm, Adiabatic processes in three-level systems, Phys. Rev. A **53**, 2501 (1996).

[268] N.V. Vitanov and S. Stenholm, Non-adiabatic effects in population transfer in three-level systems, Opt. Comm. **127**, 214 (1996);

[269] Mark. M. Kobrak and Stuart A. Rice, Coherent population transfer via a resonant intermediate state: The breakdown of adiabatic passage, Phys. Rev. A **57**, 1158 (1998).

[270] G.G. Grigoryan and Y.T. Pashayan, Adiabatic population transfer in three-level systrem with non-zero two-photon detuning, Opt. Comm. **198**, 107 (2001).

[271] B. W. Shore, J. Martin, M. P. Fewell and K. Bergmann, Coherent population transfer in multilevel systems with magnetic sublevels. I. Numerical studies, Phys. Rev. A **52**, 566 (1995).

[272] B. W. Shore, J. Martin, M. P. Fewell and K. Bergmann, Coherent population transfer in multilevel systems with magnetic sublevels. II. Algebraic analysis, Phys. Rev. A **52**, 583 (1995).

[273] R. M. Godun et. al, Efficiencies of adiabatic transfer in a multistate system, Phys. Rev. A **59**, 3775 (1999).

[274] Ignacio R. Sola, Optimal pulse sequence for population transfer in multilevel systems, Phys. Rev. A **60**, 3081 (1999)

[275] M.V. Korolkov and G.K. Paramonov, Vibrational state-selective electronic excitation of diatomic molecules by ultrashort laser pulses, Phys. Rev. A **57**, 4998 (1998)

[276] B. M. Garraway, and K.-A. Suominen, Adiabatic Passage by Light-Induced Potentials in Molecules, Phys. Rev. Lett. **80,** 932 (1998); Ignacio R. Sola, Efficiencies and robustness of adiabatic passage by light induced potentials, Phys. Rev. A **61**, 43413 (2000).

[277] Nakajima, T., M. Elk, J. Zhang, and P. Lambropoulos, Population transfer through the continuum, Phys. Rev. A **50**, R913 (1994).

[278] T. Halfmann, and K. Bergmann, J. Chem. Phys. **104**, 70687072 (1996); S. Schiemann, A. Kuhn, S. Steuerwald, and K. Bergmann, Phys. Rev. Lett. **71**, 3637 (1993); W. Suptitz, B. C. Duncan, and P. L. Gould, 1997, J. Opt. Soc. Am. **B 14**, 1001 (1997),

[279] R. G. Unanyan, B.W. Shore, K. Bergmann, Entangled-state preparation using adiabatic population transfer, Phys. Rev. A **63**, 43405 (2001).

[280] D. Grischkowsky, Coherent excitation, incoherent excitation and adiabatic states, Phys. Rev. A **14**, 802 (1976).

[281] J. R. Kuklinski, U. Gaubatz, F. T. Hioe, and K. Bergmann, Adiabatic population transfer in a three-level system driven by delayed laser pulses, Phys. Rev. A **40**, 6741 (1989).

[282] Marte, P., P. Zoller, and J. L. Hall, Coherent atomic mirrors and beam splitters by adiabatic passage in multilevel systems, Phys. Rev. A **44**, R4118 (1991).

[283] M. Weitz, B. C. Young, and S. Chu, Atomic interferometer based on adiabatic population transfer, Phys. Rev. Lett. **73**, 2563 (1994).

[284] Weitz, M., B. C. Young, and S. Chu, Atom manipulation based on delayed laser pulses in three- and four-level systems: Light shifts and transfer efficiencies, Phys. Rev. A **50**, 2438 (1994).

[285] U. Gaubatz, P. Rudecki, S. Schiemann, and K. Bergmann, Population transfer between molecular vibrational levels. A new concept and experimental results, J. Chem. Phys. **92**, 5363 (1990).

[286] T. Halfmann, and K. Bergmann, Coherent population transfer and dark resonances in SO_2, J. Chem. Phys. **104**, 70687072 (1996).

[287] S. Schiemann, A. Kuhn, S. Steuerwald, and K. Bergmann, Efficient coherent population transfer in NO molecules using pulsed lasers, Phys. Rev. Lett. **71**, 3637 (1993); Kuhn, A., S. Steuerwald, and K. Bergmann, Coherent population transfer in NO with pulsed lasers: The consequences of hyperfine structure, Doppler broadening and elec-tromagnetically induced absorption, Eur. Phys. J. D **1**,59 (1998).

[288] Kuhn, A., S. Schiemann, G. Z. He, G. Coulston, W. S. Warren, and K. Bergmann, 1992, Population transfer by stimulated Raman scattering with delayed pulses using spectrally broad light, J. Chem. Phys. 96, 42154223.

[289] Y. B. Band and P. S. Julienne, Density matrix calculation of population transfer between vibrational levels of Na_2 by stimulated Raman scattering with temporally shifted laser beams, J. Chem. Phys. **94**, 5291 (1991).

[290] A. P. Kazantsev, The acceleration of atoms by light, Sov. Phys. JETP 39, 784 (1974); Minogin, V. G., Deceleration and monochromatization of atomic beams by radiation pressure, Opt. Commun. 34, 265 (1980);

[291] R. M. Godun, M. B. dArcy, M. K. Oberthaler, G. S. Summy, and K. Burnett, Quantum accelerator modes: A tool for atom optics , Phys. Rev. A **62**, 013411(2000).

Thermoengine

[292] Max Planck, *The theory of heat radiation*, translated by Morton Masius (Dover Publications Inc., New York, 1914).

[293] M. Zemansky, *Thermodynamics*, (McGraw-Hill Book Company, Inc., New York, 1951).

[294] Norman F. Ramsey, Thermodynamics and statistical mechanics at negative absolute temperature, Phys. Rev. **103,** 20 (1956).

[295] H. Scovil and E. Schulz-Dubois, Three level masers as heat engine, Phys. Rev. Lett. **2**, 262 (1969).

[296] J. E. Guesic, E. O. Schulz-Dubois, R. W. Grasse and H.E.D. Scovil, Three level spin refrigerator and maser action at 1500mc/sec, Phys. Rev. **156,** 343 (1967).

[297] J. E. Guesic, E. O. Schulz-Dubois and H.E.D. Scovil, Quantum equivalent of a Carnot cycle, Phys. Rev. **156,** 343 (1967);

[298] Marlan O. Scully, Extracting work from a single thermal bath via quantum negentropy, Phys. Rev. Lett. **87,** 220601 (2001).

[299] Marlan O. Scully, Improving the efficiency of an ideal heat engine:the quantum afterburner, arXiv:quant-ph/105135v1 (2001).

[300] A. E. Allahverdyan and Th. M. Nieuwenhuizen, Extraction of work from a single thermal bath in the quantum regime, Phys. Rev. Lett. **85,** 1799 (2000).

[301] M. Scully, Y. Aharonov, D. J. Tannor, G. Sussmann and H. Walther, Using External Coherent Control Fields to Produce Laser Cooling Without Spontaneous Emission, to be published. ; C. Roos, D. Leibfried, A. Mundt, F. Schmidt-Kaler, J. Eschner, R. Blatt, LANL: quantph/0009034, (2000).

[302] Jochen Gemmer, Alexander Otte, and Günter Mahler, Quantum approach to derivation of the second law of thermodynamics, Phys. Rev. Lett. **86,** 1927 (2001).

[303] Jose P. Palao and Ronnie Kosloff, Jerey M. Gordon, Quantum thermodynamic cooling cycle, arXiv:quant-ph/0106048 v1 8 Jun 2001.

Trapping Methods

[304] Migdall, A., J. Prodan, W. Phillips, T. Bergeman, and H. Metcalf, First observation of magnetically trapped neutral atoms, Phys. Rev. Lett. **54**, 2596 (1985).

[305] Raab, E. M. Prentiss, A. Cable, S. Chu, and D. Pritchard, Trapping of neutral sodium atoms with radiation pressure, Phys. Rev. Lett. **59**, 2631 (1987).

[306] C.G. Townsend, N. H. Edwards, G. J. Cooper, K. P. Zetie, and C. J. Foot, Phase-space density in the magneto-optical trap , Phys. Rev. A **52**, 1423 (1995).

[307] Bergeman, T., G. Erez, and H. J. Metcalf, Magnetostatic trapping fields for neutral atoms, Phys. Rev. A **35**, 1535 (1987).

[308] Daniel Kleppner, and T. J. Greytak, , Magnetic trapping of spin-polarized atomic hydrogen, Phys. Rev. Lett. **59**, 672 (1987).

[309] Petrich, W., M. H. Anderson, J. R. Ensher, and E. A. Cornell, Stable, tightly confining magnetic trap for evaporative cooling of neutral atoms, Phys. Rev. Lett. **74**, 3352 (1995).

[310] E. Peik, Electrodynamic trap for neutral atoms, Eur. Phys. J. D **6**, 179 (1999).

[311] William H. Wing, Electrostatic trapping of neutral atomic particles, Phys. Rev. Lett. **25**, 631 (1980).

[312] J. L. Horn, D. M. Homan, C. S. Hwang, W. L. Fuqua, and K. B. MacAdam, Rev. Sci. Instrum. **69**, 4086 (1998).

Velocity Selection

[313] M. Kasevich and S. Chu, Laser cooling below a photon recoil with three-level atom, Phys. Rev. Lett. **69**, 1741 (1992).

[314] K. Moler, D. S. Weiss, M. Kasevich, and S. Chu, Theoretical analysis of velocity-selective Raman transitions, Phys. Rev. A **45**, 342 (1992).

Wigner Function and Phase Space

[315] P. Wigner, On the Quantum Correction for the Thermodynamics Equilibrium, Phys. Rev. **40**, 749 (1932).

[316] G. S. Agarwal, Master Equations in Phase-Space Formulation of Quantum Optics, Phys. Rev. **178**, 2025 (1969).

[317] This concept is also used in quadrature squeezing of light in quantum optics. Special issues on squeezed light, J. Opt. Soc. Am. B **4,** 1450 (1987), edited by H. J. Kimble and D. F. Walls.

[318] Antoine Royer, Squeezing Wigner function by pulsating harmonic potential wells, Phys. Rev. A **42**, 560 (1990).

Zeno and Anti-Zeno Effects

[319] Alfredo Luis, Zeno effect in spontaneous decay induced by coupling to an unstable level, Phys. Rev. A **64**, 032104 (2001).

[320] P. Knight, Watching a laser hot pot, Nature **344**, 493 (1990).

[321] P. Facchi, H. Nakazato and S. Pascazio, From the quantum Zeno to the inverse quantum Zeno effect, Phys. Rev. Lett. **86**, 2699 (2001).